https://www.mdc-berlin.de/de/veroeffentlichungstypen/clinical-journal-club

Als gemeinsame Einrichtung von MDC und Charité fördert das Experimental and Clinical Research Center die Zusammenarbeit zwischen Grundlagenwissenschaftlern und klinischen Forschern. Hier werden neue Ansätze für Diagnose, Prävention und Therapie von Herz-Kreislauf- und Stoffwechselerkrankungen, Krebs sowie neurologischen Erkrankungen entwickelt und zeitnah am Patienten eingesetzt. Sie sind eingeladen, uns beizutreten. Bewerben Sie sich!

The radiograph shows an extraarticular transverse fracture of the distal radius with dorsal displacement of the distal fragment, also known as a Colles' fracture. A frontal view also showed a fracture of the ulnar styloid tip. Colles' fractures typically occur after falling on an outstretched hand (FOOSH). It is a fragility fracture that indicates a diagnosis of osteoporosis in postmenopausal women, regardless of results of bone mineral density testing. The patient underwent closed reduction and casting and started on treatment for osteoporosis, followed by wrist rehabilitation.

A 57-year-old woman with a history of osteopenia presented to the emergency department with left wrist pain after slipping on ice and landing on her palm. Physical examination and a lateral radiograph of the left wrist are shown. Which of the following is the most likely diagnosis?

- Extraarticular fracture of the distal radius with dorsal displacement
- Fracture of the radial styloid
- Fracture of the scaphoid
- Intraarticular fracture of the distal radius
- Intraarticular fracture of the ulna

Eine **distale Radiusfraktur** ist ein **Bruch der Speiche in der Nähe des Handgelenks**. Sie stellt mit rund 20 Prozent aller Knochenbrüche den **häufigsten Bruch des erwachsenen Menschen** dar.

Ursachen & Typen

Der Bruch entsteht meist durch einen reflexartigen Sturz auf den Arm:

•**Colles-Fraktur**: Sturz auf die ausgestreckte Hand (häufigste Form).

•**Smith-Fraktur**: Sturz auf die gebeugte Hand.

Typische Symptome

•Starke Schmerzen bei Bewegung oder Druck.

•Schnelle Schwellung und Hämatombildung.

•Sichtbare Fehlstellung ("Bajonett-Stellung").

•Kribbeln oder Taubheit in den Fingern bei Nervenreizung.

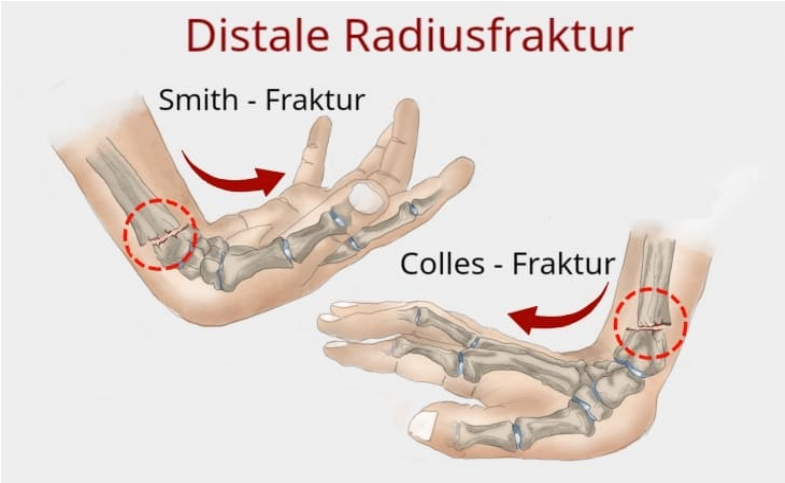

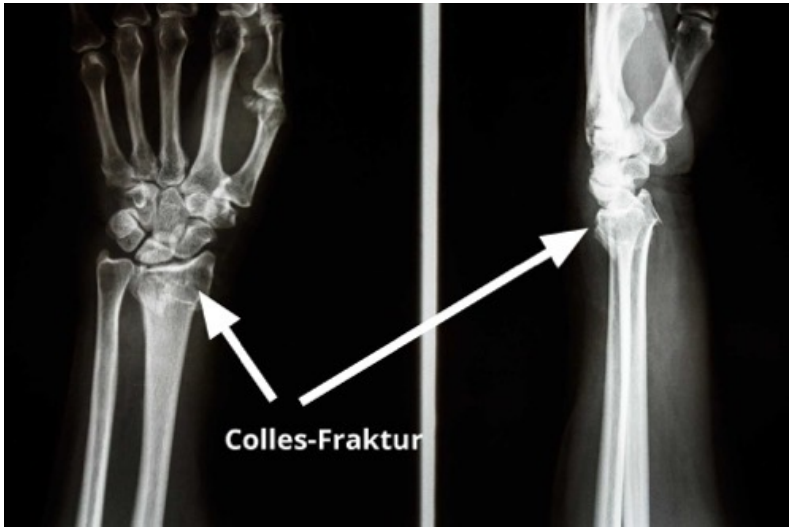

Die **Dermatomyositis** (auch Lilakrankheit genannt) ist eine **seltene, chronisch-entzündliche Autoimmunerkrankung**, die primär die **Haut und die Skelettmuskulatur** betrifft. Sie gehört zur Gruppe der Kollagenosen (diffuse Bindegewebserkrankungen) und äußert sich typischerweise durch charakteristische Hautveränderungen kombiniert mit einer fortschreitenden, symmetrischen Muskelschwäche.

Leitsymptome

•Hautveränderungen (Dermato-):

- **Heliotropes Erythem:** Eine charakteristische rot-violette (lilafarbene) Verfärbung und Schwellung der Augenlider.
- **Gottron-Papeln:** Rötliche, teils schuppende Knötchen direkt über den Fingergelenken und Streckseiten.
- **Shawl- und V-Zeichen:** Lichtempfindliche Rötungen im Nacken (Schal-Zeichen) oder auf der oberen Brust (V-Zeichen).
- **Mechaniker-Hände:** Trockene, raue und rissige Haut an den Handinnenflächen und Fingerrändern.

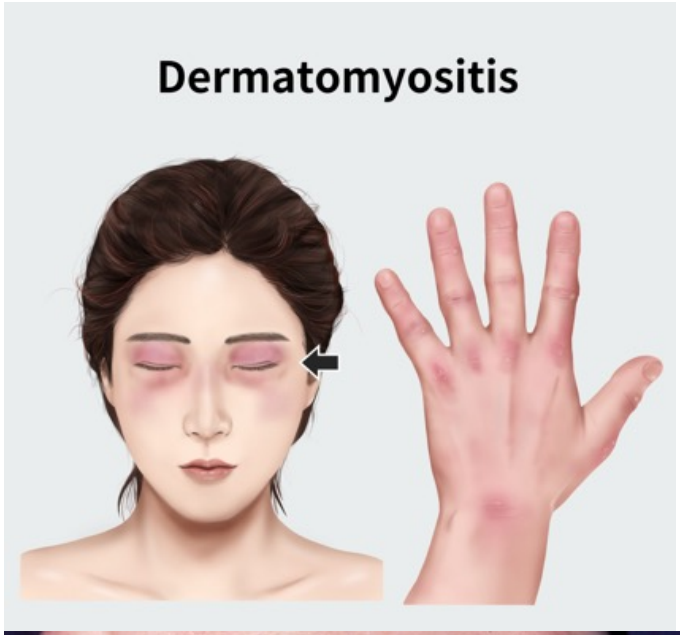

Brepocitinib ist ein neuartiger, oral einzunehmender **dualer TYK2/JAK1-Inhibitor**, der zur Behandlung schwerer, immunvermittelter Autoimmunerkrankungen entwickelt wird. Das Medikament blockiert gezielt die Tyrosinkinase 2 (TYK2) und die Januskinase 1 (JAK1), um die Signalwege entzündungsfördernder Zytokine (wie Typ-1- und Typ-2-Interferone) zu unterdrücken.

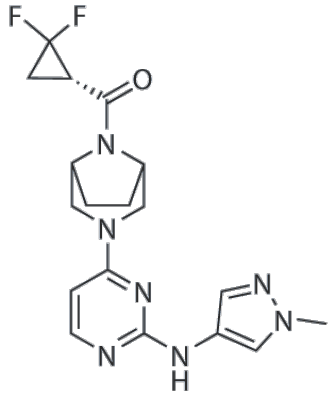

Wichtigste Anwendungsgebiete & Studienergebnisse

•**Dermatomyositis (DM):** In der zulassungsrelevanten Phase-3-Studie VALOR führte die einmal tägliche Gabe zu einer signifikanten Linderung von Haut- und Muskelbeschwerden. Besonders bedeutsam ist der **steroidsparende Effekt**: Patienten konnten ihre Kortikosteroid-Dosis drastisch senken oder die Entzündungshemmer ganz absetzen.

•**Psoriasis-Arthritis (PsA):** Phase-2-Daten zeigen eine signifikante Verbesserung der Gelenk- und Hautsymptome (Erreichen des ACR20-Endpunkts) sowie eine minimale Krankheitsaktivität bei rund 35 % der Patienten.

•**Colitis ulcerosa (CU):** In der Phase-2b-Studie VIBRATO zeigte Brepocitinib bei mittelschwerer bis schwerer aktiver CU bereits nach 8 Wochen einen signifikanten klinischen Vorteil gegenüber Placebo.

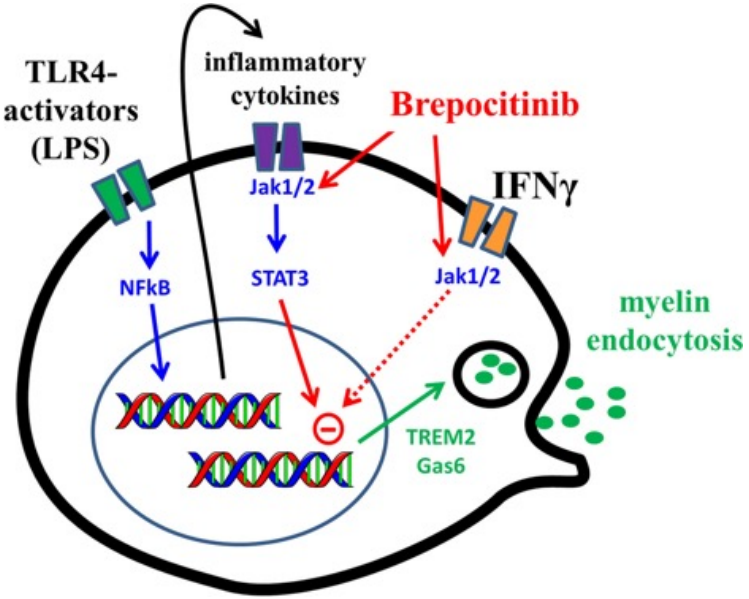

A Phase 3 Trial of Brepocitinib in Dermatomyositis

Brepocitinib is a first-in-class, oral, selective TYK2–JAK1 inhibitor that blocks cytokine signaling, which has been implicated in dermatomyositis.
In this phase 3, double-blind, randomized, placebo-controlled trial, adults with dermatomyositis were assigned in a 1:1:1 ratio to receive once-daily oral brepocitinib at a dose of 30 mg, brepocitinib at a dose of 15 mg, or placebo for 52 weeks. Standard therapies were continued, and glucocorticoids were tapered. The primary end point was the Total Improvement Score, a validated composite myositis index (with scores ranging from 0 to 100 and higher scores indicating greater improvement) at week 52. Key secondary end points, including skin disease activity, glucocorticoid tapering, and physical function, were tested in a multiplicity-controlled sequence.

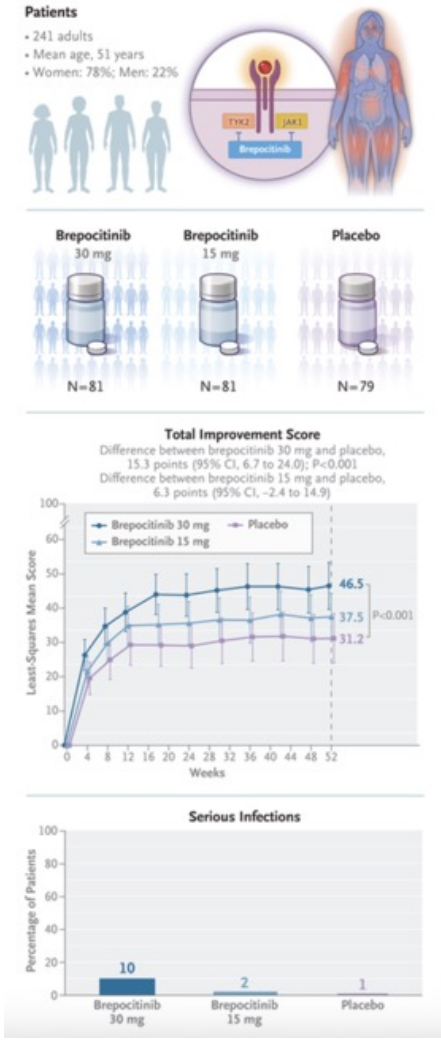

Dermatomyositis is a systemic autoimmune disease characterized by inflammation and progressive damage to the muscles, skin, lungs, joints, heart, and gastrointestinal tract. This condition often follows a chronic, unpredictable, and protracted disease course, factors that contribute to substantial morbidity, impaired quality of life, and disability in affected patients. Current therapies, including combinations of systemic glucocorticoids, nonspecific disease-modifying antirheumatic drugs (DMARDs), and intravenous immune globulin, are associated with incomplete efficacy, treatment-related toxic effects, and challenges with administration. As such, there is a substantial unmet need for safe and effective treatment options for patients with dermatomyositis.
Recent evidence regarding causative agents supports the central role of proinflammatory cytokines (including type I and II interferon, interleukin-6, interleukin-12, and interleukin-23) in the immunopathogenesis of dermatomyositis. Tyrosine kinase 2 (TYK2) and Janus kinase 1 (JAK1) mediate signal transduction of these cytokines, which provides a therapeutic rationale for targeted inhibition. Brepocitinib is an oral, selective TYK2–JAK1 inhibitor that may offer potential benefit for patients with dermatomyositis. We performed the Study to Investigate the Efficacy and Safety of Brepocitinib in Adults with Dermatomyositis (VALOR) to evaluate the efficacy and safety of brepocitinib as compared with placebo in adults with dermatomyositis.

Patients

Adults between the ages of 18 and 75 years were eligible to participate in the trial if the following criteria applied: the patients met the 2017 classification criteria of the European League Against Rheumatism–American College of Rheumatology for definite or probable idiopathic inflammatory myopathy and subclassification criteria for dermatomyositis, and they had evidence of both active muscle disease and skin disease. Active muscle disease was determined by a score of 80 to 142 on the Manual Muscle Test 8 (MMT-8), which evaluates a set of eight designated proximal, distal, and axial muscles tested bilaterally, with total scores ranging from 0 to 150 and lower scores indicating weaker muscles.

Randomization and Treatment

The patients were randomly assigned in a 1:1:1 ratio to receive once-daily oral brepocitinib at a dose of 30 mg, brepocitinib at a dose of 15 mg, or placebo.

At week 12, protocol-defined tapering of glucocorticoids was initiated, with a requirement to reduce the dose to no more than 5 mg per day by week 36 for all the patients unless clinical worsening was observed; tapering below 5 mg per day was encouraged at the investigator's discretion.

End Points

The primary efficacy end point was the mean Total Improvement Score, a weighted composite measure of improvement that integrates six core measures of myositis activity, at week 52.

The patients

Characteristic	Brepocitinib, 30 mg (N=81)	Brepocitinib, 15 mg (N=81)	Placebo (N=79)
Mean age (range) — yr	50 (21–77)	51 (23–72)	51 (20–74)
Female sex — no. (%)	65 (80)	67 (83)	55 (70)
Race or ethnic group — no. (%)†			
White	55 (68)	57 (70)	61 (77)
Asian	6 (7)	11 (14)	7 (9)
Black	6 (7)	6 (7)	4 (5)
Hispanic or Latino	23 (28)	13 (16)	21 (27)
Medical history — no. (%)			
Interstitial lung disease	19 (24)	17 (21)	11 (14)
Previous benign or malignant neoplasm	14 (17)	9 (11)	11 (14)
Atherosclerotic cardiovascular disease	5 (6)	0	2 (3)
Hypertension	27 (33)	23 (28)	23 (29)
Hyperlipidemia	13 (16)	16 (20)	17 (22)
Diabetes mellitus	10 (12)	10 (12)	11 (14)
Obesity	26 (32)	25 (31)	25 (32)
Current tobacco use	7 (9)	7 (9)	8 (10)
Testing scores			
PhGA-VAS‡	5.3±1.6	5.5±1.7	5.6±1.7
CDASI-A§	18.7±11.3	19.5±11.3	21.1±12.0
MMT-8¶	121.7±16.4	124.5±14.2	121.6±17.0
Dermatomyositis background therapy — no. (%)			
Oral glucocorticoids — no. (%)	60 (74)	58 (72)	64 (81)
Daily prednisone-equivalent dose — mg	12.2±5.7	10.7±6.2	11.3±5.9
DMARDs — no. (%)	55 (68)	57 (70)	61 (77)
≥2 Dermatomyositis-directed therapies	64 (79)	66 (82)	66 (84)
History of intravenous immune globulin or rituximab	25 (31)	24 (30)	25 (32)

Primary and Secondary End Points.

End Point	Brepocitinib, 30 mg (N=81)			Brepocitinib, 15 mg (N=81)		Placebo (N=79)
	Value	Difference from Placebo†	P Value	Value	Difference from Placebo†	Value
Primary end point						
Mean Total Improvement Score at wk 52 (95% CI)‡	46.5 (39.7 to 53.4)	15.3 (6.7 to 24.0)	<0.001	37.5 (30.6 to 44.3)	6.3 (−2.4 to 14.9)	31.2 (24.0 to 38.4)
Key secondary end points						
Change in CDASI-A from baseline at wk 52 (95% CI)§	−11.7 (−13.7 to −9.6)	−4.6 (−7.3 to −2.0)	<0.001	−9.4 (−11.5 to −7.3)	−2.4 (−5.0 to 0.2)	−7.0 (−9.2 to −4.9)
DMOMS at wk 52 (95% CI)¶	57.9 (49.5 to 66.2)	17.3 (6.8 to 27.9)	0.001	48.9 (40.5 to 57.2)	8.3 (−2.2 to 18.9)	40.5 (31.8 to 49.3)
Patients with Total Improvement Score of ≥40 at wk 52 — % (95% CI)	68 (57 to 77)	22 (7 to 37)	0.004	54 (44 to 65)	12 (−4 to 27)	44 (34 to 55)
Median time to consecutive Total Improvement Score of ≥40 — days (95% CI)‖	85 (57 to 127)	Hazard ratio, 1.60 (1.09 to 2.33)	0.02	169 (85 to 297)	Hazard ratio, 0.99 (0.66 to 1.48)	168 (85 to 254)
Patients with Total Improvement Score of ≥40 at wk 52 with minimal-to-no oral glucocorticoid use — % (95% CI)**	54 (44 to 65)	26 (11 to 40)	<0.001	41 (31 to 52)	13 (−2 to 28)	27 (18 to 37)
Patients with CDASI-A of ≥40% and ≥4-point improvement at wk 52 — % (95% CI)	62 (51 to 72)	17 (1 to 32)	0.04	59 (48 to 69)	16 (<1 to 31)	44 (34 to 55)
Patients with Total Improvement Score of ≥60 at wk 52 — % (95% CI)	46 (35 to 57)	20 (4 to 35)	0.01	29 (20 to 40)	6 (−8 to 20)	26 (18 to 38)
Change in HAQ-DI from baseline at wk 52 (95% CI)††	−0.34 (−0.49 to −0.18)	−0.30 (−0.49 to −0.10)	0.004	−0.17 (−0.32 to −0.01)	−0.13 (−0.32 to 0.07)	−0.04 (−0.21 to 0.12)
Change in CDASI-A from baseline at wk 4 (95% CI)	−6.4 (−7.7 to −5.2)	−3.0 (−4.6 to −1.4)	<0.001	−4.5 (−5.7 to −3.2)	−1.0 (−2.6 to 0.6)	−3.5 (−4.8 to −2.1)

Safety during the 52-Week Treatment Period.

Adverse Events	Brepocitinib, 30 mg (N=81)	Brepocitinib, 15 mg (N=81)	Placebo (N=79)
	number of patients (percent)		
Any adverse event	73 (90)	70 (86)	72 (91)
Serious adverse event			
Any serious event	13 (16)	7 (9)	10 (13)
Infection	8 (10)	2 (2)	1 (1)
Leading to discontinuation of brepocitinib or placebo	5 (6)	6 (7)	9 (11)
Leading to trial discontinuation	3 (4)	4 (5)	3 (4)
Adverse events of special interest†	6 (7)	4 (5)	10 (13)
Cardiovascular	1 (1)	0	2 (3)
Thromboembolic	0	0	1 (1)
Viral reactivation	4 (5)	2 (2)	4 (5)
New or recurrent cancer	0	0	2 (3)
Increase in ALT or AST level‡	1 (1)	2 (2)	1 (1)

Changes in Global Dermatomyositis Disease Activity and Glucocorticoid Sparing.

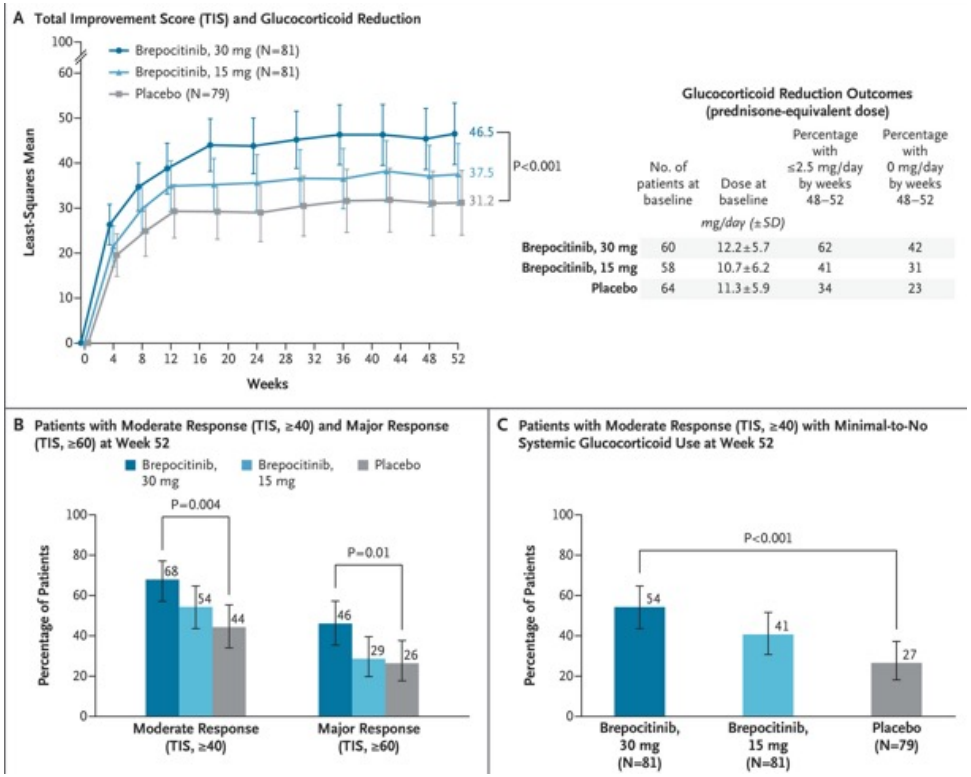

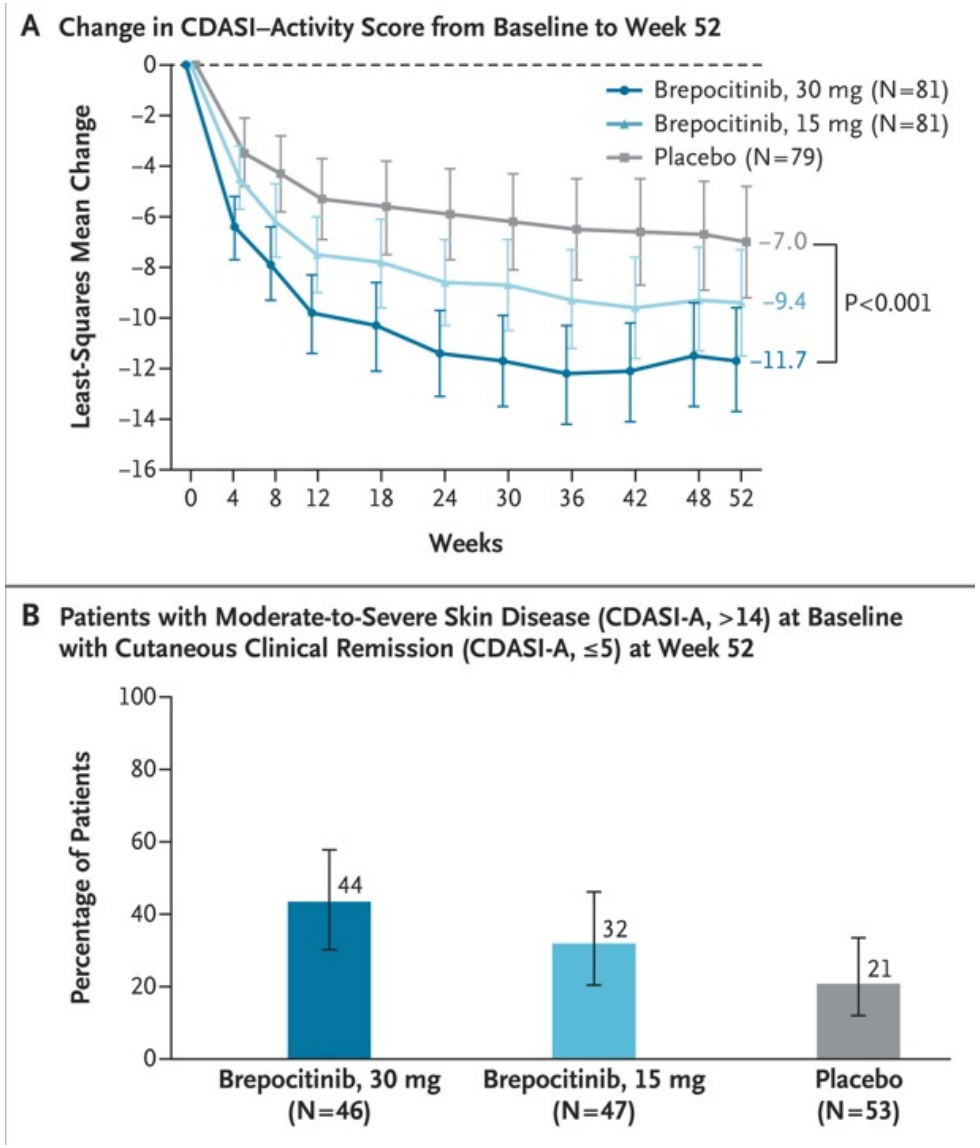

Changes in Cutaneous Dermatomyositis Disease Activity.

Panel A shows the least-squares mean change from baseline in the score on the Cutaneous Dermatomyositis Disease Area and Severity Index–Activity (CDASI-A) in the three trial groups. Scores range from 0 to 100, with higher scores indicating more severe disease activity; improvement is reflected by a decrease in the CDASI-A. Confidence intervals for the brepocitinib 15-mg dose group and for all time points other than week 4 and week 52 in the brepocitinib 30-mg group have not been adjusted for multiplicity and should not be used to infer statistical significance. Panel B shows the percentage of patients with moderate-to-severe skin disease (CDASI-A score, >14) at baseline who had cutaneous clinical remission (CDASI-A score, ≤5) at week 52. Confidence intervals have not been adjusted for multiplicity and should not be used to infer statistical significance. In both panels, I bars indicate 95% confidence intervals.

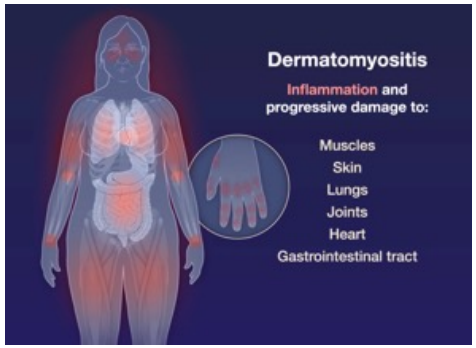

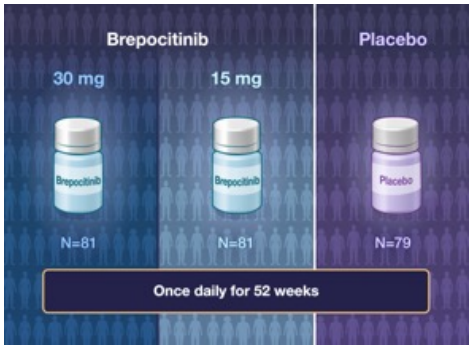

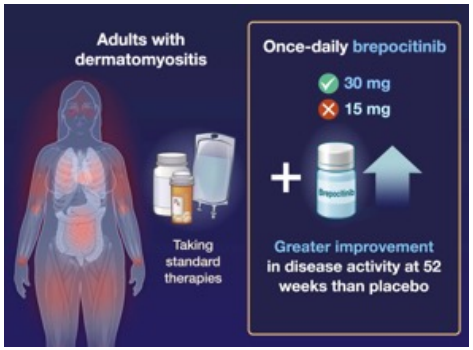

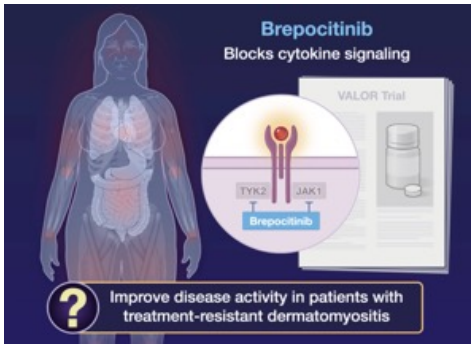

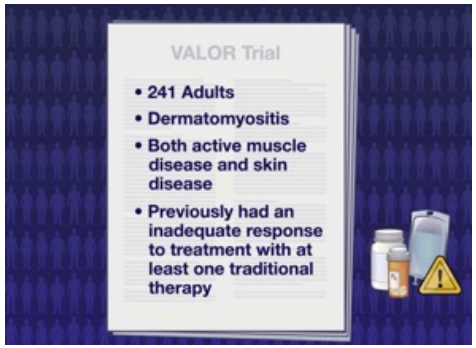

Amazing how much better the placebo group got. All three groups received the standard care.

Medium vessel occlusion (MeVO) strokes represent a critical category of acute ischemic strokes, accounting for **25% to 40% of all cases** involving a detectable vascular blockage. They occur when a blood clot obstructs mid-sized, branching cerebral arteries rather than the primary proximal trunks. While historically overshadowed by catastrophic Large Vessel Occlusions (LVOs), MeVOs are heavily recognized as major contributors to long-term neurological disability.

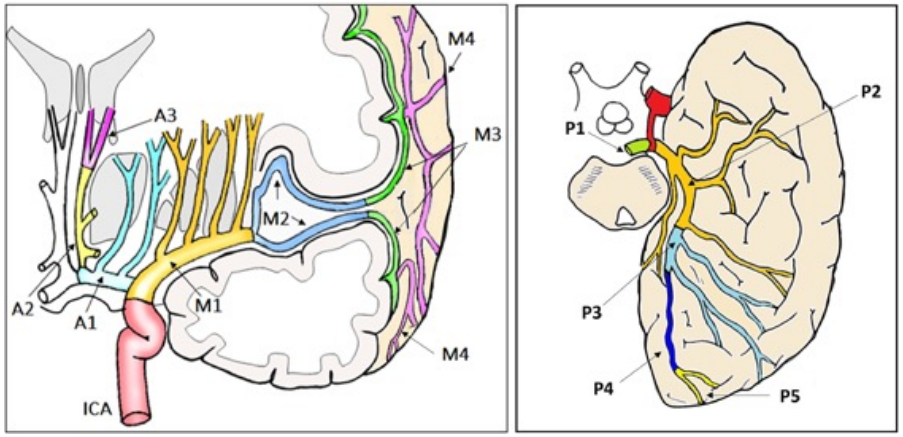

MeVO strokes impact specific segments downstream from major intracranial trunks:

- **Middle Cerebral Artery (MCA):** The M2 and M3 divisions supplying lateral cortical areas.
- **Anterior Cerebral Artery (ACA):** The A2 and A3 segments supplying medial frontal lobes.
- **Posterior Cerebral Artery (PCA):** The P2 and P3 segments supplying visual and occipital regions.

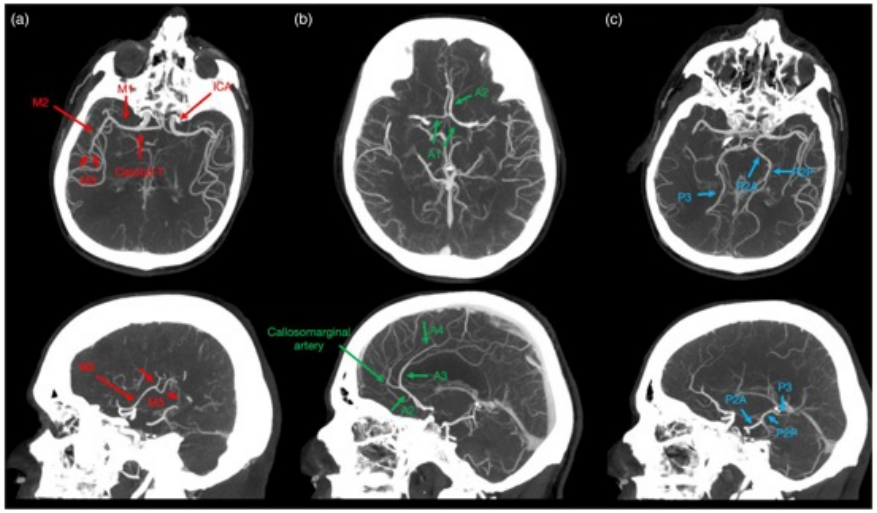

Endovascular treatment of medium-sized stroked vessels

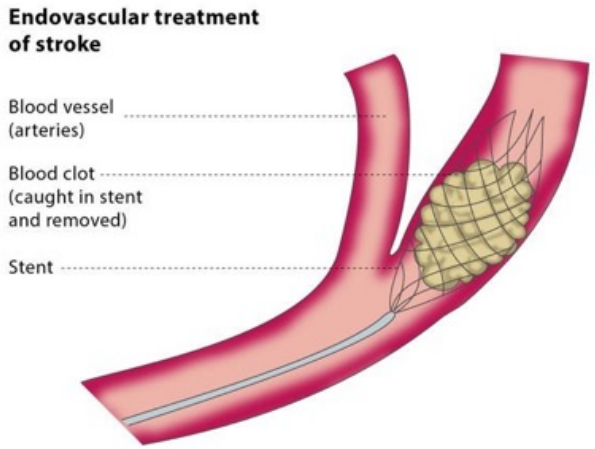

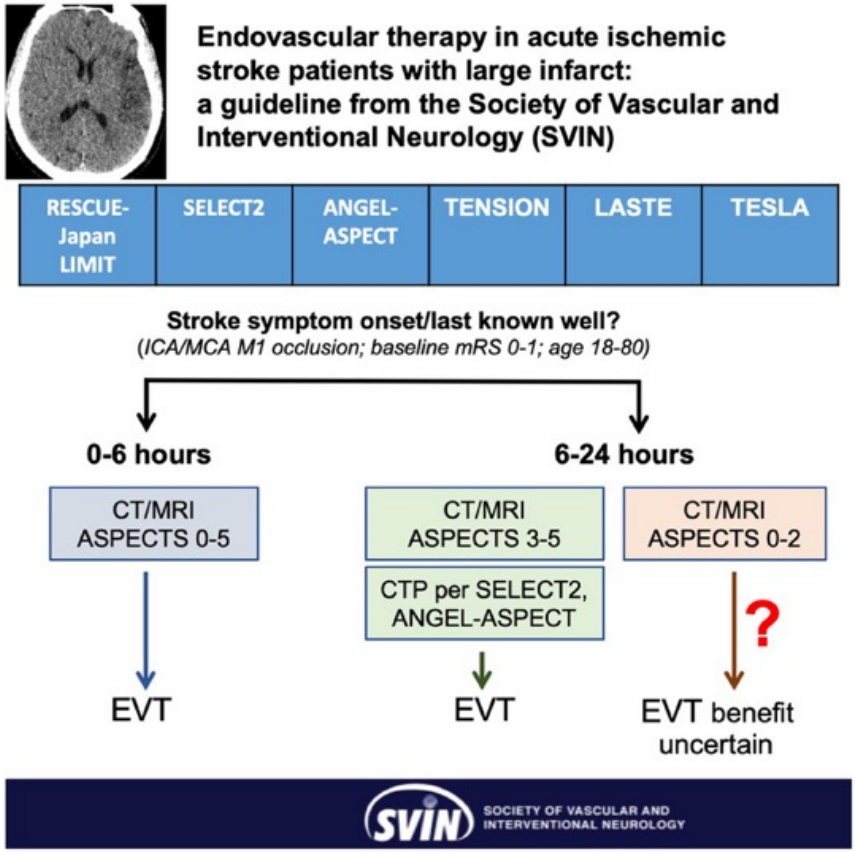

Endovascular Treatment of Medium-Vessel-Occlusion Strokes

Endovascular thrombectomy for acute ischemic stroke due to medium-vessel occlusion has had varying results across trials. Whether thrombectomy improves functional outcomes in patients with medium-vessel occlusion and moderate-to-severe deficits is unclear.

We conducted an open-label, randomized trial with blinded outcome assessment at 48 centers in China. Eligible patients were adults who presented within 24 hours after the onset of a moderate-to-severe stroke (National Institutes of Health Stroke Scale [NIHSS] score, ≥6; scale, 0 to 42, with higher scores indicating greater neurologic deficits) due to occlusion of a medium vessel. Patients were assigned in a 1:1 ratio to thrombectomy plus medical management (thrombectomy group) or medical management alone (control group). The primary outcome was functional disability as measured by the shift in the modified Rankin scale score (scale, 0 [no disability] to 6 [death]) at 90 days. Violation of the proportional-odds assumption precluded the use of shift in the modified Rankin scale score, so as prespecified, functional independence (modified Rankin scale score of 0, 1, or 2) at 90 days was used as the primary outcome. Safety outcomes were symptomatic intracranial hemorrhage and 90-day mortality.

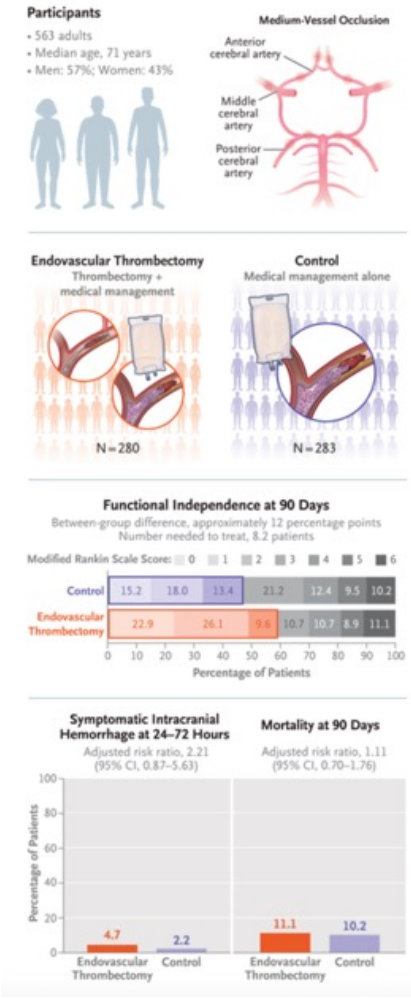

Medium-vessel occlusions account for 25 to 40% of ischemic strokes and represent an important clinical challenge. Although endovascular thrombectomy has improved outcomes in patients with large-vessel occlusions, its benefit in patients with medium-vessel occlusions remains contentious. Recent randomized trials — ESCAPE-MeVO (Endovascular Treatment to Improve Outcomes for Medium Vessel Occlusions), DISTAL (Endovascular Therapy plus Best Medical Treatment [BMT] versus BMT Alone for Medium Vessel Occlusion Stroke — A Pragmatic, International, Multicenter, Randomized Trial), and DISCOUNT (Evaluation of Mechanical Thrombectomy in Acute Ischemic Stroke Related to a Distal Arterial Occlusion) — have shown neutral or unfavorable results, a situation that challenges the extrapolation of data regarding large vessels to medium arteries.

Earlier observational studies suggested that thrombectomy for medium-vessel occlusion was technically feasible and potentially effective, but data from recent randomized trials did not reproduce these observations. In the ESCAPE-MeVO trial, which involved 530 patients, thrombectomy showed no functional benefit as compared with usual care but did lead to higher mortality and a higher incidence of symptomatic intracranial hemorrhage

Patient Population

Adults (≥18 years of age) who had a modified Rankin scale score of 0, 1, or 2 (indicating functional independence on a scale from 0 [no disability] to 6 [death]) before the stroke and who presented with moderate-to-severe clinical deficits (defined as a National Institutes of Health Stroke Scale [NIHSS] score of ≥6, on a scale from 0 to 42, with higher scores indicating greater neurologic deficits) within 24 hours after the time that they were last known to be well were eligible. Patients had to have occlusion of the codominant or nondominant M2 or M3 segment of the middle cerebral artery (MCA); the A1, A2, or A3 segment of the anterior cerebral artery; or the P1, P2, or P3 segment of the posterior cerebral artery. The diameter of the codominant or nondominant M2 segment vessel could not exceed 2.0 mm. A codominant M2 segment supplies 50% of the MCA territory, whereas a nondominant M2 segment supplies less than 50% of the MCA territory.

Outcomes

The primary outcome was functional disability at 90 days (within a window of ±14 days) in the intention-to-treat population. Functional disability was determined on the basis of the modified Rankin scale score by means of structured telephone interviews conducted with patients or caregivers by evaluators who were unaware of the treatment assignments. The planned primary analysis was assessment of an ordinal shift in the distribution of modified Rankin scale scores. In the event of violation of the proportional-odds assumption, functional independence (a modified Rankin scale score of 0, 1, or 2) was prespecified to serve as the primary outcome.

Patients

Characteristic	Thrombectomy Group (N=280)	Control Group (N=283)
Median age (IQR) — yr	71 (62–77)	71 (62–78)
Sex — no. (%)		
Male	164 (58.6)	158 (55.8)
Female	116 (41.4)	125 (44.2)
Modified Rankin scale score of 1 or 2 before stroke onset — no. (%)†	36 (12.9)	32 (11.3)
Median NIHSS score (IQR)‡	10 (8–16)	10 (7–15)
Cause of stroke — no. (%)§		
Large-artery atherosclerosis	134 (47.9)	160 (56.5)
Cardioembolism	111 (39.6)	110 (38.9)
Undetermined cause	33 (11.8)	13 (4.6)
Other determined cause	2 (0.7)	0
Occlusion site¶		
M2 segment	123 (43.9)	96 (33.9)
M3 segment	37 (13.2)	67 (23.7)
Anterior cerebral artery	66 (23.6)	63 (22.3)
Posterior cerebral artery	54 (19.3)	57 (20.1)
Intravenous thrombolysis — no. (%)	101 (36.1)	105 (37.1)
Antiplatelet therapy — no. (%)	188 (67.1)	219 (77.4)
Anticoagulation — no. (%)	80 (28.6)	81 (28.6)
Median duration (IQR) — hr		
From stroke onset to imaging	3.3 (1.9–6.1)	3.4 (1.6–6.4)
From stroke onset to randomization	5.0 (3.4–8.2)	5.0 (3.4–7.8)
From stroke onset to arterial access	5.3 (3.8–8.6)	NA
From stroke onset to revascularization	6.4 (5.0–9.3)	NA
From puncture to revascularization	1.0 (0.7–1.6)	NA
Final eTICI 2b50 to 3 — no./total no. (%)‖	206/277 (74.4)	NA
Variables on CT perfusion**		
Median lesion volume with cerebral blood flow <30% (IQR) — ml	8.4 (1.2–22.6)	4.2 (0–14.3)
Median lesion volume with Tmax >6 sec (IQR) — ml	53.9 (29.3–74.7)	37.1 (24.0–65.3)
Median mismatch ratio (IQR)††	4.3 (2.1–8.7)	5.0 (2.8–9.5)

Trial Outcomes According to Assigned Treatment.

Outcome	Thrombectomy Group (N=280)	Control Group (N=283)	Adjusted Value (95% CI)†
Primary outcome			
Median modified Rankin scale score (IQR)	2 (1 to 4)	3 (1 to 4)	—
Modified Rankin scale score of 0, 1, or 2 at 90 days — no. (%)	164 (58.6)	132 (46.6)	1.24 (1.07 to 1.44)‡
Secondary clinical outcomes§			
Modified Rankin scale score at 90 days — no. (%)			
0	64 (22.9)	43 (15.2)	1.52 (1.08 to 2.14)
0 or 1	137 (48.9)	94 (33.2)	1.47 (1.20 to 1.78)
0–3	194 (69.3)	192 (67.8)	1.01 (0.92 to 1.12)
0–4	224 (80.0)	227 (80.2)	1.00 (0.92 to 1.08)
0–5	249 (88.9)	254 (89.8)	0.99 (0.94 to 1.04)
Median NIHSS score (IQR)¶			
At 24 hr, with window of ±6 hr	9 (4 to 15)	8 (5 to 14)	0.81 (−0.27 to 1.88)
At 5–7 days or discharge	4 (1 to 10)	6 (3 to 13)	−1.27 (−2.56 to 0.03)
Barthel Index of 95 or 100 at 90 days — no. (%)‖	159 (56.8)	140 (49.5)	1.14 (0.99 to 1.31)
Median EQ-5D-5L score at 90 days (IQR)**	0.95 (0.78 to 1.00)	0.90 (0.70 to 1.00)	0.04 (−0.02 to 0.09)
Secondary imaging outcomes			
Patency at 24–72 hr on CTA or MRA — no./total no. (%)††	147/179 (82.1)	84/182 (46.2)	1.76 (1.49 to 2.09)
Intracranial hemorrhage at 24–72 hr as assessed radiologically — no. (%)	32 (11.4)	17 (6.0)	1.94 (1.12 to 3.35)
Safety outcomes			
Death — no. (%)	31 (11.1)	29 (10.2)	1.11 (0.70 to 1.76)
Symptomatic ICH at 24–72 hr — no./total no. (%)‡‡	13/275 (4.7)	6/271 (2.2)	2.21 (0.87 to 5.63)

Standard medical treatment was provided according to current guidelines and included antiplatelet therapy (one or two antiplatelet agents, at the discretion of the treating physician) and intravenous thrombolysis with alteplase or tenecteplase when patients met established eligibility criteria.

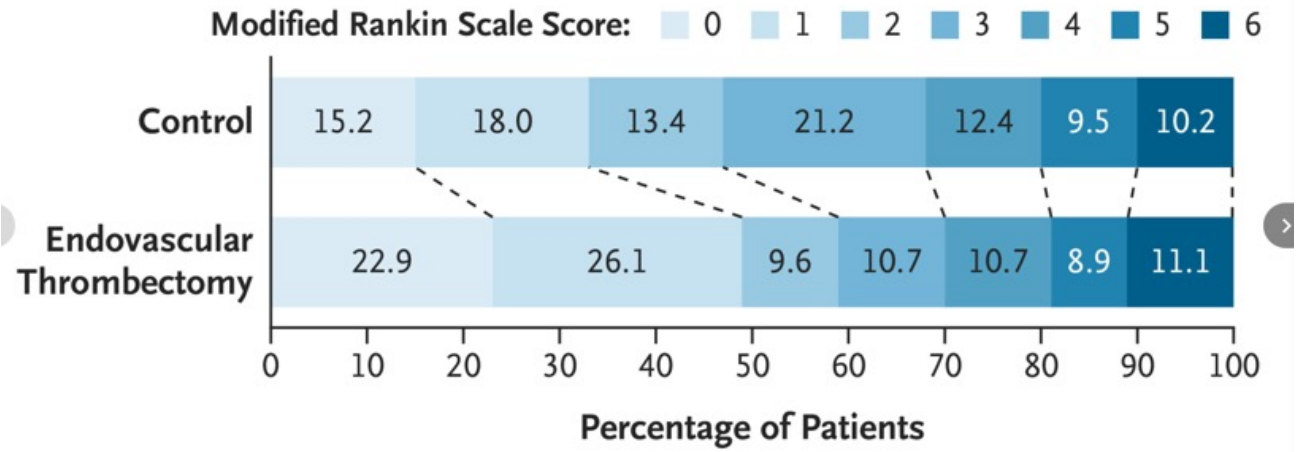

Distribution of Functional Outcomes at 90 Days (Intention-to-Treat Population).

Shown are scores on the modified Rankin scale for patients in the two treatment groups. Patients had been randomly assigned to receive endovascular thrombectomy plus medical management or medical management alone (control). The intention-to-treat population included all the patients who had undergone randomization, except for one patient in the thrombectomy group who withdrew shortly after randomization and was excluded. Scores on the modified Rankin scale range from 0 to 6, with 0 indicating no disability, 1 no clinically significant disability, 2 slight disability (patients are able to look after their own affairs without assistance but are unable to carry out all previous activities), 3 moderate disability (patients require some help but are able to walk unassisted), 4 moderately severe disability (patients are unable to attend to bodily needs without assistance and are unable to walk unassisted), 5 severe disability (patients require constant nursing care and attention), and 6 death. Percentages may not total 100 because of rounding.

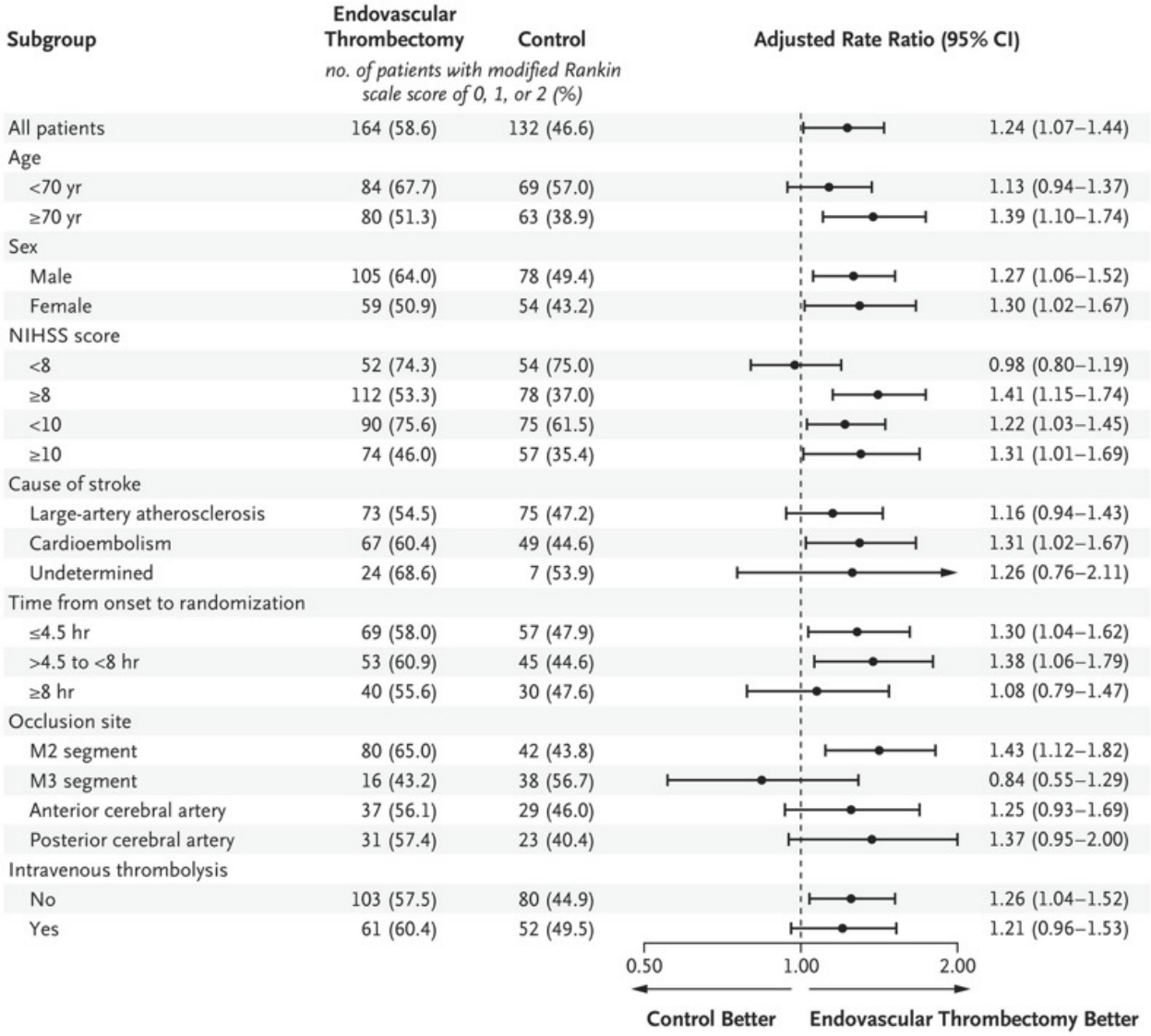

Subgroup Analyses of a Modified Rankin Scale Score of 0, 1, or 2, Indicating Functional Independence, at 90 Days (Primary Outcome).

The trial was not powered and had no prespecified correction for multiple comparisons for a definitive analysis of subgroups. Scores on the National Institutes of Health Stroke Scale (NIHSS) range from 0 to 42, with higher scores indicating greater neurologic deficits. Patients had occlusion of the medium-size segments of the middle cerebral artery (M2 or M3); the A1, A2, or A3 segment of the anterior cerebral artery; or the P1, P2, or P3 segment of the posterior cerebral artery. The arrow indicates that the confidence interval extends outside the graphed area.

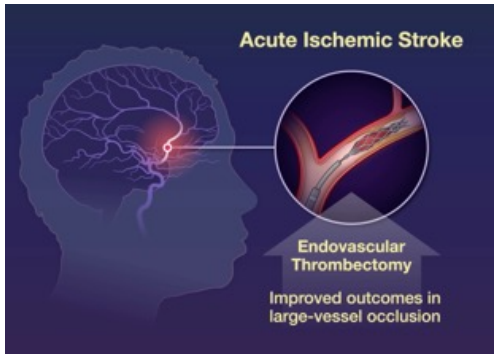
Acute Ischemic Stroke
Endovascular Thrombectomy
Improved outcomes in large-vessel occlusion

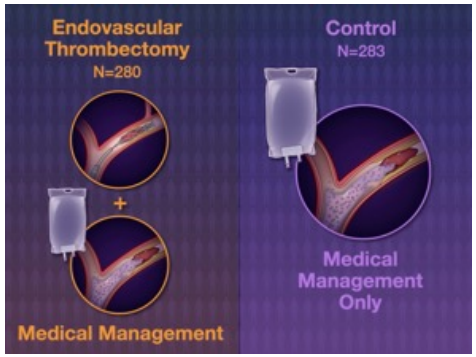
Endovascular Thrombectomy
N=280
Control
N=283
Medical Management
Medical Management Only

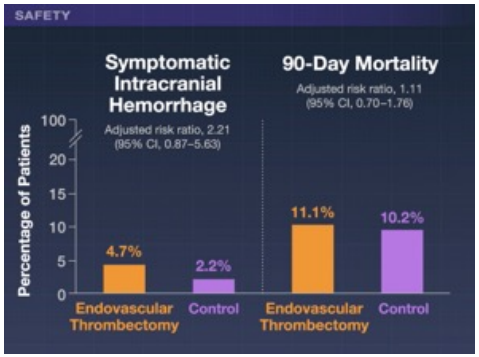
SAFETY
Symptomatic Intracranial Hemorrhage
Adjusted risk ratio, 2.21
(95% CI, 0.87–5.63)
90-Day Mortality
Adjusted risk ratio, 1.11
(95% CI, 0.70–1.76)
Percentage of Patients
100
20
15
10
5
0
4.7%
2.2%
11.1%
10.2%
Endovascular Thrombectomy
Control
Endovascular Thrombectomy
Control

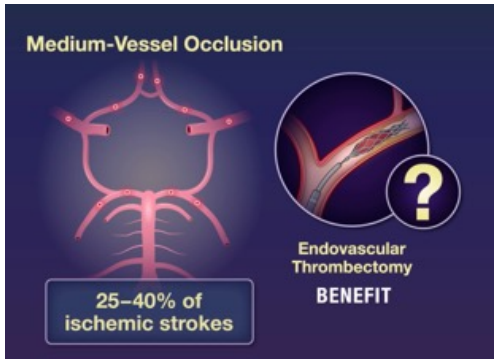
Medium-Vessel Occlusion
Endovascular Thrombectomy
BENEFIT
25–40% of ischemic strokes


PRIMARY OUTCOME
Functional Independence
Modified Rankin Scale Score
No symptoms 0 1 2 3 4 5 6 Death
Control
15.2 18.0 13.4 21.2 12.4 9.5 10.2
Endovascular Thrombectomy
22.9 26.1 9.6 10.7 10.7 8.9 11.1
0 10 20 30 40 50 60 70 80 90 100

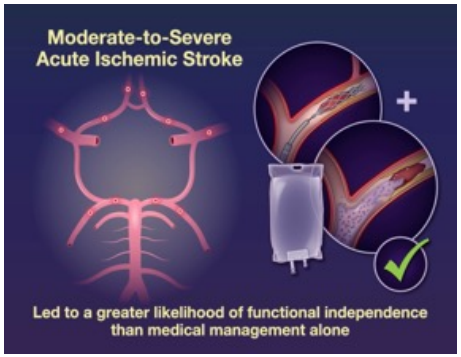
Moderate-to-Severe Acute Ischemic Stroke
Led to a greater likelihood of functional independence than medical management alone


New Trial
A new trial assesses the efficacy and safety of thrombectomy in patients with medium-vessel occlusion

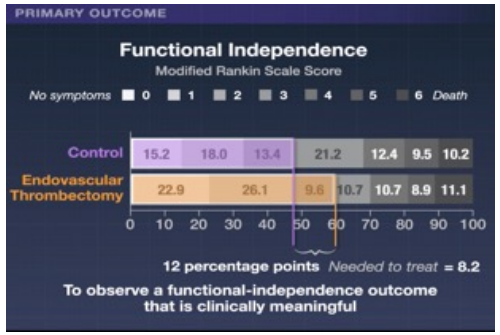
PRIMARY OUTCOME
Functional Independence
Modified Rankin Scale Score
No symptoms 0 1 2 3 4 5 6 Death
Control
15.2 18.0 13.4 21.2 12.4 9.5 10.2
Endovascular Thrombectomy
22.9 26.1 9.6 10.7 10.7 8.9 11.1
0 10 20 30 40 50 60 70 80 90 100
12 percentage points Needed to treat = 8.2
To observe a functional-independence outcome that is clinically meaningful

Ensitrelvir

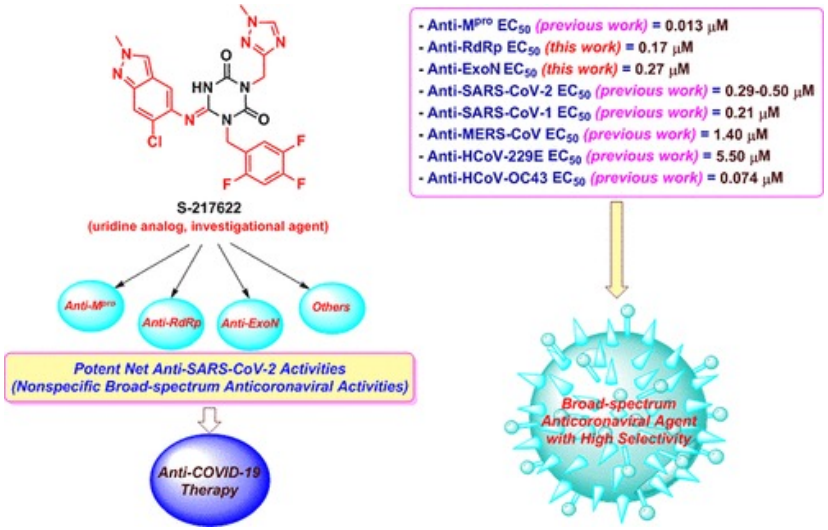

Ensitrelvir ist ein oral verabreichbares, antivirales Medikament zur Behandlung und Postexpositionsprophylaxe einer Infektion mit SARS-CoV-2 (COVID-19). Der niedermolekulare Wirkstoff wurde vom japanischen Pharmaunternehmen Shionogi entwickelt.

Wirkungsweise

•**3CL-Protease-Inhibitor:** Ensitrelvir blockiert gezielt die virale Hauptprotease (3CL-Protease) des Virus.

•**Replikationsstopp:** Das Enzym kann virale Polyproteine nicht mehr spalten. Die Virusvermehrung in den Wirtszellen bricht zusammen.

•**Kein Booster nötig:** Im Gegensatz zum bekannten Wirkstoff Nirmatrelvir benötigt Ensitrelvir keine zusätzliche Verstärkung durch Ritonavir.

Ensitrelvir for Covid-19 Postexposure Prophylaxis in Household Contacts

Ensitrelvir, an oral inhibitor of severe acute respiratory syndrome coronavirus 2 (SARS-CoV-2) 3C-like protease, is approved in Japan for the treatment of mild-to-moderate coronavirus disease 2019 (Covid-19). Previously, no antiviral agents were approved for postexposure prophylaxis in household contacts of patients with Covid-19.

In this double-blind, randomized, placebo-controlled trial, we randomly assigned persons who were SARS-CoV-2–negative on local diagnostic testing but were household contacts of a patient with Covid-19 (the index patient) to receive either ensitrelvir (375 mg on day 1 and 125 mg daily on days 2 through 5) or placebo within 72 hours after symptom onset in the index patient. The primary end point was Covid-19 (defined by a central laboratory–confirmed positive reverse-transcriptase–polymerase-chain-reaction assay and the presence of ≥1 of 14 prespecified Covid-19 symptoms lasting ≥48 hours) by day 10 in a household contact in the modified intention-to-treat population (all the participants who underwent randomization, had a central laboratory–confirmed negative RT-PCR test for SARS-CoV-2 at baseline, and received at least one dose of the trial drug or placebo).

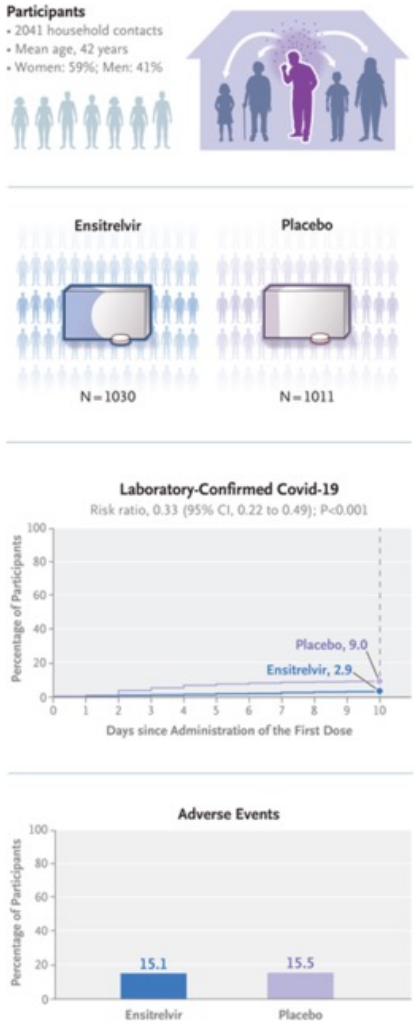

Ensitrelvir, an oral inhibitor of SARS-CoV-2 3C-like protease, has potent in vitro activity against SARS-CoV-2 variants, including omicron. Ensitrelvir is currently approved in Japan for treating mild-to-moderate Covid-19 in patients 12 years of age or older, and on the basis of the findings in the current trial, is approved in that country for postexposure prophylaxis in contacts 12 years of age or older. In patients at standard risk who had mild-to-moderate Covid-19 or asymptomatic infection, ensitrelvir was associated with significant antiviral efficacy and numerical reduction in the incidence of acute and respiratory symptoms. The phase 3 SCORPIO-SR trial (Stopping Covid-19 Progression with Early Protease Inhibitor Treatment in Standard-Risk Patients), which also enrolled patients at high risk, showed an approximate 1-day reduction in five Covid-19 symptoms when treatment was initiated within 3 days after symptom onset. Adverse effects included mild-to-moderate, reversible, dose-related decreases in high-density lipoprotein (HDL) levels and increases in triglyceride levels. In the phase 3 SCORPIO-HR (Stopping Covid-19 Progression with Early Protease Inhibitor Treatment in High-Risk Patients) trial, which enrolled nonhospitalized adults with mild-to-moderate Covid-19 who were at standard or high risk for severe Covid-19, ensitrelvir showed antiviral efficacy but did not notably reduce the time to symptom resolution. In light of the antiviral efficacy shown with ensitrelvir, we conducted a randomized, controlled trial, the phase 3 SCORPIO-PEP (Stopping Covid-19 Progression with Early Protease Inhibitor Treatment for Post-Exposure Prophylaxis) trial, to determine whether ensitrelvir would be efficacious as postexposure prophylaxis in persons exposed to SARS-CoV-2 in a household setting.

Trial Population

An index patient was defined as the first person with documented Covid-19 in a household. To be eligible, adult and pediatric index patients were required to have had at least 1 of 14 prespecified Covid-19 symptoms and a positive SARS-CoV-2 test (antigen test or reverse-transcriptase–polymerase-chain-reaction [RT-PCR] assay) within 72 hours before the participating household contact underwent randomization. The index patient received antiviral treatment at the discretion of each investigator. The intention-to-treat population included enrolled household contacts who were at least 12 years of age, had a negative local SARS-CoV-2 test as described above, and were enrolled within 72 hours after symptom onset in the index patient. The modified intention-to-treat population included all the participants who had undergone randomization, had a central laboratory–confirmed, negative RT-PCR test for SARS-CoV-2 at baseline, and received at least one dose of ensitrelvir or placebo. The intention-to-treat baseline RT-PCR–positive population included the participants who had undergone randomization and had a central laboratory–confirmed, positive RT-PCR test for SARS-CoV-2 at baseline.

Efficacy End Points

Nasopharyngeal swabs were obtained from participants on days 1, 3, 6, 10, 15, 21, and 28 for RT-PCR detection of SARS-CoV-2. The primary efficacy end point was laboratory-confirmed Covid-19 within 10 days after administration of the trial drug or placebo in a household contact who was RT-PCR negative at baseline.

Characteristics	Ensitrelvir (N=1030)	Placebo (N=1011)
Age — yr	41.8±16.9	43.0±16.1
Age range — no. (%)		
<18 yr	64 (6.2)	54 (5.3)
18–64 yr	867 (84.2)	867 (85.8)
≥65 yr	99 (9.6)	90 (8.9)
Female sex — no. (%)	584 (56.7)	627 (62.0)
Body-mass index†	26.4 (5.7)	26.6 (5.3)
Race or ethnic group — no. (%)‡		
White	632 (61.4)	615 (60.8)
Black or African American	51 (5.0)	56 (5.5)
Asian	325 (31.6)	321 (31.8)
American Indian or Alaska Native	2 (0.2)	4 (0.4)
Other	20 (1.9)	15 (1.5)
Hispanic or Latino ethnic group — no. (%)‡	620 (60.2)	623 (61.6)
Duration from symptom onset in index patient to enrollment of participant — no. of participants (%)		
<48 hr	732 (71.1)	720 (71.2)
≥48 hr	298 (28.9)	291 (28.8)
Geographic region — no. (%)		
United States	692 (67.2)	683 (67.6)
South America	7 (0.7)	4 (0.4)
Africa	6 (0.6)	5 (0.5)
Asia (except Japan)	59 (5.7)	49 (4.8)
Japan	266 (25.8)	270 (26.7)
High risk for severe illness — no. (%)§	382 (37.1)	374 (37.0)
Index patient antiviral treatment — no. (%)	140 (13.6)	134 (13.3)
Ensitrelvir¶	101 (9.8)	90 (8.9)
Nirmatrelvir or ritonavir	25 (2.4)	33 (3.3)
Molnupiravir	12 (1.2)	11 (1.1)
Trial regimen of ensitrelvir or placebo¶	2 (0.2)	0

Adverse Events (Safety Analysis Population).

Adverse Event	Ensitrelvir (N=1190)			Placebo (N=1187)		
	no. of events	*no. of patients with event*	*% of patients (95% CI)*	*no. of events*	*no. of patients with event*	*% of patients (95% CI)*
Any	303	180	15.1 (13.1–17.3)	307	184	15.5 (13.5–17.7)
Type of event†						
Infection or infestation	63	51	4.3	63	57	4.8
Nasopharyngitis	16	16	1.3	15	15	1.3
Influenza	19	13	1.1	23	19	1.6
Gastrointestinal disorder	48	42	3.5	38	31	2.6
Diarrhea	23	21	1.8	17	15	1.3
Nervous-system disorder	46	39	3.3	43	39	3.3
Headache	40	35	2.9	32	30	2.5
Respiratory, thoracic, or mediastinal disorder	40	32	2.7	40	27	2.3
Cough	14	14	1.2	9	7	0.6
Oropharyngeal pain	11	11	0.9	19	17	1.4
General disorder	26	20	1.7	31	24	2.0
Fatigue	16	13	1.1	14	12	1.0
Any serious adverse event	3	2	0.2 (0.0–0.6)	2	2	0.2 (0.0–0.6)
Any adverse event related to trial drug or placebo	23	19	1.6 (1.0–2.5)	30	21	1.8 (1.1–2.7)
Any serious adverse event related to trial drug or placebo	0	0	0.0 (0.0–0.3)	0	0	0.0 (0.0–0.3)
Any adverse event leading to drug or placebo discontinuation	1	1	<0.1 (0.0–0.5)	1	1	<0.1 (0.0–0.5)
Any adverse event leading to trial discontinuation	0	0	0.0 (0.0–0.3)	1	1	<0.1 (0.0–0.5)
Any adverse event leading to death	0	0	0.0 (0.0–0.3)	0	0	0.0 (0.0–0.3)

Nirmatrelvir and ensitrelvir are both oral antiviral medications for COVID-19 that target the same viral 3CL protease. The primary differences lie in their approval status, need for boosting medication, target patient groups, and resistance profiles.

A Incidence of Covid-19 in the Modified Intention-to-Treat Population

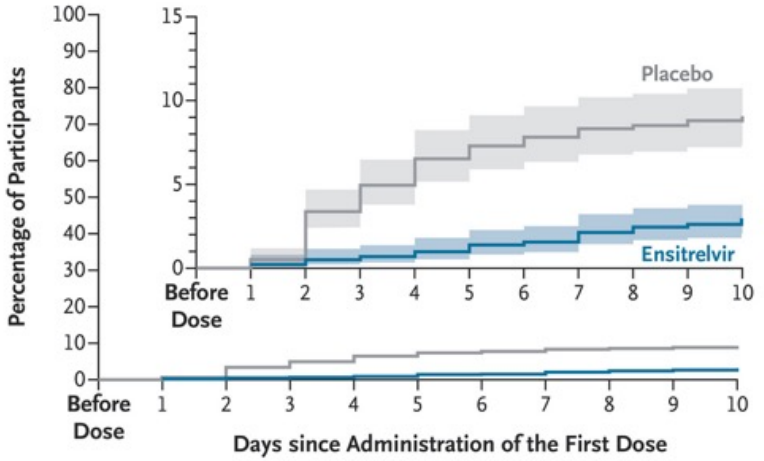

No. at Risk

Placebo	1011	1011	1006	977	961	945	937	932	927	925	922
Ensitrelvir	1030	1030	1028	1025	1023	1020	1016	1014	1008	1005	1003

B Incidence of Covid-19 in the Intention-to-Treat Population

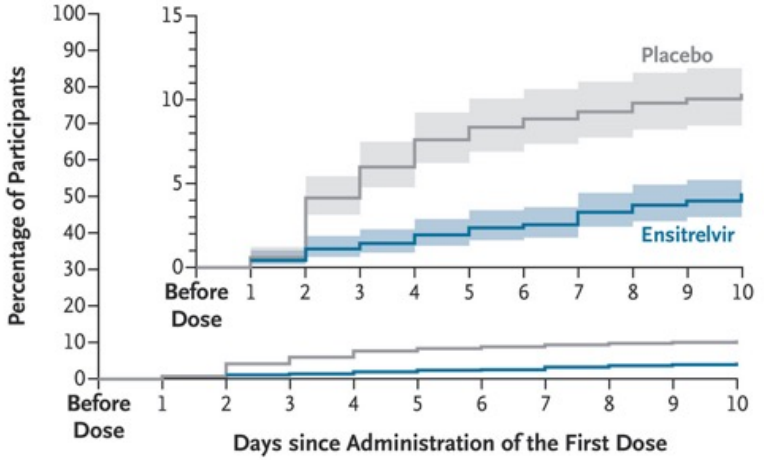

Subgroup	Ensitrelvir	Placebo	Risk Ratio (95% CI)
	no. of participants with event/total no. (%)		
Overall	30/1030 (2.9)	91/1011 (9.0)	0.33 (0.22–0.49)
Time since onset of symptoms in index patients			
<48 hr	18/732 (2.5)	74/720 (10.3)	0.26 (0.16–0.41)
≥48 hr	12/298 (4.0)	17/291 (5.8)	0.69 (0.33–1.42)
Geographic region			
Japan	11/266 (4.1)	62/270 (23.0)	0.18 (0.10–0.33)
United States	15/692 (2.2)	25/683 (3.7)	0.60 (0.32–1.12)
Rest of the world	4/72 (5.6)	4/58 (6.9)	0.84 (0.27–2.61)
Risk factors			
Present	9/382 (2.4)	37/374 (9.9)	0.24 (0.12–0.49)
Absent	21/648 (3.2)	54/637 (8.5)	0.39 (0.24–0.62)
Age of household contact			
<18 yr	1/64 (1.6)	2/54 (3.7)	0.42 (0.04–4.57)
18–64 yr	26/867 (3.0)	78/867 (9.0)	0.34 (0.23–0.52)
≥65 yr	3/99 (3.0)	11/90 (12.2)	0.25 (0.08–0.82)
Type of treatment in index patient			
Any Covid-19–specific	4/144 (2.8)	26/139 (18.7)	0.16 (0.06–0.40)
No treatment	26/886 (2.9)	65/872 (7.5)	0.40 (0.26–0.61)
Upper respiratory symptoms in index patient			
Present	25/853 (2.9)	73/821 (8.9)	0.34 (0.22–0.52)
Absent	5/176 (2.8)	18/190 (9.5)	0.30 (0.13–0.72)
Age of index patient			
<12 yr	1/45 (2.2)	6/43 (14.0)	0.16 (0.01–1.82)
12–17 yr	3/94 (3.2)	13/90 (14.4)	0.22 (0.07–0.72)
≥18 yr	26/891 (2.9)	72/878 (8.2)	0.37 (0.24–0.56)

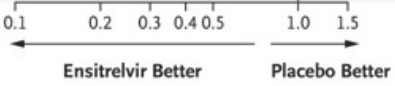

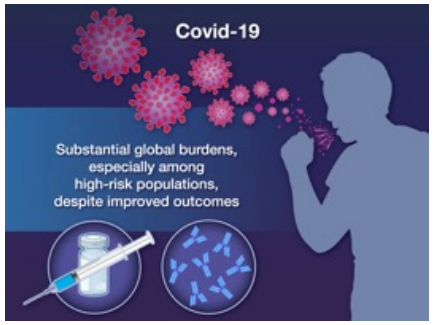
Covid-19
Substantial global burdens, especially among high-risk populations, despite improved outcomes


SCORPIO-PEP Trial
Ensitrelvir
Efficacy and safety as a postexposure prophylaxis in household contacts of index patients with Covid-19

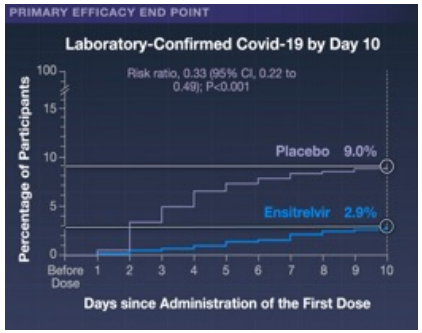
PRIMARY EFFICACY END POINT
Laboratory-Confirmed Covid-19 by Day 10
Risk ratio, 0.33 (95% CI, 0.22 to 0.49); P<0.001
Placebo 9.0%
Ensitrelvir 2.9%
Percentage of Participants
Before Dose
Days since Administration of the First Dose


Ensitrelvir
More effective than placebo in preventing Covid-19 in household contacts of patients with SARS-CoV-2 infection

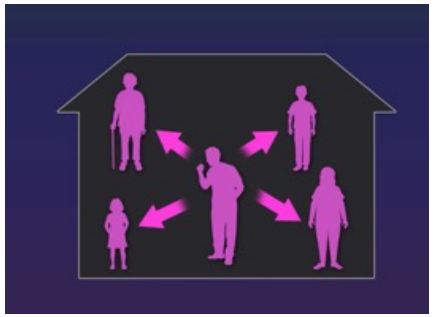

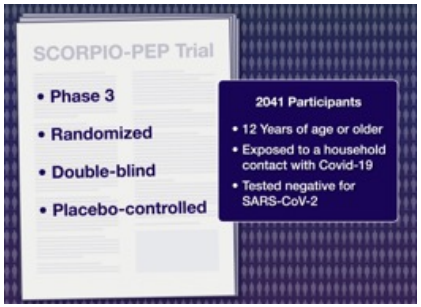
SCORPIO-PEP Trial
• Phase 3
• Randomized
• Double-blind
• Placebo-controlled
2041 Participants
• 12 Years of age or older
• Exposed to a household contact with Covid-19
• Tested negative for SARS-CoV-2

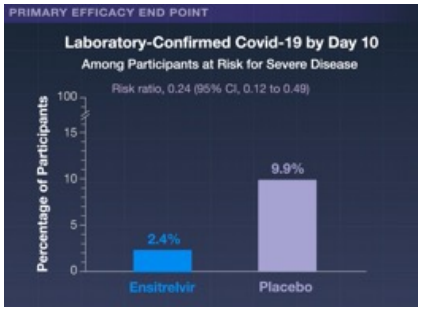
PRIMARY EFFICACY END POINT
Laboratory-Confirmed Covid-19 by Day 10
Among Participants at Risk for Severe Disease
Risk ratio, 0.24 (95% CI, 0.12 to 0.49)
Percentage of Participants
2.4%
9.9%
Ensitrelvir
Placebo

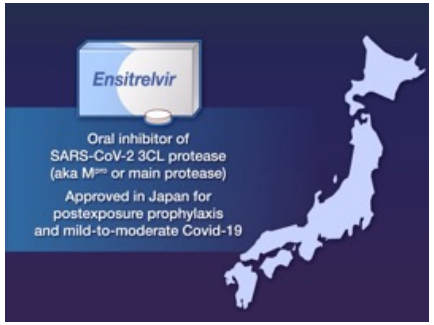
Ensitrelvir
Oral inhibitor of SARS-CoV-2 3CL protease (aka Mpro or main protease)
Approved in Japan for postexposure prophylaxis and mild-to-moderate Covid-19

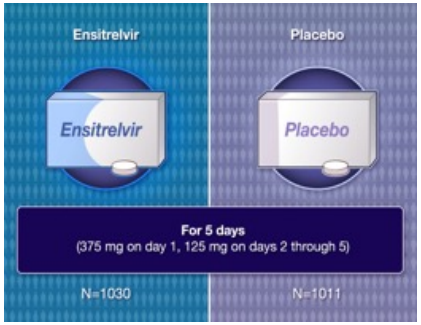
Ensitrelvir
Placebo
Ensitrelvir
Placebo
For 5 days
(375 mg on day 1, 125 mg on days 2 through 5)
N=1030
N=1011

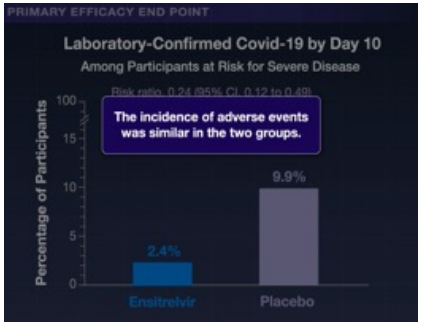
PRIMARY EFFICACY END POINT
Laboratory-Confirmed Covid-19 by Day 10
Among Participants at Risk for Severe Disease
The incidence of adverse events was similar in the two groups.
Percentage of Participants
2.4%
9.9%
Ensitrelvir
Placebo

IgA Nephropathie

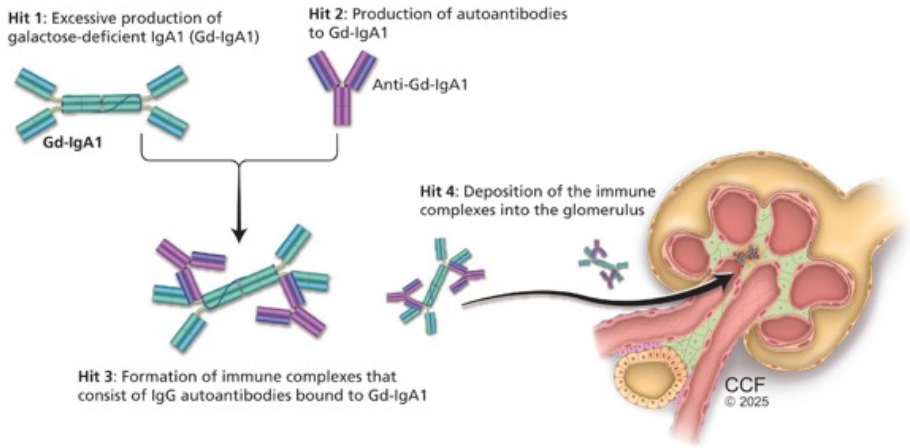

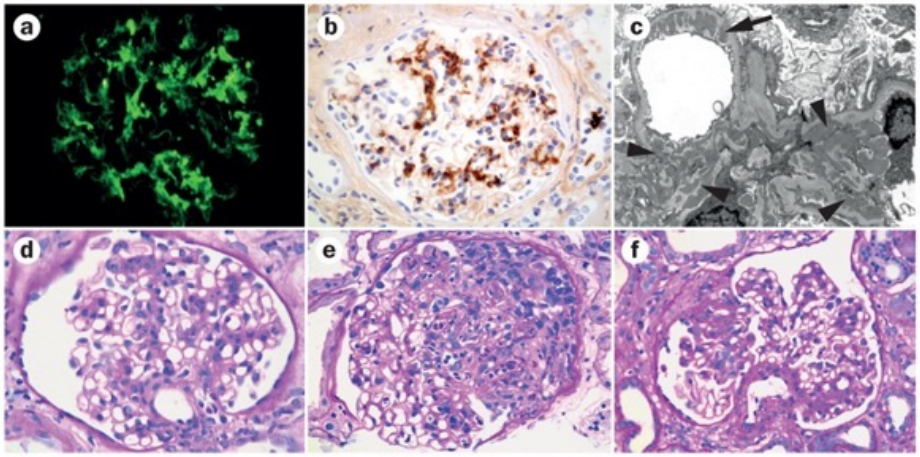

Die Pathogenese der **IgA-Nephropathie (IgAN, Morbus Berger)** wird heute über das etablierte **„Multi-Hit-Modell“ (Vier-Treffer-Hypothese)** erklärt. Es beschreibt eine Kaskade, bei der eine genetische Veranlagung, Schleimhaut-Immunreaktionen und die Bildung abnormaler Immunkomplexe zu einer chronischen Entzündung der Nierenkörperchen führen.

- **Treffer 1: Überproduktion von Galaktose-defizientem IgA1 (Gd-IgA1.** Durch eine genetische Veranlagung und getriggert durch Schleimhautinfektionen (z. B. der Atemwege oder des Darms) produzieren B-Lymphozyten eine abnorme Form des Immunglobulins A1. Diesem **Gd-IgA1** fehlt die Zuckerverbindung Galaktose in der sogenannten Scharnierregion (Hinge-Region) des Antikörpers.

APRIL und **BAFF** sind zwei lebenswichtige Zytokine (Proteine) des Immunsystems, die eng zusammenarbeiten, um B-Lymphozyten zu aktivieren, zu differenzieren und ihr Überleben zu sichern. Sie spielen eine Schlüsselrolle bei der Bildung unseres Antikörpergedächtnisses, können bei Fehlfunktionen aber auch Autoimmunerkrankungen auslösen

•**BAFF** (*B-cell activating factor*): Ist essenziell für das Überleben und die Reifung von B-Zellen. Es sorgt dafür, dass sich unreife B-Zellen im Körper verteilen können und regt die Produktion von Antikörpern an.

•**APRIL** (*a proliferation-inducing ligand*): Fördert das Wachstum, die Reifung und das Überleben von langlebigen Plasmazellen im Knochenmark. Zudem ist es maßgeblich an der Klassenwechsel-Rekombination (CSR) beteiligt, also der Anpassung der Antikörper an spezifische Krankheitserreger.

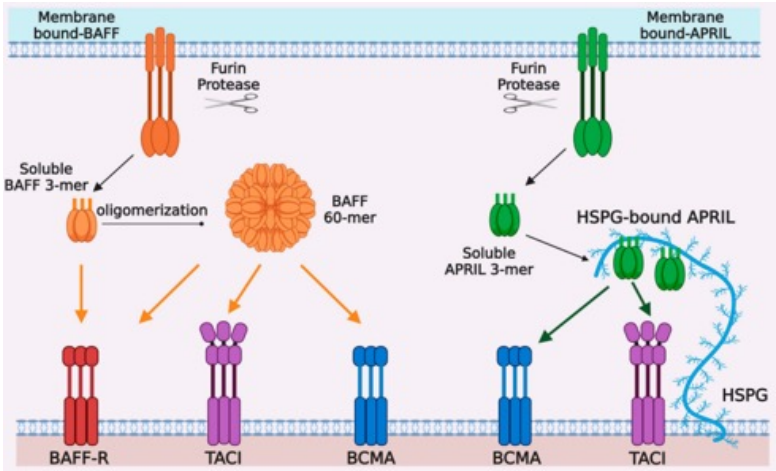

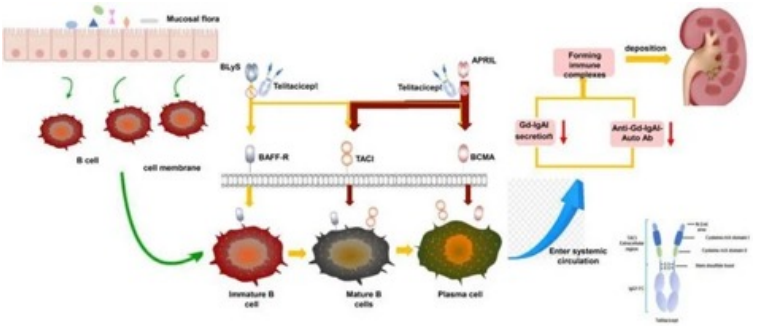

Telitacicept

Telitacicept for IgA Nephropathy — Interim Analysis of a Phase 3 Trial

The pathogenesis of IgA nephropathy is mediated by B-cell activating factor (BAFF) and a proliferation-inducing ligand (APRIL). Telitacicept is a fusion protein that targets and neutralizes both BAFF and APRIL and, as such, might be effective in IgA nephropathy.

We now report a prespecified interim analysis of a phase 3, multicenter, double-blind, randomized, placebo-controlled trial, which enrolled adults with biopsy-proven IgA nephropathy and persistent proteinuria (protein level, ≥1.0 g per day), despite appropriate supportive care. Patients were randomly assigned in a 1:1 ratio to receive subcutaneous once-weekly telitacicept (240 mg) or matching placebo. The primary end point was the geometric mean ratio of the 24-hour urinary protein-to-creatinine ratio at 39 weeks relative to baseline. Safety was also evaluated.

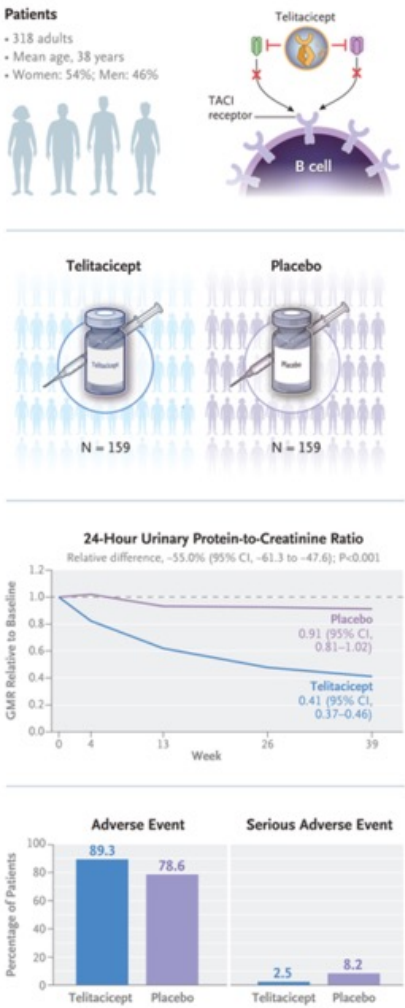

A large body of data suggests that cellular homeostasis and IgA production are critically regulated by cytokines of the tumor necrosis factor superfamily, principally B-cell activating factor (BAFF) and a proliferation-inducing ligand (APRIL). Elevated serum levels of both BAFF and APRIL have been documented in patients with IgA nephropathy and correlate with disease severity, which suggests this signaling axis as a possible therapeutic target. Therefore, interrupting this pathway may constitute a disease-modifying strategy that targets a fundamental step in its pathogenesis. Telitacicept is a recombinant fusion protein composed of the extracellular domain of the human transmembrane activator and CAML interactor (TACI) receptor and the Fc domain of human IgG1. By mimicking the TACI receptor, telitacicept acts as a decoy that can simultaneously bind to and neutralize both BAFF and APRIL, thereby inhibiting B-cell maturation, survival, and immunoglobulin production. On the basis of studies conducted in China, telitacicept has gained regulatory approval and shown a favorable safety profile for three autoimmune conditions: systemic lupus erythematosus, rheumatoid arthritis, and generalized myasthenia gravis. A previously published phase 2 study showed the clinical efficacy of telitacicept in patients with IgA nephropathy and showed a reduction in levels of galactose-deficient IgA1. We now report prespecified results from stage A of a phase 3 trial of telitacicept for IgA nephropathy (TELIGAN), which was designed to evaluate the effect of telitacicept on proteinuria over a period of 39 weeks.

Patients

Adults (≥18 years of age) with biopsy-proven primary IgA nephropathy were eligible. Key inclusion criteria were persistent proteinuria (24-hour urinary protein-to-creatinine ratio [with both protein and creatinine measured in grams] of ≥0.8 or a 24-hour urinary total protein level of ≥1.0 g per day) and an estimated glomerular filtration rate (GFR) of 30 ml per minute per 1.73 m^2 of body-surface area or higher, calculated with the use of the Chronic Kidney Disease Epidemiology Collaboration (CKD-EPI) equation.

End Points

The primary efficacy end point for the stage A analysis was the geometric mean ratio of the 24-hour urinary protein-to-creatinine ratio at week 39 relative to baseline. Secondary efficacy end points at week 39 included the geometric mean ratio of the estimated GFR relative to baseline, the geometric mean ratio of the 24-hour urinary albumin-to-creatinine ratio relative to baseline, a decline in the estimated GFR of 30% or more, and a 24-hour urinary protein-to-creatinine ratio of less than 0.8. Exploratory end points included the geometric mean ratio of the 24-hour urinary total protein level relative to baseline. Pharmacodynamic end points included changes in circulating B-cell counts and serum immunoglobulin levels. Safety end points included the incidence and severity of adverse events, serious adverse events, and changes in laboratory measures and vital signs.

Characteristic	Telitacicept (N=159)	Placebo (N=159)
Age — yr	37.8±9.4	38.6±10.0
Sex — no. (%)		
Male	77 (48.4)	70 (44.0)
Female	82 (51.6)	89 (56.0)
Body-mass index†	25.0±4.4	25.4±4.3
Disease duration — mo	51.8±52.5	47.2±43.3
Interval from biopsy to randomization — mo	52.4±52.5	47.8±43.2
MEST-C scores — no./total no. (%)‡§		
M score		
M0	24/117 (20.5)	27/128 (21.1)
M1	93/117 (79.5)	101/128 (78.9)
E score		
E0	76/117 (65.0)	90/128 (70.3)
E1	41/117 (35.0)	38/128 (29.7)
S score		
S0	29/117 (24.8)	37/128 (28.9)
S1	88/117 (75.2)	91/128 (71.1)
T score		
T0	69/117 (59.0)	81/128 (63.3)
T1 or T2	48/117 (41.0)	47/128 (36.7)
C score		
C0	51/96 (53.1)	57/102 (55.9)
C1 or C2	45/96 (46.9)	45/102 (44.1)
Median 24-hr urinary protein-to-creatinine ratio (range)‡¶	1.23 (0.47–5.86)	1.29 (0.54–6.59)
Estimated glomerular filtration rate		
Mean — ml/min/1.73 m^2	76.53±26.95	74.43±27.20
Distribution — no. (%)		
30 to <45 ml/min/1.73 m^2	19 (11.9)	23 (14.5)
45 to <60 ml/min/1.73 m^2	34 (21.4)	34 (21.4)
≥60 ml/min/1.73 m^2	106 (66.7)	102 (64.2)
Hematuria — no. (%)‡	113 (71.1)	112 (70.4)
Diabetes — no. (%)‡	30 (18.9)	26 (16.4)
Blood pressure — mm Hg		
Systolic	116.6±11.0	117.9±10.8
Diastolic	77.8±8.2	78.3±8.1
Use of SGLT2 inhibitor — no. (%)	56 (35.2)	55 (34.6)
Use of MRA — no. (%)‡	7 (4.4)	9 (5.7)
Use of endothelin A receptor antagonist — no. (%)‡	0	1 (0.6)

Adverse Events.

Event	Telitacicept (N=159)	Placebo (N=159)
	no. of patients (%)	
Adverse event	142 (89.3)	125 (78.6)
Serious adverse event	4 (2.5)	13 (8.2)
Adverse events considered to be related to the trial regimen		
Any adverse event	123 (77.4)	77 (48.4)
Serious adverse event	0	1 (0.6)
Adverse event leading to interruption of the regimen	25 (15.7)	28 (17.6)
Adverse event leading to discontinuation of the regimen	1 (0.6)	2 (1.3)
Adverse event leading to withdrawal from the trial	2 (1.3)	2 (1.3)
Adverse event leading to death	0	0
Adverse events with an incidence of ≥5% in either group		
Upper respiratory tract infection	65 (40.9)	58 (36.5)
Urinary tract infection	13 (8.2)	9 (5.7)
Respiratory tract infection	8 (5.0)	6 (3.8)
Bronchitis	3 (1.9)	10 (6.3)
Cough	12 (7.5)	9 (5.7)
Diarrhea	3 (1.9)	8 (5.0)
Injection-site reaction†	80 (50.3)	22 (13.8)
Mild	71 (44.7)	20 (12.6)
Moderate	14 (8.8)	2 (1.3)
Severe	2 (1.3)	0
Injection-site pruritus	21 (13.2)	3 (1.9)
Injection-site pain	10 (6.3)	9 (5.7)
Pyrexia	6 (3.8)	9 (5.7)
Blood IgM decreased	39 (24.5)	1 (0.6)
Blood IgG decreased	21 (13.2)	0
Weight increased	9 (5.7)	3 (1.9)

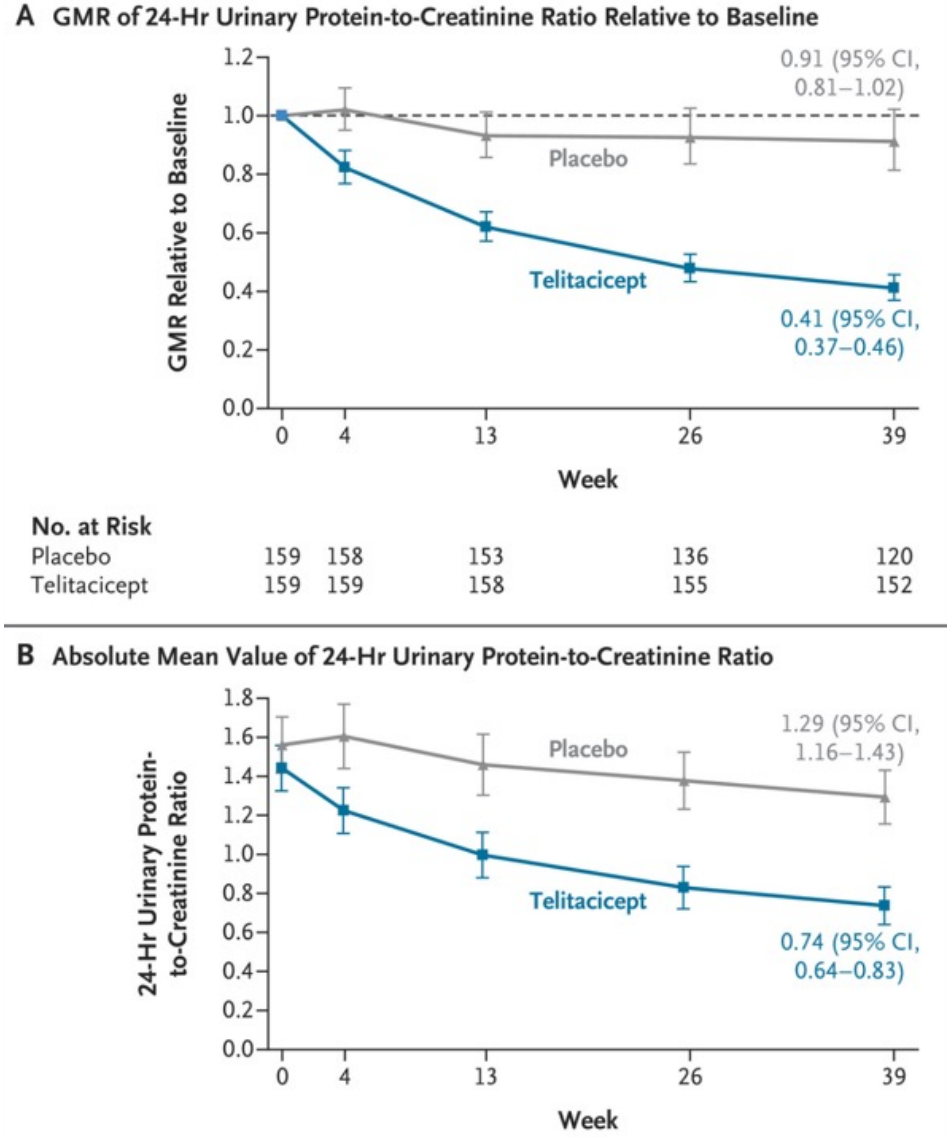

Changes in 24-Hour Urinary Protein-to-Creatinine Ratio over a Period of 39 Weeks.

Panel A shows the geometric mean ratio of 24-hour urinary protein-to-creatinine ratio relative to baseline at weeks 4, 13, 26, and 39; both protein and creatinine were measured in grams. The plotted treatment effects are based on a mixed-effects model for the log-transformed ratio of 24-hour urinary protein-to-creatinine ratio. The number at each visit is the number of patients with nonmissing values, excluding the data after the use of prohibited medications or therapies (including rescue therapy). Panel B shows the absolute mean value of 24-hour urinary protein-to-creatinine ratio over time. I bars indicate 95% confidence intervals. Only the confidence intervals for the geometric mean ratio of the 24-hour urinary protein-to-creatinine ratio relative to baseline at week 39 were adjusted for multiplicity; the other confidence intervals are descriptive and should not be used for hypothesis testing.

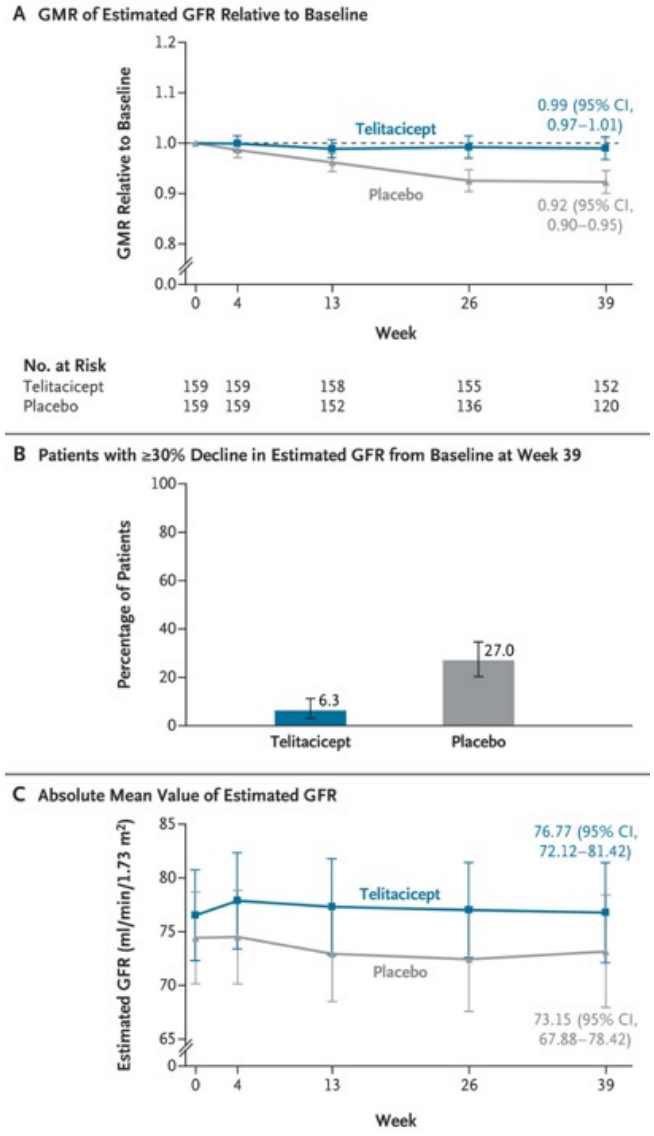

Changes in Estimated Glomerular Filtration Rate (GFR) over a Period of 39 Weeks.

Panel A shows the geometric mean ratio of the estimated GFR relative to baseline at weeks 4, 13, 26 and 39. The plotted treatment effects are based on a mixed-effects model for the log-transformed ratio of the estimated GFR. The number at each visit is the number of patients with nonmissing values, excluding the data after the use of prohibited medications or therapies (including rescue therapy). Panel B shows the percentage of patients with a decline in the estimated GFR of at least 30% from baseline at week 39. Panel C shows the absolute mean value of the estimated GFR over time. I bars indicate 95% confidence intervals, which have not been adjusted for multiplicity and should not be used for hypothesis testing.

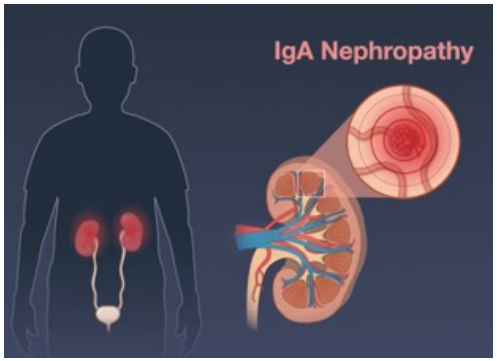
IgA Nephropathy

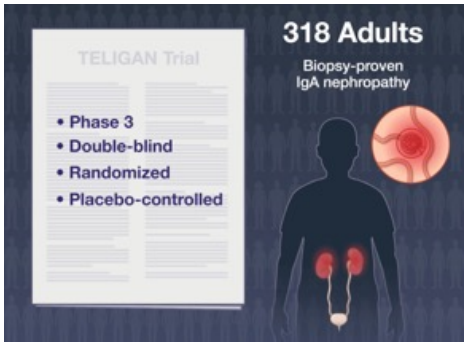
TELIGAN Trial
318 Adults
Biopsy-proven IgA nephropathy
• Phase 3
• Double-blind
• Randomized
• Placebo-controlled

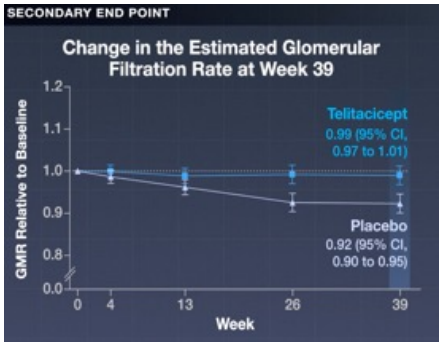
SECONDARY END POINT
Change in the Estimated Glomerular Filtration Rate at Week 39
GMR Relative to Baseline
1.2
1.1
1.0
0.9
0.8
0.0
Telitacicept
0.99 (95% CI, 0.97 to 1.01)
Placebo
0.92 (95% CI, 0.90 to 0.95)
0
4
13
26
39
Week

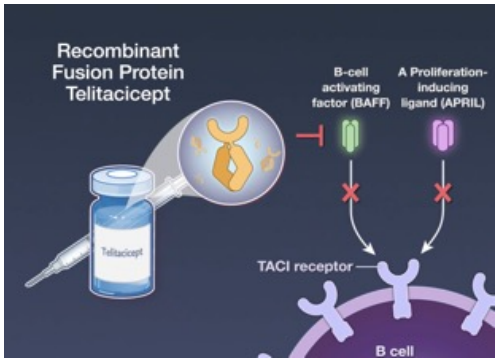
Recombinant Fusion Protein Telitacicept
B-cell activating factor (BAFF)
A Proliferation-inducing ligand (APRIL)
TACI receptor
B cell

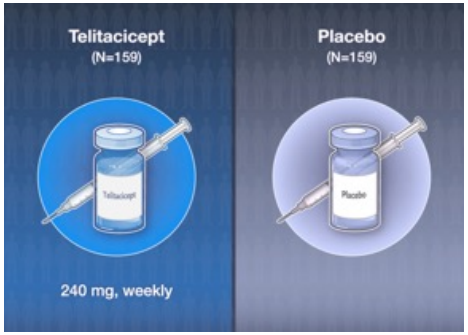
Telitacicept
(N=159)
Placebo
(N=159)
240 mg, weekly

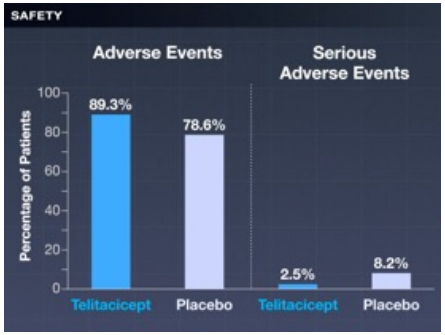
SAFETY
Adverse Events
Serious Adverse Events
Percentage of Patients
100
80
60
40
20
0
89.3%
78.6%
2.5%
8.2%
Telitacicept
Placebo
Telitacicept
Placebo


Clinical efficacy
Phase 2 Trial

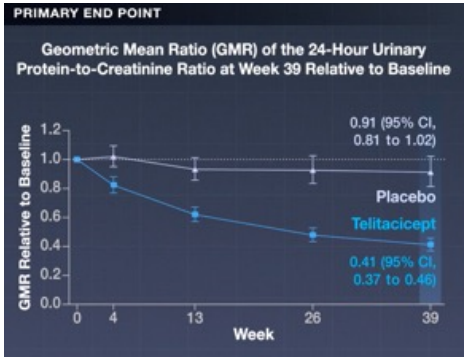
PRIMARY END POINT
Geometric Mean Ratio (GMR) of the 24-Hour Urinary Protein-to-Creatinine Ratio at Week 39 Relative to Baseline
GMR Relative to Baseline
1.2
1.0
0.8
0.6
0.4
0.2
0.0
0.91 (95% CI, 0.81 to 1.02)
Placebo
Telitacicept
0.41 (95% CI, 0.37 to 0.46)
0
4
13
26
39
Week

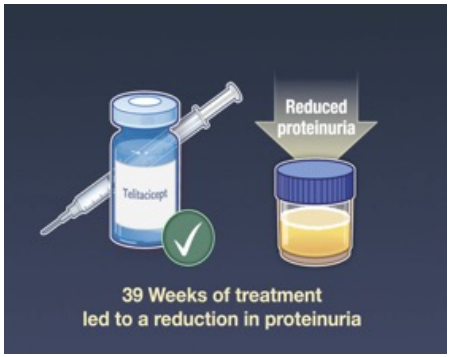
Reduced proteinuria
39 Weeks of treatment
led to a reduction in proteinuria

Inflammatory Myopathies

Summary

Inflammatory myopathies are a heterogeneous group of autoimmune diseases characterized by immune-mediated damage to skeletal muscle. They are classified into five major subtypes: inclusion-body myositis, immune-mediated necrotizing myopathies, antisynthetase syndrome, overlapping myositis, and dermatomyositis, each with distinct clinical features and outcomes. Inclusion-body myositis and immune-mediated necrotizing myopathies primarily affect muscle, with prognosis largely determined by functional impairment, whereas antisynthetase syndrome, overlapping myositis, and dermatomyositis are systemic diseases that can involve the skin, joints, and lungs and may be life-threatening. The majority of inflammatory myopathies are associated with myositis-specific autoantibodies, which inform diagnosis, subtype classification, and prognosis. Advances in understanding the distinct pathomechanisms underlying each subgroup now enable increasingly targeted therapeutic approaches.

Inflammatory Myopathies

- Inflammatory myopathies are a heterogeneous group of autoimmune diseases defined by immune-mediated damage to skeletal muscle tissue.
- Inflammatory myopathies are subdivided into inclusion-body myositis, immune-mediated necrotizing myopathies, antisynthetase syndrome, myositis occurring in the spectrum of connective-tissue diseases (overlapping myositis), and dermatomyositis.
- In inclusion-body myositis and immune-mediated necrotizing myopathies, muscle involvement is predominant and the prognosis is primarily functional.
- Antisynthetase syndrome, overlapping myositis, and dermatomyositis are systemic diseases that can affect the skin, joints, and lungs and can be life-threatening.
- The majority of inflammatory myopathies are associated with a myositis-specific autoantibody, the presence of which determines the diagnosis, subtype, and prognosis.
- Each myositis subgroup is characterized by distinct pathomechanisms that now allow for targeted therapeutic approaches.

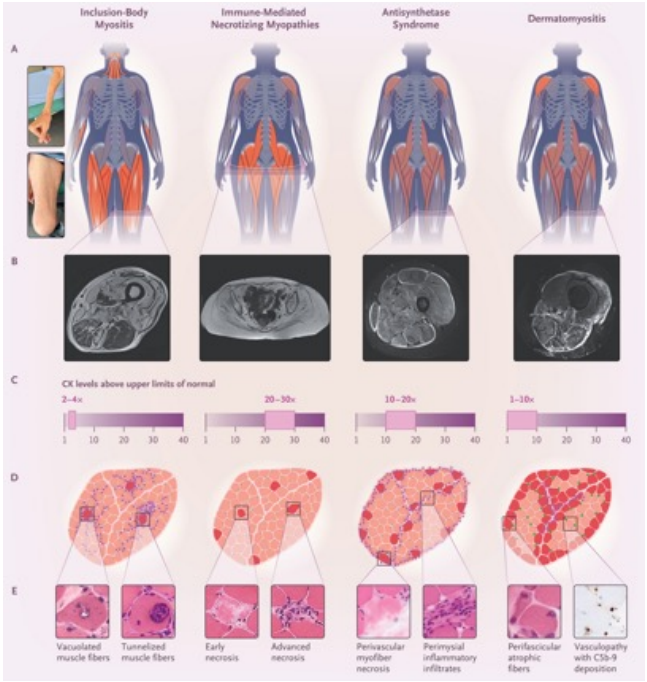

Patterns of Muscle Involvement in the Four Major Types of Idiopathic Inflammatory Myopathies. Shown is a comparative analysis of four idiopathic inflammatory myopathy subtypes. Panel A shows the distribution of muscle weakness (dark red areas indicate severe and frequent involvement) and typical muscle atrophy of finger flexors and quadriceps in inclusion-body myositis. Panel B shows characteristic MRI images (corresponding to either muscle damage or muscle edema). Panel C shows elevations in creatine kinase (CK) levels above the upper limit of normal (pink shading). Panel D is a schematic diagram of the pathological features showing affected muscle fibers (red areas), inflammatory infiltrates (purple dots), and vascular changes when present (green dots); and Panel E shows key microscopic findings (400× magnification). In the depiction of a patient with inclusion-body myositis, key specific features are involvement of the muscles of swallowing, finger flexors, and quadriceps; MRI (axial T1-weighted image of left thigh) showing fatty infiltration of the quadriceps with undulating fascia sign; pathological features, including scattered fiber damage and dense endomysial inflammation within the muscle fascicles; and key findings such as vacuolated or tunnelized muscle fibers, often surrounded by lymphocytes. In the example of a patient with immune-mediated necrotizing myopathy, the proximal muscles (scapular and pelvic girdle, with the pelvis predominant) are primarily affected. MRI (axial T1-weighted image of pelvic girdle) shows complete fatty infiltration of the gluteus muscles in a patient with very severe muscle damage. Pathological testing shows minimal inflammation with random fiber damage and muscle fibers in various stages of necrosis, from early (hyalinized fibers) to advanced (macrophage-mediated clearance). As shown in the illustration of antisynthetase syndrome, the proximal muscles (scapular and pelvic girdle) are primarily affected. MRI (axial T2-weighted short tau inversion recovery relaxation image of left thigh) shows muscle hypersignal corresponding to inflammation as well as the disease activity and fascia hypersignal that are frequently observed in patients with antisynthetase syndrome. Pathological evaluation shows characteristic perifascicular myofiber necrosis with perimysial inflammatory infiltrates and perivascular inflammation. Like immune-mediated necrotizing myopathy and antisynthetase syndrome, dermatomyositis primarily involves proximal muscles (scapular and pelvic girdle, with the scapula predominant). MRI (axial T2-weighted short tau inversion recovery relaxation image of left thigh) shows edema related to the degree of inflammation and disease activity in muscle and subcutaneous tissue. Pathological testing further shows clustered fiber damage at the fascicle periphery but with atrophic fibers, as well as perivascular inflammation with vasculopathy illustrated by endocapillary C5b-9 deposition.

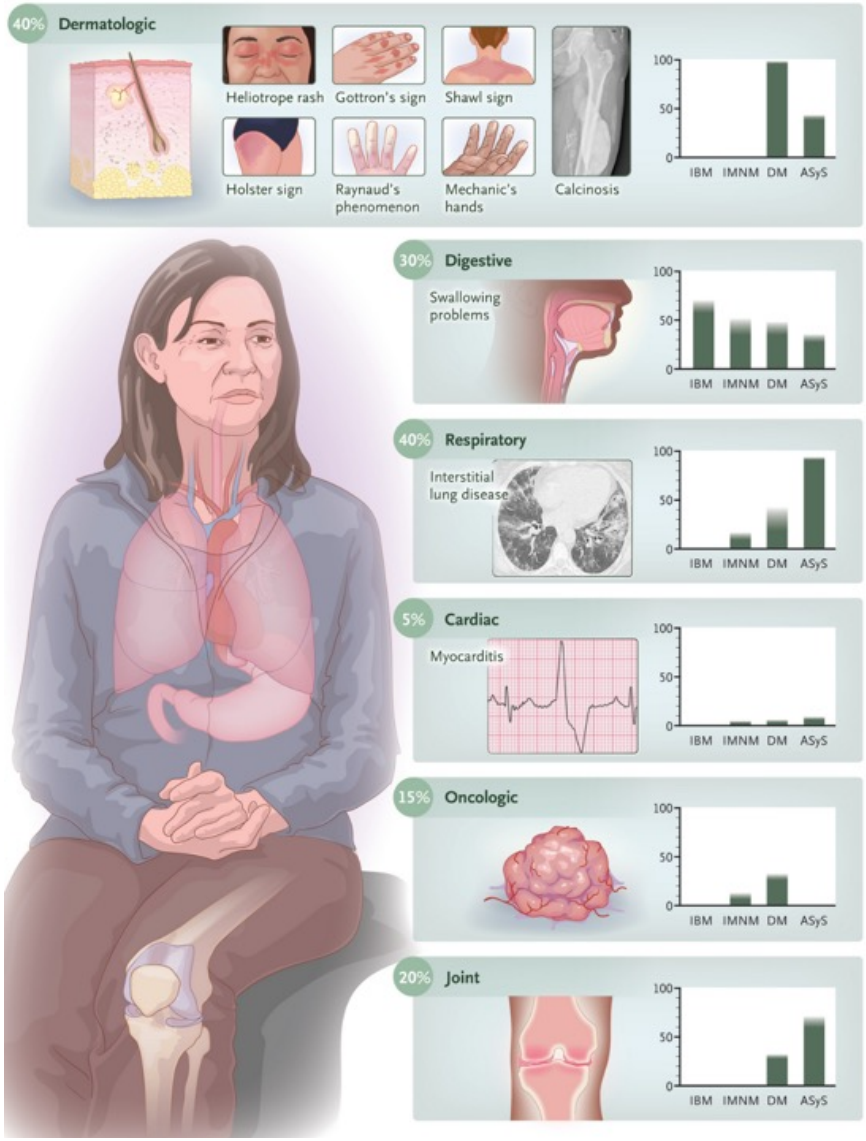

Spectrum of Extramuscular Involvement in the Four Main Groups of Idiopathic Inflammatory Myopathy.

Shown are the most common types of tissue involvement in idiopathic inflammatory myopathy. For each subgroup of myositis, the frequency of tissue involvement is shown on a bar chart. Respiratory involvement (nonspecific interstitial pneumonia or organized pneumonia) and skin lesions (erythematous) are the most common manifestations. The most common dermatological manifestations (erythematous or not) are heliotrope rash (dermatomyositis [DM]), Gottron's papules (DM), shawl sign (DM), holster sign (DM), Raynaud's phenomenon (DM, antisynthetase syndrome [ASyS], and overlap myositis), mechanic's hands (ASyS), and calcinosis (skin damage). Digestive involvement is dominated by dysphagia. The presence of cancer of any type is common. Symptomatic cardiac involvement is rare and may be associated with ventricular dysfunction, arrhythmias, or conduction disorders. IBM denotes inclusion-body myositis, and IMNM immune-mediated necrotizing myopathy.

Myositis-Specific and Myositis-Associated Autoantibody

IIM Subtype and Autoantibody	Immunoassay Available?	Assessment of Immunoassay Quality†	Clinical Features or Prognosis	Cancer Risk[26]
Inclusion-body myositis				
Seronegative				Low
Anti-cN1A	Yes	Awareness of limitations indicated	Worse prognosis than seronegative IBM	Low
Immune-mediated necrotizing myopathy				
Seronegative				High
Anti-HMGCR	Yes	Acceptable	Better muscle function prognosis in patients who have received statins than in those who have not	Intermediate
Anti-SRP	Yes	Acceptable	Severe weakness, frequent mild ILD	Low
Antisynthetase syndrome				
Anti–Jo-1	Yes	Acceptable	Most frequent, classic phenotype (myositis, arthritis, ILD)	Low
Anti–PL-7	Yes	Acceptable	Worse prognosis owing to more severe ILD	Low
Anti–PL-12	Yes	Acceptable	Worse prognosis owing to more severe ILD	Low
Anti-EJ	Yes	Awareness of limitations indicated	Constant ILD	Low
Anti-OJ	Yes	Serious concerns	Frequent ILD, arthritis and fever	High[27]
Anti-KS	Yes	Acceptable	Frequent amyopathy, sicca syndrome	Low
Anti-Zo	Yes	Awareness of limitations indicated	Classic phenotype (myositis, arthritis, ILD)	Low
Anti-Ha	Yes	Awareness of limitations indicated	Predominant muscle involvement, frequent skin lesions, infrequent ILD	Low
Other‡	No	Immunoassays not yet available for routine detection		Low
Dermatomyositis				
Seronegative				High if age >40 yr at onset
Anti–TIF-1γ	Yes	Awareness of limitations indicated	Psoriasis-like, poikiloderma, ovoid palatal patch	High
Anti-NXP2	Yes	Acceptable	Intestinal vasculopathy, skin edema, calcinosis	High
Anti–Mi-2	Yes	Acceptable	High creatine kinase level, photodistributed rash	Intermediate
Anti-MDA5	Yes	Acceptable	Severe ILD, amyopathic, arthritis, cutaneous ulcers	Intermediate
Anti-SAE	Yes	Awareness of limitations indicated	OP ILD pattern, "angel wing" rash on back	Intermediate
Overlap myositis				
Seronegative				Low
Anti-PM/Scl	Yes	Acceptable	NSIP or OP ILD pattern, skin thickening, sclerodactyly	Low
Anti-Ku	Yes	Acceptable	Arthralgia, ILD, glomerulonephritis, sclerodactyly	Low
Anti-RNP	Yes	Acceptable	ILD, arthralgia, sclerodactyly	Low

Conclusions

The management of idiopathic inflammatory myopathies has evolved, reflecting advancements in clinical immunopathological testing. The refinement of the diagnosis and classification of these myopathies through the identification of myositis-specific autoantibodies has helped clarify the challenges of each patient subgroup, as well as the underlying pathologic mechanisms. These advancements have led to substantial changes in the therapeutic landscape of idiopathic inflammatory myopathies, supported by major breakthroughs in hemato-oncology therapies. Key innovations include interferon pathway blockers for dermatomyositis, antibody-depletion therapy that has shown promising results in severe antisynthetase syndrome and immune-mediated necrotizing myopathy, and new drugs that are being tested for the treatment of inclusion-body myositis. The results of ongoing clinical trials will provide further insights into the effectiveness of these treatments.

Cerebral Syphilitic Gumma

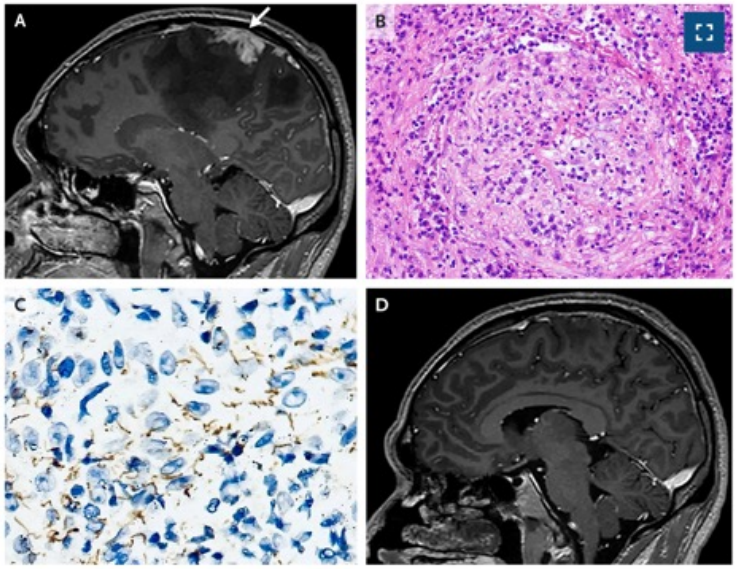

A 50-year-old man presented to the emergency department with a 1-month history of headache and worsening weakness of the left arm and leg. Physical examination was notable for the patient's inability to raise his left arm against gravity or lift his left leg against resistance. Magnetic resonance imaging of the brain after the administration of contrast material showed an enhancing lesion with extensive surrounding edema adjacent to the cerebral falx in the right frontoparietal lobe (Panel A, arrow; T1-weighted, sagittal view). A serum *Treponema pallidum* particle agglutination (TPPA) assay was positive, and the titer was 1:16 on a toluidine red unheated serum test (TRUST). Testing for human immunodeficiency virus was negative. An analysis of the cerebrospinal fluid showed a lymphocytic pleocytosis with a positive TPPA result. Histopathological analysis of a biopsy sample of the brain lesion showed abundant plasma-cell infiltration with arteriolitis (Panel B) and spirochetes on immunohistochemical staining (Panel C). A diagnosis of cerebral syphilitic gumma — a rare manifestation of long-standing syphilis — was made. Treatment with a 2-week course of intravenous penicillin was given. Seven weeks after the completion of treatment, the weakness of the left side had abated, the brain lesion had substantially decreased in size (Panel D), and the TRUST titer had decreased to 1:2.

Ein **syphilitisches Gumma** (Plural: *Gummen* oder *Gummata*) ist eine charakteristische, entzündliche Gewebeveränderung (Granulom), die im **Tertiärstadium (Spätstadium) einer Infektion mit *Treponema pallidum*** auftritt. Durch den breiten Einsatz von Antibiotika sind diese Läsionen heute in Industrieländern sehr selten geworden.

Haupteigenschaften und Gewebelehre

•**Konsistenz:** Die Knoten fühlen sich prall-elastisch und gummiartig an.

•**Gewebezerfall:** Im Zentrum der Läsion befindet sich eine Zone abgestorbenen Gewebes (Koagulationsnekrose).

•**Mikroskopischer Befund:** Das Zentrum wird von einer Wand aus Entzündungszellen umschlossen. Dazu gehören Lymphozyten, Plasmazellen, Makrophagen und mehrkernige Riesenzellen.

•**Gefäßveränderungen:** Typisch ist eine Entzündung der kleinen Arterien (Endarteritis obliterans), die bis zum Gefäßverschluss führen kann.

•**Erregernachweis:** Im Gegensatz zu frühen Krankheitsstadien sind im Gumma fast keine intakten Bakterien mehr nachweisbar. Es handelt sich primär um eine immunologische Überreaktion des Körpers.

Inhalation Injury from House Fire Smoke

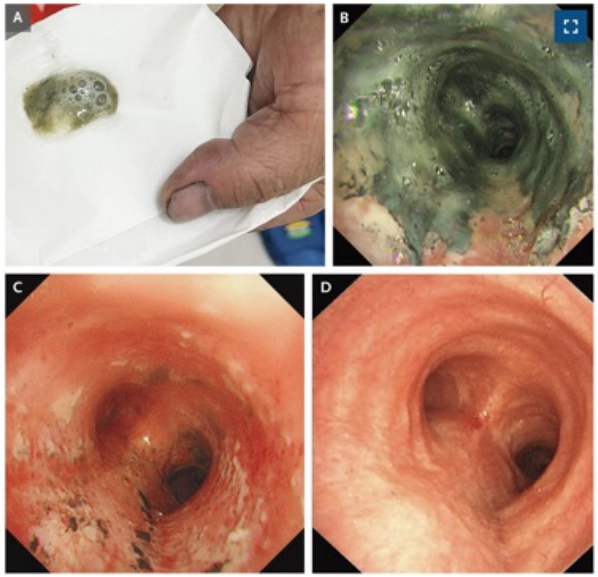

A 55-year-old man presented to the emergency department with cough, chest pain, and worsening dyspnea after being trapped in a burning house for 10 minutes. His heart rate was 120 beats per minute, his respiratory rate 30 breaths per minute, and his oxygen saturation 92% while he was receiving supplemental oxygen through a nasal cannula at a rate of 4 liters per minute. On physical examination, the patient was covered in soot but had no burn injuries. His sputum was carbonaceous (Panel A). Diffuse expiratory wheezing was present on auscultation. Carboxyhemoglobin testing was not available. Computed tomography of the chest revealed segmental mucus plugging. Owing to serious concern about inhalation injury, flexible bronchoscopy was performed to confirm the diagnosis and determine the severity of the injury. After copious secretions were removed from the airway with suction, carbonaceous deposits that extended from the subglottic region to the distal segmental airways were seen (Panel B and video). After therapeutic bronchoalveolar lavage was performed, erythema and edema of the airway mucosa were noted (Panel C). A diagnosis of severe inhalation injury from smoke was made. Treatment with inhaled bronchodilators and supplemental oxygen was administered. The patient was discharged 1 week later. At a follow-up visit 4 weeks after discharge, repeat bronchoscopy showed no abnormalities (Panel D).

VIDEO

Carbonaceous Deposits on Bronchoscopy 0m 19s

Central Retinal-Vein Occlusion

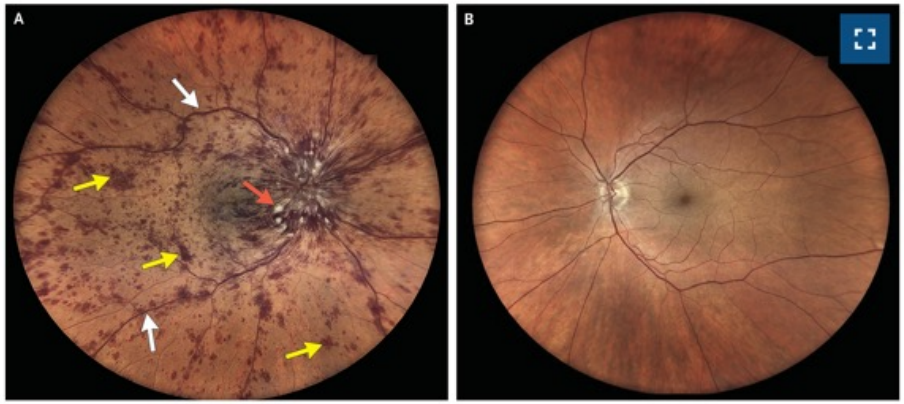

A 65-year-old woman with diabetes, hypertension, and dyslipidemia presented to the ophthalmology clinic with a 14-hour history of painless, progressively worsening, blurry vision in the right eye. Physical examination was notable for a visual acuity of 20/400 in the right eye, with the patient unable to see fingers in the peripheral visual fields. There was also a relative afferent pupillary defect in the right eye. Examination of the left eye was normal. Funduscopy of the right eye showed retinal hemorrhages (Panel A, yellow arrows) and marked venous dilatation (Panel A, white arrows) in all four quadrants — findings known as a "blood and thunder" appearance. Cotton-wool spots (Panel A, red arrow) and optic-disk edema were also seen. Funduscopy of the left eye was normal (Panel B). A diagnosis of central retinal-vein occlusion was made. Central retinal-vein occlusion occurs when an acute thrombus obstructs venous outflow from a proximal retinal vein, resulting in sudden-onset, painless vision loss. Fluorescein angiography confirmed ischemic injury, and optical coherence tomography identified severe macular edema. Improved control of cardiovascular disease risk factors was initiated to prevent the occurrence of central retinal-vein occlusion in the contralateral eye. Treatment with anti–vascular endothelial growth factor injections was given. At the 3-month follow-up visit, the patient's visual acuity in the right eye was 20/80, with persistent blind spots from residual macular scarring.

Case 14-2026: A 50-Year-Old Woman with Vaginal Bleeding and Anemia

Edema

Muscle Weakness

Hair loss

Heavy Vaginal bleeding

Discoloration („vitiligo“)

The patient had been in her usual state of health, with leg edema that was attributed to chronic venous insufficiency, until 6 months before the current presentation, when increased swelling and new weakness developed in the legs. Before the onset of these symptoms, she had been physically active. She first noted that her legs felt more tired and sore than usual after normal physical activity, and the symptoms were accompanied by increased swelling and a feeling of heaviness in the legs. Over the course of the next 2 months, the leg weakness progressed to the point that she was unable to rise from a seated position or climb stairs. The patient also noted that her arms felt heavy, and she had difficulty reaching and holding them above her head. During this time, she had intermittent fever that resolved with the use of acetaminophen.

Four months before the current presentation, hair loss developed. What started as patchy hair loss coalesced into larger areas, which prompted the patient to shave her head. When the hair grew back, it was thin and patchy, and she began shaving her head regularly and wearing hats. No scalp pruritus was present, but the patient noted discoloration of the scalp.

The blood levels of thyrotropin, electrolytes, and glucose were normal, as were results of tests of kidney function. The hemoglobin level was 4.3 g per deciliter (reference range, 12.0 to 16.0), which was a decrease from the baseline level of 8.1 g per deciliter recorded 2 years earlier. The white-cell count was 3370 per microliter (reference range, 4000 to 11,000), the platelet count 123,000 per microliter (reference range 150,000 to 450,000), and the erythrocyte sedimentation rate (ESR) 73 mm per hour (reference range, 0 to 29); other laboratory test results are shown. The patient was instructed to present to a local emergency department for evaluation and treatment of anemia.

Transthoracic echocardiography, which was performed to evaluate for a cardiac cause of leg edema, showed concentric left ventricular hypertrophy with a normal left ventricular ejection fraction, a mildly dilated right ventricle with mild right ventricular hypertrophy, mild-to-moderate tricuspid regurgitation, and an estimated right ventricular systolic pressure of 29 mm Hg; the main pulmonary artery measured 3.1 cm in diameter. A diagnosis of high-output heart failure leading to pulmonary hypertension was considered. Treatment with furosemide was started, and the leg edema decreased. On hospital day 6, the patient was discharged with plans for follow-up in the cardiology clinic.

Variable	Reference Range, Adults, This Hospital†	1 Mo before Current Presentation	2 Wk before Current Presentation	On Current Presentation
Hemoglobin (g/dl)	12.0–16.0	4.3	9.1	7.2
Hematocrit (%)	36.0–46.0	16.3	31.7	22.2
Mean corpuscular volume (fl)	80.0–100.0	66.8	76.6	78.2
White-cell count (per μl)	4000–11,000	3370	3100	5690
Differential count (per μl)				
Neutrophils	1920–7600	—	—	4430
Lymphocytes	720–4100	—	—	600
Monocytes	160–1100	—	—	600
Eosinophils	0–500	—	—	0
Basophils	0–150	—	—	0
Platelet count (per μl)	150,000–450,000	123,000	52,000	39,000
C-reactive protein (mg/liter)	<8.0	—	—	9.9
Erythrocyte sedimentation rate (mm/hr)	0–29	73	—	88
Aspartate aminotransferase (U/liter)	9–32	49	74	111
Alanine aminotransferase (U/liter)	7–33	31	52	64
Alkaline phosphatase (U/liter)	30–100	48	87	78
Total bilirubin (mg/dl)	0.0–1.0	0.4	1.4	2.5
Direct bilirubin (mg/dl)	0.0–0.3	—	—	0.4
Albumin (g/dl)	3.3–5.0	3.0	3.0	3.2
Total protein (g/dl)	6.0–8.3	8.6	9.1	9.2
Iron (μg/dl)	30–160	17	—	—
Transferrin saturation (%)	14–50	5	—	—
Iron-binding capacity (μg/dl)	230–404	358	—	—
Ferritin (μg/liter)	10–200	10	—	350
Creatine kinase (U/liter)	40–150	—	—	268
Lactate dehydrogenase (U/liter)	110–210	—	—	611
Haptoglobin (mg/dl)	30–200	—	—	<10

Anemia, thrombocytopenia, continued bleeding
Iron losses, possible immune hemolysis

On the day of the current presentation, the patient was evaluated in the primary care clinic of this hospital. She reported ongoing heavy vaginal bleeding with multiple clots, fatigue, and dyspnea on exertion. There was no rash, headache, vision changes, or joint pain. She was brought to the emergency department of this hospital for evaluation and treatment.

On examination, the temporal temperature was 38.1°C, the blood pressure 136/69 mm Hg, the heart rate 98 beats per minute, the respiratory rate 20 breaths per minute, and the oxygen saturation 100% while the patient was breathing ambient air. The body-mass index (the weight in kilograms divided by the square of the height in meters) was 24.7. She had diffuse hair thinning with areas of hypopigmentation and hyperpigmentation involving the entire scalp and bowls of the ears. Cervical lymphadenopathy was present. She had no tenderness on palpation of the abdomen, but splenomegaly was present. The external genitalia were normal. Multiple clots were present in the vagina, and the cervix was deviated posteriorly and to the left. The uterus was mobile on bimanual examination, with an estimated size equivalent to that of a uterus at 10 weeks' gestation. She had no edema in the legs. Strength was 3/5 on shoulder abduction, elbow flexion, and hip flexion and was otherwise 5/5. Atrophy of the biceps, triceps, and deltoids was noted.

Vitiligo, lymphadenopathy, muscle atrophy, thrombocytopenia, dyspnea

The patient's medical history included hypertension, migraines, and triphasic Raynaud's phenomenon that had developed 3 years before the current presentation. In addition, she had a history of alcohol use disorder but reported having stopped alcohol consumption 2 years before the current presentation. Medications included ferrous gluconate, furosemide, and polyethylene glycol as needed for constipation. She had no known adverse reactions to medications and no family history of heritable bleeding disorders. The patient worked in sales, and she lived alone in a suburb of Boston. She had smoked approximately five cigarettes per day for the past 20 years and smoked marijuana on most days.

A chest radiograph showed mild enlargement of the cardiac silhouette, diffuse interstitial opacities, a patchy airspace opacity at the base of the right lung, thickening of the right paratracheal stripe, and increased density in the left mediastinum. Computed tomography (CT) of the chest and of the abdomen and pelvis, performed after the administration of intravenous contrast material, showed mild bilateral supraclavicular lymphadenopathy and mild-to-moderate bilateral intrathoracic lymphadenopathy; the main pulmonary artery was 3.6 cm in diameter. Splenomegaly was present, with the spleen measuring 18.6 cm in the craniocaudal dimension (reference value, ≤13). She had small-volume ascites and borderline enlarged, multistation abdominopelvic lymphadenopathy.

Vaginal bleeding continued. The patient passed large clots, and the bleeding required multiple pad changes per hour. After transfusion, the hemoglobin level was 7.0 g per deciliter; two additional units of packed red cells were transfused.

The hemoglobin level was 7.2 g per deciliter, and the platelet count was 39,000 per microliter; other laboratory test results are shown. Results of coagulation tests were normal. A peripheral-blood smear showed marked anisopoikilocytosis with numerous hypochromic forms but no schistocytes, spherocytes, or red-cell agglutination. Urinalysis showed 3+ blood (reference value, negative) and 2+ protein (reference value, negative); examination of the urine sediment showed 10 to 20 red cells per high-power field (reference range, 0 to 2). A direct antiglobulin test was negative.
Two units of packed red cells were transfused. Four hours after completion of the second transfusion, the temporal temperature increased to 39.1°C. A sample of blood was obtained for culture, and imaging studies were obtained.

Heavy proteinuria and erythrocyturia

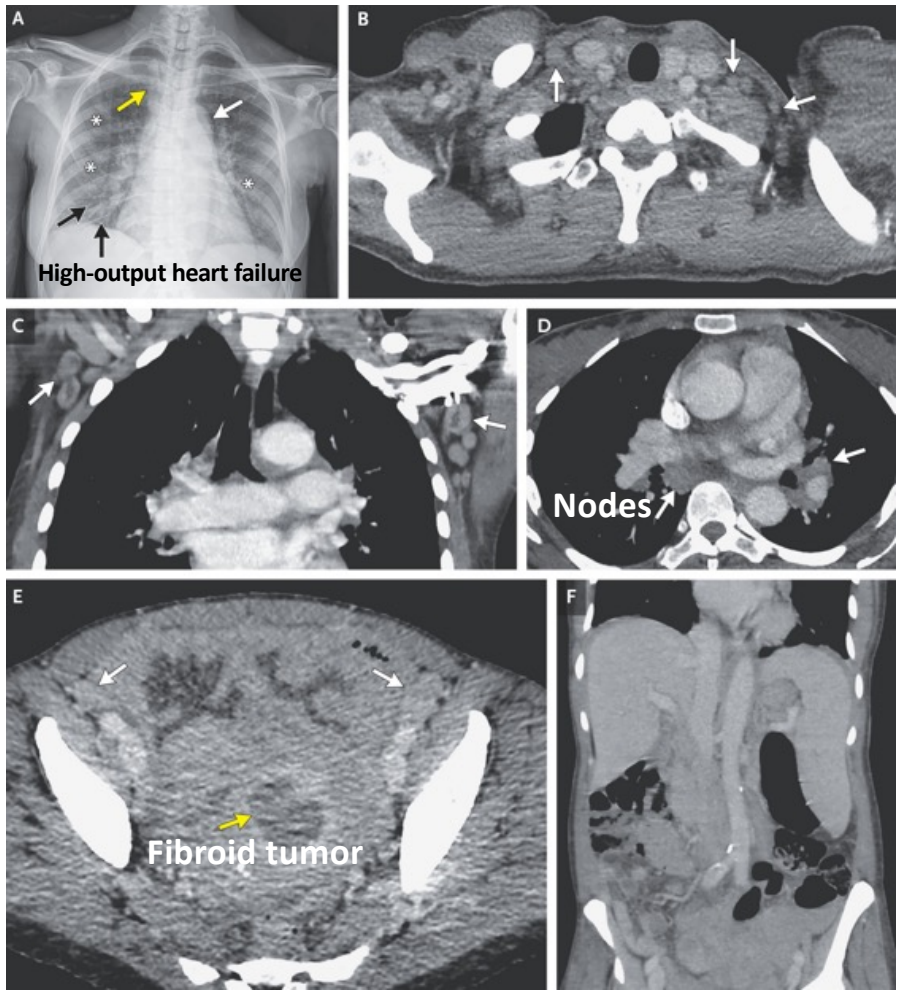

Differential Diagnosis

This 50-year-old woman presented with acute and life-threatening vaginal bleeding for which she received emergency supportive care. However, determining the correct diagnosis to explain her presentation requires consideration of her progressive signs and symptoms over the preceding weeks, months, and years. In developing a differential diagnosis, I will begin by grouping her signs and symptoms into three phases of illness: immune initiation, immune activation, and immune culmination.

Immune Initiation

The first phase of this patient's illness started with the development of Raynaud's phenomenon 3 years before the current presentation, followed by irregular vaginal bleeding associated with uterine fibroids and systemic symptoms that include proximal muscle weakness, leg edema, fever, alopecia, dyspnea on exertion, and fatigue.

Immune Activation

The second phase of this patient's illness is characterized by signs that point to more substantial activation of the immune system — leukopenia, thrombocytopenia, an elevated ESR, an elevated globulin gap, and cardiac ultrasound findings from another hospital. I suspect that the lymphadenopathy, splenomegaly, and proteinuria were most likely also present during this phase.

Immune Culmination

The third phase of this patient's illness is marked by an emergency presentation to this hospital with fibroid-related hemorrhage requiring aggressive transfusion support. I suspect that this patient's bleeding is most likely a consequence of profound thrombocytopenia.

Explaining Escalating Clinical Acuity

One loose end in considering a diagnosis of SLE is the need to explain why this patient's clinical status worsened so quickly and profoundly. Could SLE have been provoked by the recent administration of intravenous iron or packed red cells at the other hospital? Alternatively, could SLE have been an immune risk factor for the development of another hematologic process, such as lymphoma or multicentric Castleman disease? During the admission to this hospital, she had a possible febrile transfusion reaction. This event reinforces my theory that she has an autoimmune disease that could react to red-cell transfusion, which supports the explanatory model of a provoking factor that shifted SLE from the "immune activation" to the "immune culmination" phase of illness. However, it is possible that autoimmune disease was a risk factor for the development of cancer, or that cancer explains her entire course of illness.

I suspect that this patient has SLE. Therefore, my next diagnostic step would be to rapidly and noninvasively evaluate for this disease with serologic testing for autoantibodies and to concurrently assess for a hematologic cancer with the use of flow cytometry. If these tests do not provide enough diagnostic confidence to begin treatment, I would plan to administer packed red cells and platelets and move forward with prompt tissue sampling.

Initial Diagnostic Testing

An immunofluorescence assay performed on Hep-2 (human epithelial) cells showed antinuclear antibodies (ANA) with a homogeneous pattern (titer, 1:640) and ANA with a speckled cytoplasmic pattern (titer, 1:80). Specific antibody testing was positive for anti-Smith antibodies, anti-ribonucleoprotein (anti-RNP) antibodies, anti–cyclic citrullinated protein, and rheumatoid factor and was equivocal for antibodies against Sjögren's syndrome–related antigen A (anti-Ro antibodies). Antibodies against Sjögren's syndrome–related antigen B (anti-La antibodies) and anti–double-stranded DNA antibodies were not detected, and an autoimmune inflammatory myopathy IgG panel was negative. A skin punch-biopsy specimen, which was obtained from the left postauricular area of the scalp, showed marked alopecia with miniaturization of the few remaining hair follicles, perifollicular and epidermal interface dermatitis with vacuolar changes and pigment incontinence, and markedly increased deposition of dermal mucin. The histologic findings of interface dermatitis combined with dermal mucin deposition help to establish the diagnosis of a systemic autoimmune rheumatic disease. The positive serologic tests taken together with the skin-biopsy findings support the diagnosis of SLE.

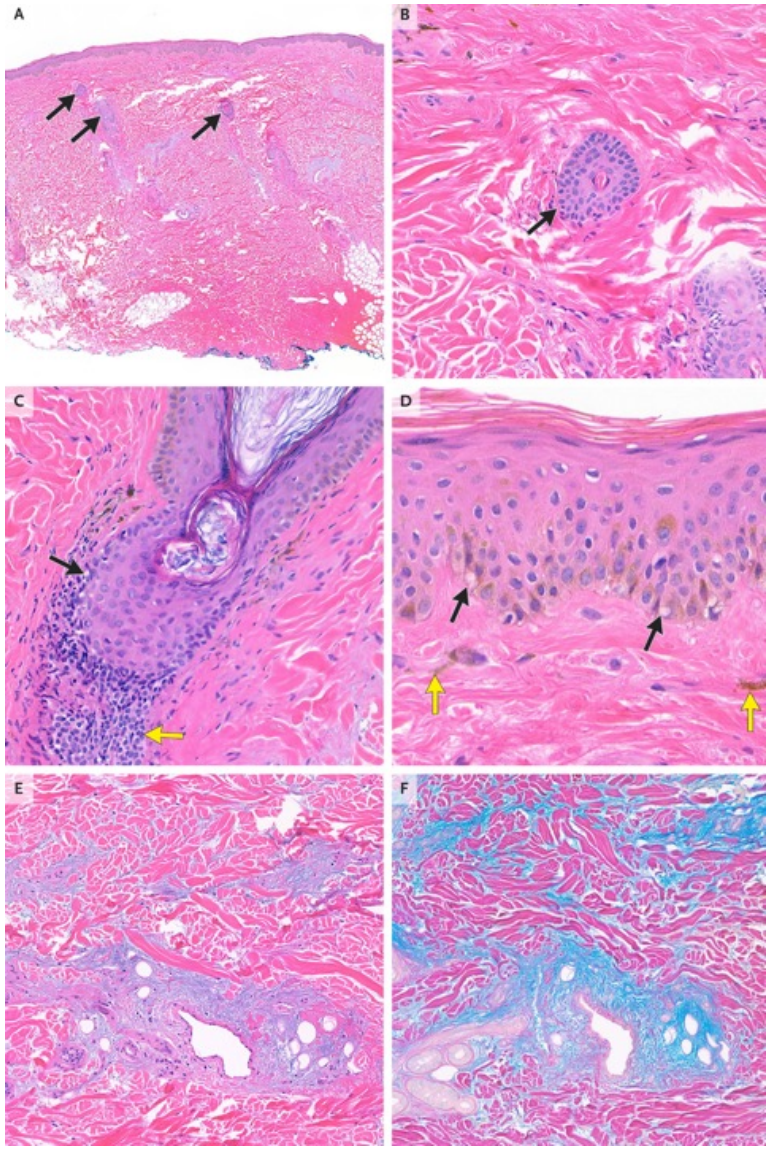

Biopsy Specimen of the Left Postauricular Scalp.

Hematoxylin and eosin staining of a skin punch-biopsy specimen obtained from the left postauricular scalp shows alopecia (Panel A), along with miniaturization of the hair follicles (Panel B). The few remaining hair follicles are markedly reduced in size (Panels A and B, arrows). Perifollicular interface dermatitis (Panel C) is present with a lymphocytic inflammatory infiltrate (yellow arrow) and vacuolar changes of the follicular epithelium (black arrow). Epidermal interface dermatitis (Panel D) is present with vacuolar changes (black arrows) and dermal pigment incontinence (yellow arrows) with sparse inflammation. Markedly increased deposition of dermal mucin is present, as evidenced by the grayish-blue coloration pooling around vessels and interspersed between dermal collagen bundles (Panel E). Colloidal iron staining (Panel F) confirms the increased dermal mucin deposition (in blue).

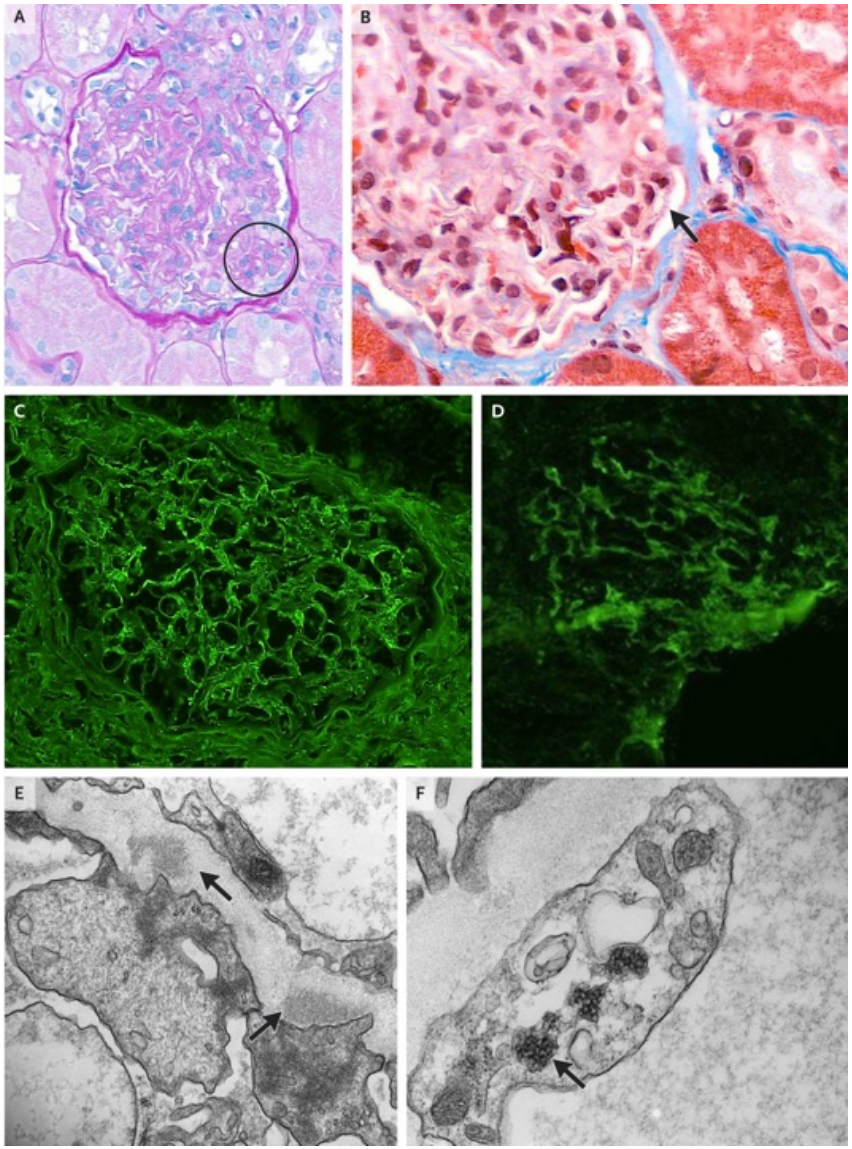

Biopsy Specimen of the Kidney.

Periodic acid–Schiff staining (Panel A) shows mild endocapillary proliferation, identified in 3 glomeruli (18%) (circle). Trichrome staining (Panel B) shows membranous glomerular deposits (arrow). Immunofluorescence staining shows focal and segmental, predominantly membranous deposits in the glomerular basement membrane, which are positive for IgG (Panel C) and C1q (Panel D), as well as C3, IgA, IgM, and kappa and lambda light chains (not shown). Images from electron microscopy (Panels E and F) show subepithelial deposits (Panel E, arrows) and mesangial deposits (not shown), as well as numerous tubuloreticular structures (Panel F, arrow), which are associated with systemic interferon activity and are commonly seen in patients with lupus nephritis.

Even before the results of the kidney biopsy became available, treatment with hydroxychloroquine was initiated for SLE on the basis of its benefits in reducing flares, limiting organ damage, and improving survival. In patients with idiopathic inflammatory myopathy, treatment with glucocorticoids would usually be considered. However, because of ongoing evaluation of multistation lymphadenopathy and splenomegaly, the patient instead received intravenous immune globulin, after which muscle strength quickly improved to 4+/5 in all proximal muscle groups.

A lymph-node biopsy specimen showed granulomatous changes without evidence of cancer. Treatment for lupus nephritis was initiated with a triple therapy approach, which consisted of glucocorticoids, mycophenolate mofetil, and plans for outpatient belimumab (anti-BLyS) initiation. Treatment with trimethoprim–sulfamethoxazole was started for prophylaxis against *Pneumocystis jirovecii* pneumonia.

Belimumab was added to the patient's treatment regimen 2 months after hospital discharge. She has maintained close follow-up, and her creatine kinase levels have normalized. The creatinine levels have remained normal, and proteinuria has resolved. She has had complete normalization of proximal muscle strength, resolution of alopecia, and an increase in energy.

Final Diagnosis

Overlap syndrome of systemic lupus erythematosus and idiopathic inflammatory myopathy.

An **ischemic stroke** is a life-threatening medical emergency that occurs when a blood clot or fatty plaque **blocks blood flow to the brain**, depriving brain tissue of vital oxygen and nutrients. It is the most common type of stroke, accounting for roughly **85% to 87% of all cases** globally. Within minutes of a blockage, brain cells begin to die, making immediate emergency medical care critical to minimize permanent disability or death.

Recognize the Signs: Think F.A.S.T.
Stroke symptoms always happen suddenly. Use the clinical **F.A.S.T.** acronym to quickly check for symptoms:

•**F - Face Drooping**: One side of the face sags or feels numb, resulting in an uneven smile.

•**A - Arm Weakness**: One arm feels weak or numb; if both arms are raised, one drifts downward.

•**S - Speech Difficulty**: Speech is slurred, garbled, or difficult to understand.

•**T - Time to Call Emergency Services**: Call emergency services immediately if you notice *any* of these signs, even if they temporarily disappear.

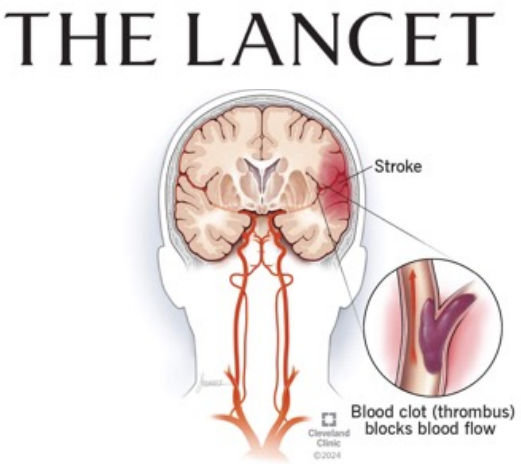

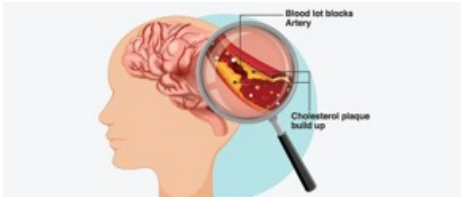

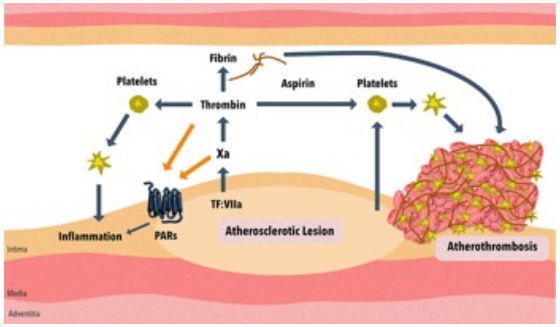

Die **Duale Plättchenhemmung**, oft als DAPT (Dual Antiplatelet Therapy) bezeichnet, kombiniert Aspirin (ASS) mit einem sogenannten P2Y12-Hemmer (z. B. Clopidogrel, Ticagrelor). Diese Kombination verhindert, dass Blutplättchen verklumpen, und wird vor allem nach Herzinfarkten, Schlaganfällen oder dem Einsetzen von Herz-Stents eingesetzt.

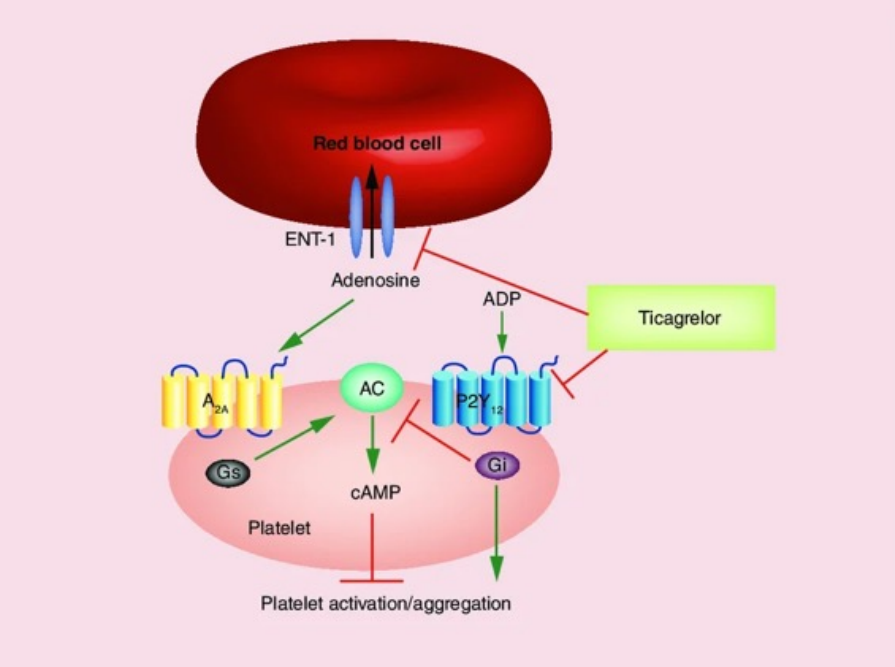

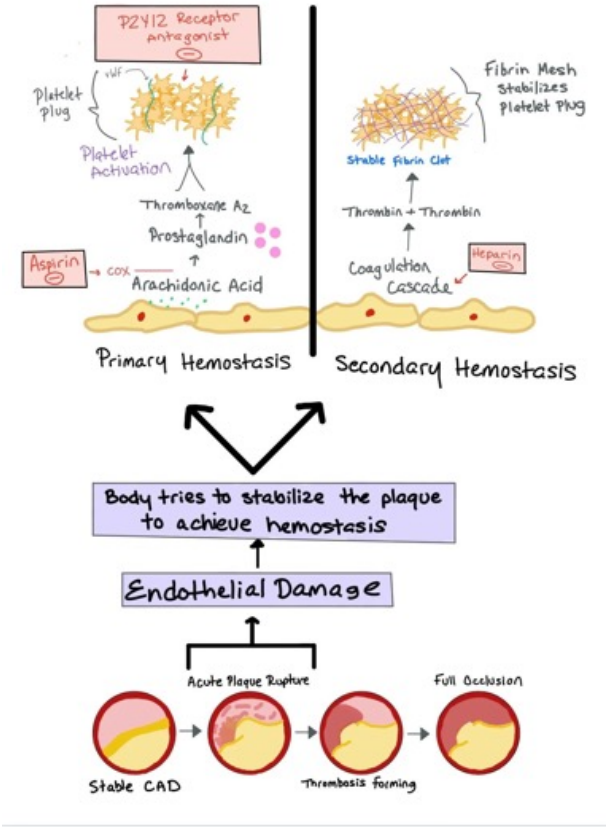

Ticagrelor with aspirin dual antiplatelet therapy combined with intravenous thrombolysis in patients with ischaemic stroke in China (TAPIS): a multicentre, double-blind, randomised controlled trial

Summary

Background Evidence supporting the early addition of antiplatelet therapy to intravenous thrombolysis in patients with acute ischaemic stroke remains inconclusive. We aimed to investigate the efficacy and safety of early oral dual antiplatelet therapy (DAPT), started within 6 h of onset, as an adjunct to intravenous thrombolysis.

Methods TAPIS was a randomised, double-blind, placebo-controlled trial done in 60 hospitals across China. We enrolled patients treated with intravenous thrombolysis for ischaemic stroke, with a National Institutes of Health Stroke Scale score of 4–10. We randomly assigned (1:1) patients to receive oral aspirin plus ticagrelor (DAPT group) or corresponding placebo within 6 h of stroke onset, either before, during, or after receiving thrombolysis. Ticagrelor or placebo was continued for days 2–7 in each group, with open-label aspirin administered for days 2–90. Patients, clinicians, and investigators were masked to the group assignment. The primary efficacy outcome was an excellent functional outcome (modified Rankin Scale score 0–1) at 90 days. The primary safety outcome was symptomatic intracranial haemorrhage within 36 h. This trial was registered with ClinicalTrials.gov (NCT06316570) and is completed.

Findings Between April 3, 2024, and Sept 30, 2025, we randomly assigned 1382 patients to the early DAPT (n=690 [49·9%]) or placebo (n=692 [50·1%]) groups. The median age was 65·6 years (IQR 58·3–72·0), 991 (71·7%) were men, and 391 (28·3%) were women. At 90 days, 474 (68·7%) patients in the early DAPT group and 429 (62·0%) in the placebo group achieved excellent functional outcomes (risk ratio 1·11 [95% CI 1·03–1·20; p=0·0089). Symptomatic intracranial haemorrhage within 36 h occurred in six (0·9%) patients in the early DAPT group versus five (0·7%) in the control group (risk ratio 1·20 [95% CI 0·37–3·93; p=0.76).

Interpretation Among patients treated with intravenous thrombolysis for moderate ischaemic stroke, initiation of oral DAPT within 6 h of onset improved the likelihood of excellent functional outcomes at 90 days. Although no significant between-group difference in symptomatic intracranial haemorrhage was detected, wide CIs precluded exclusion of a small increased risk.

Funding National Natural Science Foundation of China, Capital's Funds for Health Improvement and Research, Noncommunicable Chronic Diseases-National Science and Technology Major Project, Beijing Municipal Science & Technology Commission, and the New Cornerstone Science Foundation.

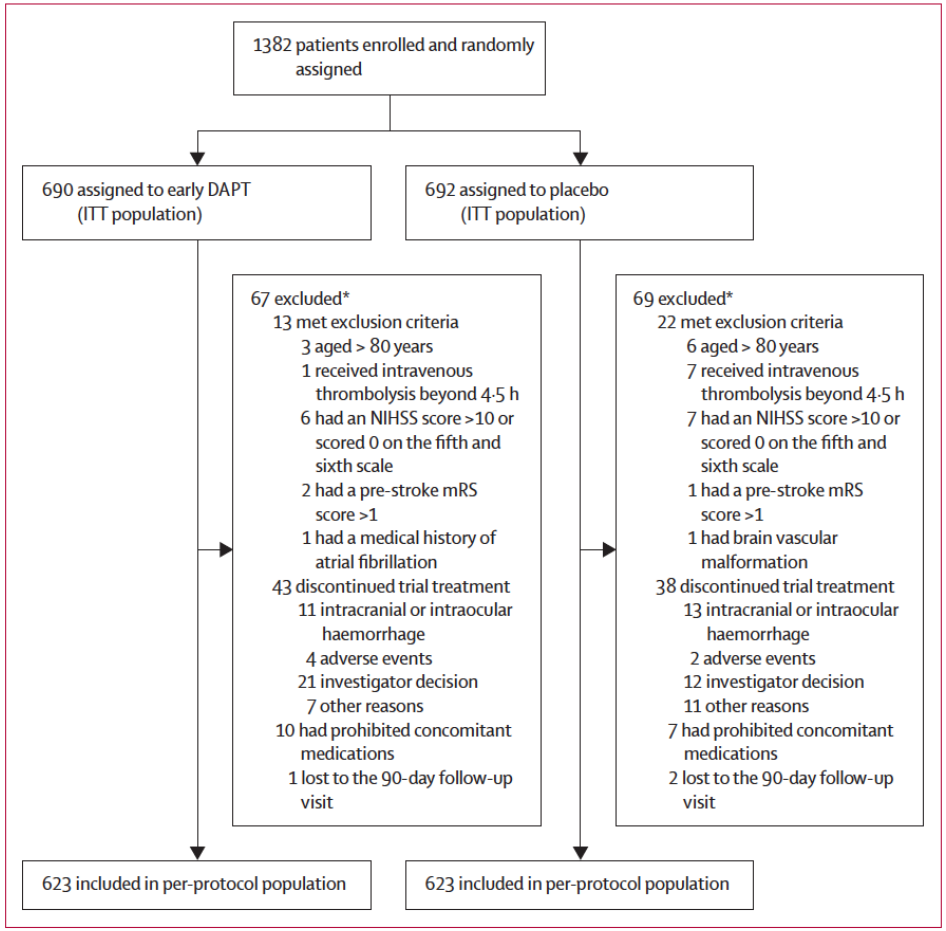

Figure 1: **Trial profile**
DAPT=dual antiplatelet therapy. ITT=intention to treat. mRS=modified Rankin Scale. NIHSS=National Institutes of Health Stroke Scale. *A single reason was recorded in screening logs. Some patients might have had multiple reasons for exclusion.

	Early DAPT (n=690)	Placebo (n=692)
Age, years	65·1 (57·9–71·9)	66·1 (59·0–72·1)
Sex		
Male	495 (71·7%)	496 (71·7%)
Female	195 (28·3%)	196 (28·3%)
BMI, kg/m²	23·7 (21·9–26·0)	24·1 (22·0–26·6)
Blood pressure, mm Hg		
Systolic	153 (140–166)	153 (140–166)
Diastolic	87 (78–96)	87 (80–96)
Current smoking	237 (34·3%)	238 (34·4%)
Current drinking	121 (17·5%)	99 (14·3%)
Previous antiplatelet therapy*	72 (10·4%)	60 (8·7%)
Medical history		
Ischaemic stroke	168 (24·3%)	165 (23·8%)
Ischaemic heart disease	77 (11·2%)	84 (12·1%)
Type 2 diabetes	159 (23·0%)	159 (23·0%)
Hypertension	420 (60·9%)	412 (59·5%)
mRS score before stroke onset		
0	625 (90·6%)	631 (91·2%)
1	63 (9·1%)	60 (8·7%)
2	2 (0·3%)	1 (0·1%)
NIHSS score before intravenous thrombolysis	6 (5–7)	6 (6–8)
Thrombolytic agents		
Alteplase	340 (49·3%)	321 (46·4%)
Tenecteplase	350 (50·7%)	371 (53·6%)
TOAST classification		
Large-artery atherosclerosis	284 (41·2%)	285 (41·2%)
Cardioembolic	5 (0·7%)	5 (0·7%)
Small-artery occlusion	370 (53·6%)	366 (52·9%)
Other determined cause	13 (1·9%)	10 (1·4%)
Undetermined cause	18 (2·6%)	26 (3·8%)
Time from onset to randomisation, min†	240 (172–292)	240 (171–300)
Time from onset to intravenous thrombolysis initiation, min	156 (112–210)	155 (110–209)
Time from intravenous thrombolysis initiation to randomisation, min	65 (16–112)	66 (17–111)
Timing of randomisation		
Before intravenous thrombolysis	113 (16·4%)	107 (15·5%)
During intravenous thrombolysis	92 (13·3%)	86 (12·4%)
After intravenous thrombolysis	485 (70·3%)	499 (72·1%)

Data are n (%) or median (IQR). Percentages might not total 100 because of rounding. DAPT=dual antiplatelet therapy. mRS=modified Rankin Scale. NIHSS=National Institutes of Health Stroke Scale. *Previous antiplatelet therapy within 1 month before this onset. †The first dose of study medication was administered at the time of randomisation; therefore, time from onset to randomisation equals time from onset to study drug administration.

Table 1: **Baseline characteristics**

	Early DAPT (n=690)	Placebo (n=692)	Effect size (95% CI)*	p value
Primary efficacy outcome				
mRS score 0–1 at 90 days	474/690 (68·7%)	429/692 (62·0%)	1·11 (1·03–1·20)	0·0089
Secondary efficacy outcomes				
mRS score 0–2 at 90 days	550/690 (79·7%)	517/692 (74·7%)	1·07 (1·01–1·13)	0·027
Ordinal mRS score at 90 days†	..	..	1·24 (1·02–1·50)	0·029
0	222/690 (32·2%)	204/692 (29·5%)	..	..
1	252/690 (36·5%)	225/692 (32·5%)	..	..
2	76/690 (11·0%)	88/692 (12·7%)	..	..
3	87/690 (12·6%)	106/692 (15·3%)	..	..
4	23/690 (3·3%)	38/692 (5·5%)	..	..
5	11/690 (1·6%)	8/692 (1·2%)	..	..
6	19/690 (2·8%)	23/692 (3·3%)	..	..
NIHSS score decreasing by ≥4 points at 7 days from baseline	400/690 (58·0%)	377/692 (54·5%)	1·06 (0·97–1·17)	0·19
EQ-5D-VAS score at 90 days‡	90 (78–95)	88 (70–95)	1·00 (0·00–2·00)	0·024
EQ-5D-5L score at 90 days‡	1·0 (0·9–1·0)	1·0 (0·8–1·0)	0·00 (0·00–0·00)	0·056
Barthel Index 95–100 at 90 days§	553/689 (80·3%)	514/690 (74·5%)	1·08 (1·02–1·14)	0·011
Recurrence of ischaemic stroke within 90 days¶	27/690 (3·9%)	24/692 (3·5%)	1·17 (0·67–2·05)	0·57
Safety outcomes				
Symptomatic intracranial haemorrhage within 36 h‖	6/690 (0·9%)	5/692 (0·7%)	1·20 (0·37–3·93)	0·76
Symptomatic intracranial haemorrhage within 7 days‖	7/690 (1·0%)	6/692 (0·9%)	1·17 (0·39–3·47)	0·78
Symptomatic intracranial haemorrhage with parenchymal haematoma type 2 within 36 h**	6/690 (0·9%)	5/692 (0·7%)	1·20 (0·37–3·93)	0·76
Symptomatic intracranial haemorrhage with parenchymal haematoma type 2 within 7 days**	6/690 (0·9%)	6/692 (0·9%)	1·00 (0·32–3·10)	>0·99
Any bleeding within 90 days††	50/690 (7·2%)	42/692 (6·1%)	1·19 (0·80–1·78)	0·38
Minor	37/690 (5·4%)	33/692 (4·8%)	..	..
Moderate	2/690 (0·3%)	0/692 (0·0%)	..	..
Severe or life-threatening	11/690 (1·6%)	9/692 (1·3%)	..	..
Adverse events within 90 days	109/690 (15·8%)	103/692 (14·9%)	1·06 (0·83–1·36)	0·64
Serious adverse events within 90 days	48/690 (7·0%)	48/692 (6·9%)	1·00 (0·68–1·48)	0·99

Data are n/N (%) or median (IQR), unless otherwise indicated. DAPT=dual antiplatelet therapy. EQ-5D-5L=EuroQol Group 5-Dimension 5-Level Self-Report Questionnaire. EQ-5D-VAS=EQ-5D Visual Analogue Scale. mRS=modified Rankin Scale. NIHSS=National Institutes of Health Stroke Scale. *The effect size is a risk ratio unless otherwise indicated. The widths of CIs for difference or risks for secondary outcomes were not adjusted for multiple comparisons, so no conclusions can be drawn from these data. †The common odds ratio (95% CI) is provided for ordinal score on the mRS at 90 days. ‡The median difference (95% CI) is provided for EQ-5D-VAS and EQ-5D-5L scores at 90 days. Data on the EQ-5D-VAS and EQ-5D-5L scores at 90 days were missing for three patients (one in the early DAPT group and two in the placebo group). §Data on the Barthel Index at 90 days were missing for three patients (one in the early DAPT group and two in the placebo group). ¶The hazard ratio (95% CI) is provided for recurrence of ischaemic stroke within 90 days. ‖Symptomatic intracranial haemorrhage was defined according to the ECASS-III criteria. **Symptomatic intracranial haemorrhage with parenchymal hematoma type 2 was defined by the SITS-MOST criteria. ††A bleeding event was defined according to the GUSTO criteria.

Table 2: **Efficacy and safety outcomes in the intention-to-treat population**

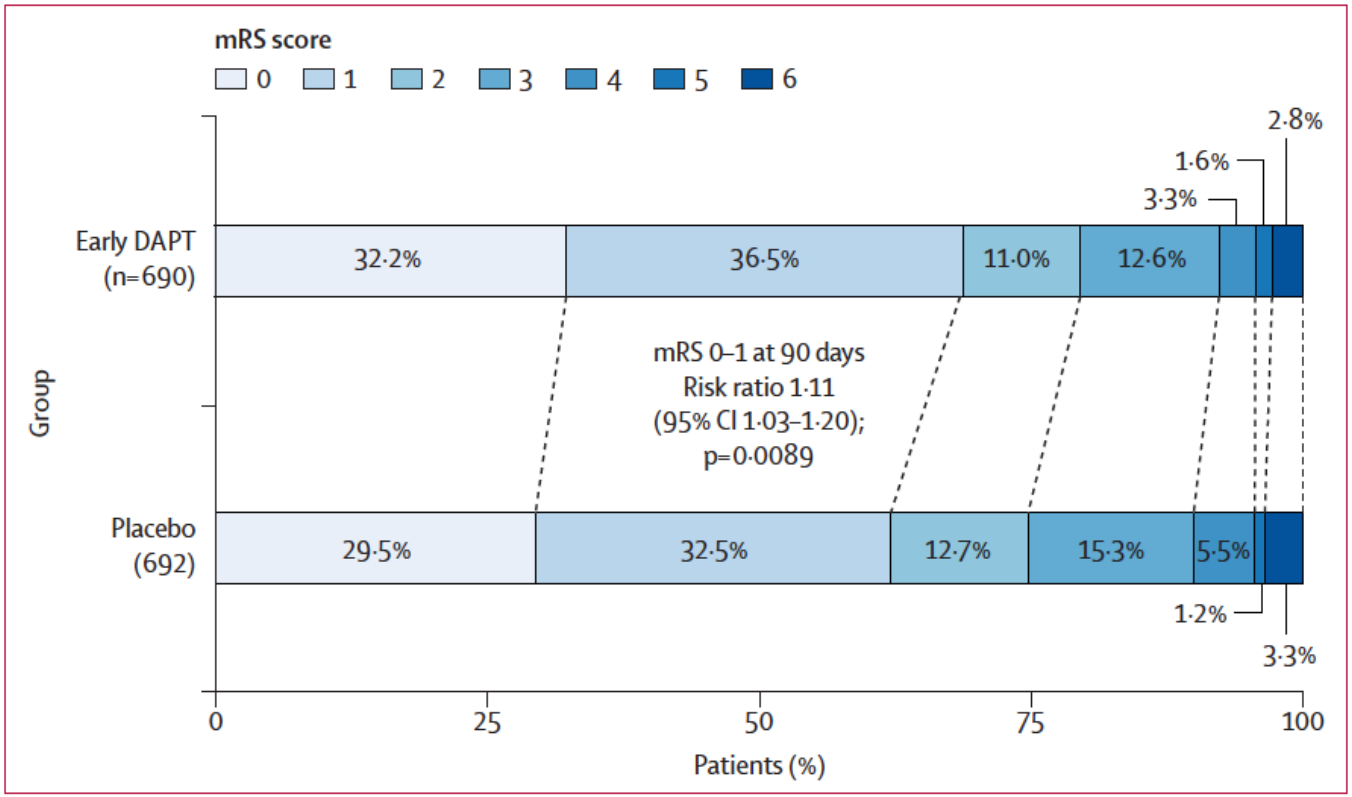

Figure 2: **Distribution of mRS scores at 90 days in the intention-to-treat population**
DAPT=dual antiplatelet therapy. mRS=modified Rankin Scale. Percentages might not amount to 100% because of rounding.

	Early DAPT group	Placebo group	Risk ratio (95%CI)	$p_{interaction}$
Age (years)				
<65	261/342 (76·3%)	209/321 (65·1%)	1·17 (1·06–1·29)	0·11
≥65	213/348 (61·2%)	220/371 (59·3%)	1·03 (0·92–1·16)	
Sex				
Female	134/195 (68·7%)	113/196 (57·7%)	1·19 (1·02–1·39)	0·26
Male	340/495 (68·7%)	316/496 (63·7%)	1·08 (0·99–1·18)	
Time from onset to randomisation (min)				
<240	239/332 (72·0%)	227/335 (67·8%)	1·06 (0·96–1·17)	0·26
≥240	235/358 (65·6%)	202/357 (56·6%)	1·16 (1·03–1·31)	
NIHSS score before intravenous thrombolysis				
<6	133/174 (76·4%)	115/163 (70·6%)	1·08 (0·95–1·23)	0·74
≥6	341/516 (66·1%)	314/529 (59·4%)	1·11 (1·01–1·22)	
TOAST classification				
Large-artery atherosclerosis	185/284 (65·1%)	168/285 (58·9%)	1·11 (0·97–1·26)	0·84
Small-artery occlusion	268/370 (72·4%)	237/366 (64·8%)	1·12 (1·01–1·23)	
Others	21/36 (58·3%)	24/41 (58·5%)	1·00 (0·68–1·45)	
Thrombolytic agent				
Alteplase	233/340 (68·5%)	195/321 (60·7%)	1·13 (1·01–1·26)	0·68
Tenecteplase	241/350 (68·9%)	234/371 (63·1%)	1·09 (0·98–1·21)	
History of ischaemic stroke				
No	372/522 (71·3%)	339/527 (64·3%)	1·11 (1·02–1·20)	0·96
Yes	102/168 (60·7%)	90/165 (54·5%)	1·11 (0·93–1·34)	
Type 2 diabetes				
No	376/531 (70·8%)	340/533 (63·8%)	1·11 (1·02–1·21)	0·94
Yes	98/159 (61·6%)	89/159 (56·0%)	1·10 (0·92–1·32)	
Hypertension				
No	191/270 (70·7%)	189/280 (67·5%)	1·05 (0·94–1·17)	0·21
Yes	283/420 (67·4%)	240/412 (58·3%)	1·16 (1·04–1·29)	
Timing of randomisation				
Before intravenous thrombolysis	80/113 (70·8%)	77/107 (72·0%)	0·98 (0·83–1·16)	0·33
During intravenous thrombolysis	63/92 (68·5%)	53/86 (61·6%)	1·11 (0·89–1·38)	
After intravenous thrombolysis	331/485 (68·2%)	299/499 (59·9%)	1·14 (1·04–1·25)	
Overall	**474/690 (68·7%)**	**429/692 (62·0%)**	**1·11 (1·03–1·20)**	

Figure 3: **Subgroup analysis of the primary efficacy outcome in the intention-to-treat population**
Data are n/N (%), unless otherwise indicated. Comparisons are unadjusted for multiplicity. Effect sizes are shown by prespecified subgroups. DAPT=dual antiplatelet therapy. NIHSS=National Institutes of Health Stroke Scale.

Research in context

Evidence before this study

We searched PubMed for randomised trials published from database inception to March 15, 2026, assessing the efficacy of antiplatelet therapy within 24 h after intravenous thrombolysis in patients with acute ischaemic stroke, using the terms "antiplatelet", "intravenous thrombolysis", and "ischaemic stroke".

Previous randomised trials have reported conflicting findings on the efficacy and safety of intravenous antiplatelet agents as adjunctive therapy to intravenous thrombolysis. The ARTIS trial, among the first large-sample randomised clinical trials assessing the efficacy of intravenous aspirin within 90 min after alteplase treatment, was prematurely terminated because of worse safety outcomes than with alteplase alone. Similarly, the MOST trial showed no clinical benefit of adjunctive intravenous eptifibatide but found increased mortality. By contrast, the ASSET-IT trial suggested that tirofiban use within 60 min after intravenous thrombolysis improved functional outcomes with an acceptable risk of symptomatic intracranial haemorrhage.

Evidence on oral antiplatelet therapy remains scarce. The EAST trial showed safety but no additional benefit of antiplatelet treatment with clopidogrel plus aspirin in patients with mild neurological deficits treated with intravenous thrombolysis. The TREND-IVT trial, designed to investigate whether patients with moderate-to-severe ischaemic stroke benefit from a single loading dose of oral aspirin adjunctive to thrombolysis, is still ongoing. To date, there is a paucity of evidence supporting early oral antiplatelet therapy for patients with stroke treated with intravenous thrombolysis, particularly those with moderate neurological severity.

Added value of this study

The TAPIS trial, a double-blind, randomised controlled trial enrolling 1382 patients with acute ischaemic stroke from 60 sites in China, suggests that in patients with acute ischaemic stroke with a National Institutes of Health Stroke Scale score of 4–10 who received thrombolysis, early initiation (within 6 h of symptom onset) of oral dual antiplatelet therapy with ticagrelor plus aspirin was associated with an improved likelihood of excellent functional outcomes (a modified Rankin Scale score of 0–1) at 90 days. Moreover, no statistically significant difference in the risk of symptomatic intracranial haemorrhage was detected between the early dual antiplatelet therapy group and the placebo control group, with wide CIs that did not rule out a modest increase in risk.

Implications of all the available evidence

The TAPIS trial showed benefits of ticagrelor–aspirin dual antiplatelet therapy within 6 h of onset on functional outcomes in patients with acute ischaemic stroke who received thrombolysis, providing high-quality evidence that might inform clinical decision-making regarding early adjunctive oral antiplatelet therapy in this population.

Eine **komplizierte Harnwegsinfektion (cUTI)** liegt vor, wenn eine Entzündung der Harnwege mit Faktoren einhergeht, die das Risiko für ein **Therapieversagen oder schwere Komplikationen (wie eine Urosepsis) deutlich erhöhen**. Im Gegensatz zu einer unkomplizierten Blasenentzündung betrifft sie häufiger die oberen Harnwege (Nieren) oder tritt bei Personen mit anatomischen Besonderheiten oder geschwächtem Immunsystem auf.

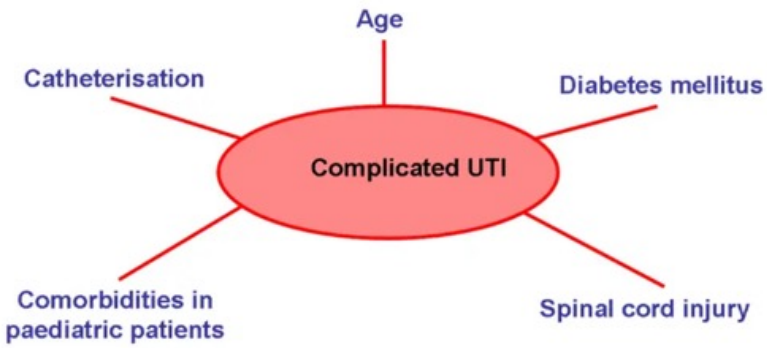

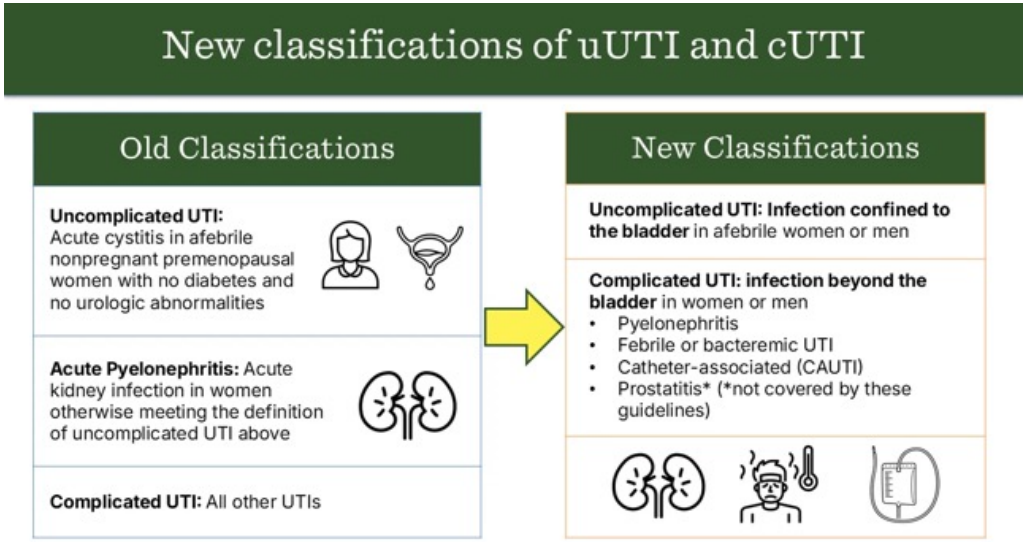

Efficacy and safety of cefepime–nacubactam and aztreonam–nacubactam compared with imipenem–cilastatin for complicated urinary tract infection or acute uncomplicated pyelonephritis (Integral-1): a double-blind,

Summary

Background Nacubactam (OP0595) is a newly developed diazabicyclooctane β-lactamase inhibitor used in combination with cefepime or aztreonam. We assessed the efficacy and safety of cefepime–nacubactam and aztreonam–nacubactam versus imipenem–cilastatin in complicated urinary tract infection (cUTI) or acute uncomplicated pyelonephritis.

Methods The Integral-1 global, phase 3, multicentre, randomised, double-blind study recruited adults (aged ≥18 years) with cUTI or acute uncomplicated pyelonephritis at 79 sites in Bulgaria, China, Czech Republic, Estonia, Georgia, Japan, Latvia, Lithuania, and Slovakia. Patients were randomly assigned (2:1:1) to receive intravenous cefepime (2 g) plus nacubactam (1 g), aztreonam (2 g) plus nacubactam (1 g), or imipenem (1 g) plus cilastatin (1 g) every 8 h for 5–14 days. Randomisation was stratified by diagnosis and geographical region. The primary endpoint was the proportion of patients achieving composite clinical and microbiological success at test of cure in the microbiological modified intention-to-treat population—all patients who were randomly assigned, received any amount of the study drug, and had a baseline qualifying pathogen that was susceptible to imipenem and meropenem. The prespecified non-inferiority margin was more than 15 percentage points difference; the superiority margin was more than zero percentage points difference, for the lower bound of the two-sided 95% CI for imipenem–cilastatin. Safety was assessed in all patients who received at least one dose of study drug. This study is registered with ClinicalTrials.gov, NCT05887908.

Findings Between May 22, 2023, and Nov 26, 2024, 614 patients were randomly assigned and 431 were included in the primary efficacy analysis (cefepime–nacubactam [n=214], aztreonam–nacubactam [n=112], or imipenem–cilastatin [n=105]); 228 patients (53%) were male and 203 (47%) were female. The primary endpoint was achieved by 176 (82%) of 214, 81 (72%) of 112, and 64 (61%) of 105 patients in the cefepime–nacubactam, aztreonam–nacubactam, and imipenem–cilastatin groups, respectively. The percentage difference in the success rate versus imipenem–cilastatin was 21·3% (95% CI 10·9 to 32·0) for cefepime–nacubactam (non-inferior and superior), and 11·4% (–1·2 to 23·7) for aztreonam–nacubactam (non-inferior). Treatment-emergent adverse events were reported in 100 (33%) of 306, 45 (30%) of 152, and 65 (43%) of 150 patients in the cefepime–nacubactam, aztreonam–nacubactam, and imipenem–cilastatin groups, respectively. No treatment-related deaths occurred.

Interpretation Cefepime–nacubactam and aztreonam–nacubactam are potential treatment options for Gram-negative cUTI and acute uncomplicated pyelonephritis, including infections caused by antimicrobial-resistant strains.

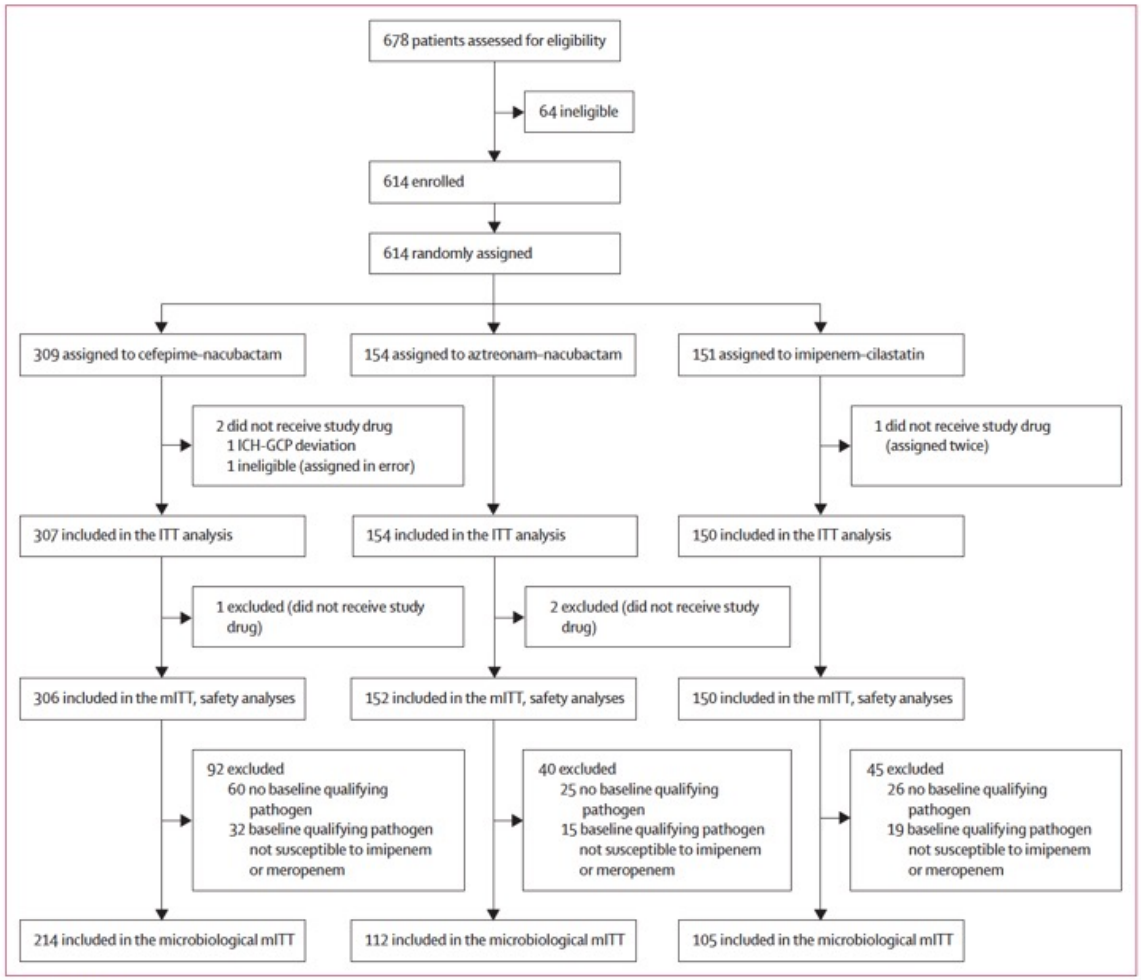

Figure: **Trial profile**
The ITT population was defined as all patients who were randomly allocated to treatment. The mITT and safety populations were defined as all patients who met the ITT criteria and received any amount of the study drug. The microbiological mITT population was defined as all patients who met the mITT criteria and had a baseline qualifying pathogen that was susceptible to imipenem and meropenem. ICH-GCP=International Council for Harmonisation–Good Clinical Practice. ITT=intention-to-treat. mITT=modified ITT.

	Cefepime–nacubactam (n=214)	Aztreonam–nacubactam (n=112)	Imipenem–cilastatin (n=105)	Total (n=431)
Age, years	63·62 (14·83)	66·41 (14·04)	65·46 (15·57)	64·79 (14·83)
Sex				
Male	111 (52%)	61 (54%)	56 (53%)	228 (53%)
Female	103 (48%)	51 (46%)	49 (47%)	203 (47%)
Race				
Asian (Japanese)	12 (6%)	6 (5%)	5 (5%)	23 (5%)
Asian (Chinese)	23 (11%)	9 (8%)	7 (7%)	39 (9%)
Asian (other)	0	1 (<1%)	0	1 (<1%)
White	179 (84%)	96 (86%)	93 (89%)	368 (85%)
Geographical region				
Japan	12 (6%)	6 (5%)	5 (5%)	23 (5%)
China	23 (11%)	10 (9%)	7 (7%)	40 (9%)
Other*	179 (84%)	96 (86%)	93 (89%)	368 (85%)
Weight, kg	79·11 (17·75)	81·26 (19·20)	77·47 (17·48)	79·27 (18·08)
Body mass index, kg/m²	27·52 (5·42)	28·49 (5·37)	26·94 (5·59)	27·62 (5·46)
Primary infection type				
Complicated urinary tract infection	137 (64%)	76 (68%)	73 (70%)	286 (66%)
Acute uncomplicated pyelonephritis	77 (36%)	36 (32%)	32 (30%)	145 (34%)
Creatinine clearance, mL/min				
Total	86·9 (34·9; n=212)	87·8 (40·1)	82·0 (32·4; n=104)	85·9 (35·8; n=428)
<30	1 (<1%)	3 (3%)	0	4 (1%)
30 to <60	46 (21%)	30 (27%)	27 (26%)	103 (24%)
60 to <90	77 (36%)	30 (27%)	44 (42%)	151 (35%)
90 to <240	88 (41%)	49 (44%)	33 (31%)	170 (39%)
Secondary bacteraemia	15 (7%)	9 (8%)	10 (10%)	34 (8%)
Prior short-acting antibacterial therapy	18 (8%)	12 (11%)	12 (11%)	42 (10%)
Resistance type				
ESBL-positive	48 (22%)	34 (30%)	27 (26%)	109 (25%)
Escherichia coli	34 (16%)	25 (22%)	21 (20%)	80 (19%)
Klebsiella pneumoniae	15 (7%)	8 (7%)	6 (6%)	29 (7%)
Proteus mirabilis	0	1 (<1%)	0	1 (<1%)

Data are n (%) or mean (SD). mITT=modified intention-to-treat. ESBL=extended-spectrum β-lactamases. *Includes Bulgaria, Czech Republic, Estonia, Georgia, Latvia, Lithuania, and Slovakia. ESBL defined as testing with a ceftazidime broth microdilution minimum inhibitory concentration of 2 μg/mL or greater, and a 5 mm or greater increase in zone size when tested with ceftazidime-clavulanate or cefotaxime-clavulanate disks, compared with the zone size for discs containing the agent alone.

Table 1: **Patient demographics and background characteristics (microbiological mITT population)**

	Cefepime–nacubactam (n=214)	Aztreonam–nacubactam (n=112)	Imipenem–cilastatin (n=105)	Total (n=431)
Baseline pathogen				
Escherichia coli	162 (76%)	89 (80%)	76 (72%)	327 (76%)
Klebsiella pneumoniae	32 (15%)	12 (11%)	16 (15%)	60 (14%)
Proteus mirabilis	2 (1%)	7 (6%)	2 (2%)	11 (3%)
Klebsiella oxytoca	5 (2%)	2 (2%)	1 (1%)	8 (2%)
Pseudomonas aeruginosa	5 (2%)	1 (1%)	2 (2%)	8 (2%)
Enterobacter hormaechei	4 (2%)	1 (1%)	2 (2%)	7 (2%)
Citrobacter freundii	2 (1%)	1 (1%)	1 (1%)	4 (1%)
Klebsiella variicola	2 (1%)	1 (1%)	1 (1%)	4 (1%)
Providencia rettgeri	1 (<1%)	0	2 (2%)	3 (1%)
Citrobacter koseri	1 (<1%)	0	1 (1%)	2 (<1%)
Klebsiella aerogenes	1 (<1%)	1 (1%)	0	2 (<1%)
Proteus hauseri	2 (1%)	0	0	2 (<1%)
Acinetobacter junii	0	1 (1%)	0	1 (<1%)
Citrobacter spp	0	0	1 (1%)	1 (<1%)
Enterobacter spp	0	0	1 (1%)	1 (<1%)
Enterobacter bugandensis	1 (<1%)	0	0	1 (<1%)
Raoultella ornithinolytica	1 (<1%)	0	0	1 (<1%)
Serratia marcescens	1 (<1%)	0	0	1 (<1%)
Polymicrobial infection	8 (4%)	4 (4%)	1 (1%)	13 (3%)
Escherichia coli and *Klebsiella pneumoniae*	4 (2%)	0	0	4 (1%)
Escherichia coli and *Pseudomonas aeruginosa*	2 (1%)	1 (1%)	0	3 (1%)
Escherichia coli and *Proteus mirabilis*	1 (<1%)	1 (1%)	0	2 (<1%)
Klebsiella oxytoca and *Klebsiella pneumoniae*	0	2 (2%)	0	2 (<1%)
Klebsiella pneumoniae and *Providencia rettgeri*	1 (<1%)	0	1 (1%)	2 (<1%)

mITT=modified intention-to-treat.

Table 2: **Summary of baseline pathogens (microbiological mITT population)**

	Cefepime–nacubactam (n=214)	Aztreonam–nacubactam (n=112)	Imipenem–cilastatin (n=105)	Treatment difference (95% CI)	
				Cefepime–nacubactam *vs* imipenem–cilastatin	Aztreonam–nacubactam *vs* imipenem–cilastatin
Composite clinical and microbiological success					
Success	176 (82·2% [76·5 to 87·1])	81 (72·3% [63·1 to 80·4])	64 (61·0% [50·9 to 70·3])	21·3% (10·9 to 32·0)	11·4% (–1·2 to 23·7)
Failure	26 (12%)	27 (24%)	34 (32%)	..	..
Indeterminate	12 (6%)	4 (4%)	7 (7%)	..	..
Clinical outcome					
Cure	195 (91·1% [86·5 to 94·6])	103 (92·0% [85·3 to 96·3])	92 (87·6% [79·8 to 93·2])	3·5% (–3·3 to 11·8)	4·3% (–3·9 to 13·0)
Failure	7 (3%)	3 (3%)	5 (5%)	..	..
Indeterminate	12 (6%)	6 (5%)	8 (8%)	..	..
Microbiological outcome					
Eradication	184 (86·0% [80·6 to 90·3])	83 (74·1% [65·0 to 81·9])	67 (63·8% [53·9 to 73·0])	22·2% (12·2 to 32·7)	10·3% (–2·0 to 22·5)
Persistence	0	0	0	..	..
Recurrence	14 (7%)	22 (20%)	28 (27%)	..	..
Indeterminate	16 (7%)	7 (6%)	10 (10%)	..	..

Data are n (% [95% CI]). mITT=modified intention-to-treat.

Table 3: **Clinical and microbiological success rates and outcomes at test of cure visit and between-group comparisons (mITT)**

	Cefepime–nacubactam (n=214)	Aztreonam–nacubactam (n=112)	Imipenem–cilastatin (n=105)	Treatment difference (95% CI)	
				Cefepime–nacubactam *vs* imipenem–cilastatin	Aztreonam–nacubactam *vs* imipenem–cilastatin
End of treatment					
Composite clinical and microbiological success					
Success	199 (93·0% [88·7 to 96·0])	102 (91·1% [84·2 to 95·6])	94 (89·5% [82·0 to 94·7])	3·5% (−2·7 to 11·3)	1·5% (−6·6 to 10·0)
Failure	10 (5%)	5 (4%)	7 (7%)	..	..
Indeterminate	5 (2%)	5 (4%)	4 (4%)	..	..
Clinical outcome					
Cure	204 (95·3% [91·6 to 97·7])	106 (94·6% [88·7 to 98·0])	100 (95·2% [89·2 to 98·4])	0·1% (−4·6 to 6·4)	−0·6% (−7·1 to 6·0)
Failure	5 (2%)	1 (1%)	1 (1%)	..	..
Indeterminate	5 (2%)	5 (4%)	4 (4%)	..	..
Microbiological outcome					
Eradication	203 (94·9% [91·0 to 97·4])	105 (93·8% [87·5 to 97·5])	95 (90·5% [83·2 to 95·3])	4·4% (−1·3 to 11·9)	3·3% (−4·2 to 11·2)
Persistence	0	0	0	..	..
Recurrence	0	3 (3%)	1 (1%)	..	..
Indeterminate	11 (5%)	4 (4%)	9 (9%)	..	..
Follow-up					
Composite clinical and microbiological success					
Success	147 (68·7% [62·0 to 74·8])	73 (65·2% [55·6 to 73·9])	65 (61·9% [51·9 to 71·2])	6·8% (−4·1 to 18·1)	3·3% (−9·5 to 16·0)
Failure	54 (25%)	34 (30%)	34 (32%)	..	..
Indeterminate	13 (6%)	5 (4%)	6 (6%)	..	..
Clinical outcome					
Cure	188 (87·9% [82·7 to 91·9])	98 (87·5% [79·9 to 93·0])	89 (84·8% [76·4 to 91·0])	3·1% (−4·5 to 12·1)	2·7% (−6·6 to 12·3)
Failure	7 (3%)	4 (4%)	2 (2%)	..	..
Recurrence	6 (3%)	5 (4%)	7 (7%)	..	..
Indeterminate	13 (6%)	5 (4%)	7 (7%)	..	..
Microbiological outcome					
Eradication*	157 (73·4% [66·9 to 79·2])	75 (67·0% [57·4 to 75·6])	68 (64·8% [54·8 to 73·8])	8·6% (−2·0 to 19·7)	2·2% (−10·4 to 14·8)
Presumed eradication†	56 (26%)	30 (27%)	18 (17%)	..	..
Persistence	0	0	1 (1%)	..	..
Recurrence	40 (19%)	29 (26%)	25 (24%)	..	..
Indeterminate	17 (8%)	8 (7%)	11 (10%)	..	..

Data are n (% [95% CI]). CFM= colony-forming units. mITT=modified intention-to-treat. *Includes presumed eradication. †Presumed eradication was assessed at follow-up and categorised as eradication only if the baseline qualifying Gram-negative pathogen was eradicated (reduced to <10^5 CFU/mL) at the test of cure visit, and a urine sample could not be collected but there was a clinical outcome of cure at follow-up; therefore, a urine sample should also have been collected at follow-up, unless the baseline qualifying Gram-negative pathogen was eradicated (reduced to <10^5 CFU/mL) at the treatment of cure visit.

Table 4: **Clinical and microbiological success rates and outcomes at end of treatment visit and follow-up visit and between-group comparisons (microbiological mITT population)**

	Cefepime–nacubactam (n=306)	Aztreonam–nacubactam (n=152)	Imipenem–cilastatin (n=150)	Total (n=608)
Any adverse event	102 (33% [208])	47 (31% [105])	66 (44% [135])	215 (35% [448])
Any serious adverse event	6 (2% [7])	4 (3% [4])	5 (3% [7])	15 (2% [18])
Any adverse event leading to death	1 (<1% [1])	0	0	1 (<1% [1])
Any treatment-emergent adverse event	100 (33% [203])	45 (30% [99])	65 (43% [132])	210 (35% [434])
Mild	67 (22%)	35 (23%)	42 (28%)	144 (24%)
Moderate	28 (9%)	9 (6%)	20 (13%)	57 (9%)
Severe	5 (2%)	1 (1%)	3 (2%)	9 (1%)
Any adverse drug reaction	44 (14% [58])	15 (10% [29])	27 (18% [40])	86 (14% [127])
Mild	35 (11%)	14 (9%)	19 (13%)	68 (11%)
Moderate	8 (3%)	0	7 (5%)	15 (2%)
Severe	1 (<1%)	1 (1%)	1 (1%)	3 (<1%)
Any intravenous procedure-related treatment-emergent adverse event	14 (5% [15])	5 (3% [6])	8 (5% [12])	27 (4% [33])
Any serious treatment-emergent adverse event	6 (2% [7])	4 (3% [4])	5 (3% [7])	15 (2% [18])
Any treatment-emergent adverse event leading to discontinuation of study drug	7 (2% [10])	2 (1% [2])	2 (1% [3])	11 (2% [15])
Any treatment-emergent adverse event leading to discontinuation of study	7 (2% [7])	2 (1% [2])	1 (1% [2])	10 (2% [11])
Treatment-emergent adverse events by System Organ Class and MedDRA preferred term (experienced by ≥2% of patients in any treatment group)				
Gastrointestinal disorders	32 (10% [37])	13 (9% [18])	28 (19% [36])	73 (12% [91])
Diarrhoea	14 (5% [14])	3 (2% [3])	6 (4% [6])	23 (4% [23])
Nausea	5 (2% [5])	1 (1% [1])	10 (7% [10])	16 (3% [16])
Constipation	6 (2% [6])	3 (2% [3])	4 (3% [6])	13 (2% [15])
Vomiting	2 (<1% [2])	1 (1% [1])	5 (3% [5])	8 (1% [8])
Abdominal pain upper	1 (<1% [1])	1 (1% [1])	3 (2% [3])	5 (1% [5])
Infections and infestations	18 (6% [18])	14 (9% [14])	16 (11% [20])	48 (8% [52])
Asymptomatic bacteriuria	3 (1% [3])	7 (5% [7])	5 (3% [5])	15 (2% [15])
Nervous system disorders*	16 (5% [18])	9 (6% [9])	9 (6% [10])	34 (6% [37])
Headache	10 (3% [11])	8 (5% [8])	6 (4% [6])	24 (4% [25])
General disorder and administration site conditions	8 (3% [8])	5 (3% [5])	12 (8% [17])	25 (4% [30])
Pyrexia	4 (1% [4])	2 (1% [2])	3 (2% [3])	9 (1% [9])
Metabolism and nutrition disorders	11 (4% [17])	4 (3% [4])	4 (3% [8])	19 (3% [31])
Hypokalaemia	6 (2% [6])	1 (1% [1])	2 (1% [2])	9 (1% [9])
Skin and subcutaneous tissue disorders	8 (3% [8])	4 (3% [4])	4 (3% [4])	16 (3% [16])
Rash	2 (<1% [2])	2 (1% [2])	4 (3% [4])	8 (1% [8])
Vascular disorders	11 (4% [11])	5 (3% [5])	0	16 (3% [16])
Hypertension	5 (2% [5])	3 (2% [3])	0	8 (1% [8])

Data are n, participants (% [n, events]). Events are coded by System Organ Class and preferred term according to MedDRA version 26.0. MedDRA=Medical Dictionary for Regulatory Activities. *All nervous system disorders other than headache occurred at a frequency of less than 2%: cefepime–nacubactam, dizziness (three treatment-emergent adverse events in three patients [1%]), and cervical radiculopathy, dizziness postural, encephalopathy, and radiculopathy (one treatment-emergent adverse event in one patient [<1%] each); aztreonam–nacubactam, cerebral infarction (one treatment-emergent adverse event in one patient [<1%]); imipenem–cilastatin, neuralgia, paraesthesia, presyncope, and tremor (one treatment-emergent adverse event in one patient [<1%] each).

Table 5: **Overall summary of adverse events, treatment-emergent adverse events, adverse drug reactions, and breakdown of treatment-emergent adverse events occurring in minimum 2% of patients in any treatment group by System Organ Class and MedDRA preferred term (safety population)**

Implications of all the available evidence

Integral-1 showed that cefepime–nacubactam and aztreonam–nacubactam are effective and well tolerated for the treatment of cUTI or acute uncomplicated pyelonephritis and related secondary bacteraemia caused by Gram-negative bacteria except *Acinetobacter* species, including antimicrobial-resistant strains. It was necessary to exclude patients with carbapenem-resistant pathogens, given that imipenem, a carbapenem, was used as the active comparator. Adding the results of this study to those of the existing pharmacokinetic and non-clinical pharmacology studies strengthens the evidence that supports cefepime–nacubactam and aztreonam–nacubactam as important new treatments for antimicrobial-resistant Gram-negative bacterial infections. A clinical trial to assess efficacy of cefepime–nacubactam and aztreonam–nacubactam for infections caused by carbapenem-resistant Enterobacterales (Integral-2) is ongoing.

Gavi (Die Impfallianz)

Die Globale Allianz für Impfstoffe und Immunisierung (GAVI) ist eine öffentlich-private globale Gesundheitspartnerschaft. Sie hat das Ziel, die globale Gesundheitsversorgung zu verbessern, indem sie den Zugang zu neuen und untergenutzten Impfstoffen für Kinder in den ärmsten Ländern der Welt massiv ausweitet und finanziert.

•**Beteiligte:** Regierungen, die Weltgesundheitsorganisation (WHO), UNICEF, die Weltbank, die Bill & Melinda Gates Foundation sowie Impfstoffhersteller.

•**Fokus:** Bekämpfung von Infektionskrankheiten wie Malaria, Ebola, Pneumokokken und HPV.

•**Weitere Informationen:** Offizielle Einblicke, Hilfsprojekte und Spendenmöglichkeiten finden Sie direkt auf der Webseite von Gavi, die Impfallianz.

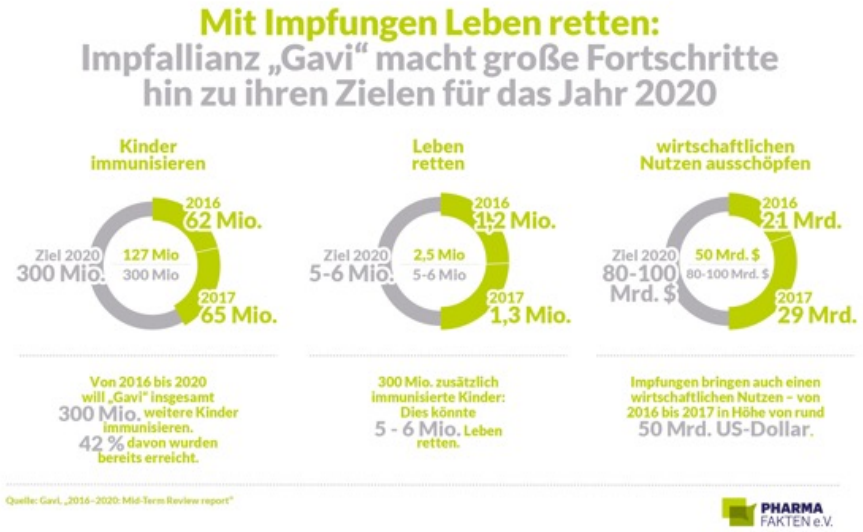

Quantifying relative health impact across Gavi, the Vaccine Alliance's portfolio in 117 countries at the subregional level: a modelling study

Summary

Background Estimates of vaccine impact have typically been used to quantify the effects of, and inform, immunisation strategies. Given the growing resource constraints on health systems worldwide, robust estimates of vaccine impact that allow comparison across different vaccines are now more crucial for decision making than ever. Building on previous modelling studies, we aimed to estimate vaccine impact ratios for an expanded portfolio of Gavi, the Vaccine Alliance-supported vaccination programmes against 14 vaccine-preventable diseases across 117 low-income and middle-income countries using multiple models.

Methods In this modelling study, we have presented Vaccine Impact Modelling Consortium estimates of vaccine impact ratios, defined as deaths or disability-adjusted life-years averted per 1000 vaccinations, for the Gavi portfolio of vaccines. Modelling groups used standardised inputs for demographic data and vaccination coverage assumptions, including a no-vaccination counterfactual, and accounted for structural, parameter, and stochastic uncertainty to produce burden estimates. These estimates were then compared to calculate vaccine impact ratios, disaggregated by immunisation activity type and geographical subregions for vaccinations given between 2000 and 2030 (or 2000 and 2040 for cholera).

Findings Overall, we observed human papillomavirus (11·24 [95% uncertainty interval 10·88–11·64]) and measles (6·09 [4·90–7·07])vaccines averting a higher number of deaths per 1000 vaccinations than others. For other vaccines, the impact ratios varied across subregions and activity types. Due to parameter, structural, and stochastic uncertainty, the ranges of these ratios often overlap.

Interpretation Decisions around which vaccines to use are increasingly important in the context of Gavi's country vaccine budgets. Robust metrics that allow comparison between vaccines are thus essential to inform discussions. The vaccine impact ratios presented in this study can be used to complement other evidence to support effective planning and prioritisation in national immunisation programmes.

	Deaths averted per 1000 vaccinations (95% uncertainty interval)	DALYs averted per 1000 vaccinations (95% uncertainty interval)
Cholera	0·20 (0·13–0·56)	6·13 (4·81–12·61)
COVID-19	0·12 (0·08–0·18)	4·03 (2·86–6·19)
Hib	2·22 (1·81–2·61)	150·37 (124·74–176·12)
HepB	5·00 (4·47–5·58)	141·94 (127·28–157·71)
HPV	11·24 (10·88–11·64)	523·04 (499·92–547·11)
Japanese encephalitis	0·18 (0·10–0·30)	80·57 (55·55–106·80)
Malaria	2·78 (2·16–3·53)	203·04 (156·99–259·97)
Measles	6·09 (4·90–7·07)	411·01 (331·63–476·14)
Meningitis	0·66 (0·49–0·85)	42·78 (31·90–54·91)
PCV	1·53 (0·87–2·09)	104·91 (61·47–142·93)
Rota	0·80 (0·49–1·04)	46·07 (25·78–61·78)
Rubella	0·22 (0·12–0·35)	16·78 (11·91 23·51)
Typhoid	0·68 (0·21–1·72)	26·57 (7·96–70·69)
Yellow fever	1·86 (0·52–4·23)	72·26 (20·06–165·63)

Diseases have been ordered alphabetically. Deaths for rubella reflect deaths related to Congenital Rubella Syndrome. Malaria refers to the combined value of RTS,S and R21 vaccine effect. COVID-19 refers to an average of different COVID-19 vaccine product effects informed by the most prevalent vaccine product per country. Meningitis refers to the combined effect of MenA and MenACWYX vaccination. DALYs=disability-adjusted life-years. Hib=*Haemophilus influenzae* type b. HepB=hepatitis B. HPV=human papillomavirus. PCV=pneumococcal conjugate vaccine. Rota=rotavirus.

Table 1: **Mean and 95% uncertainty interval of bootstrap mean impact ratio of deaths and DALYs averted per 1000 vaccinations for all activities**

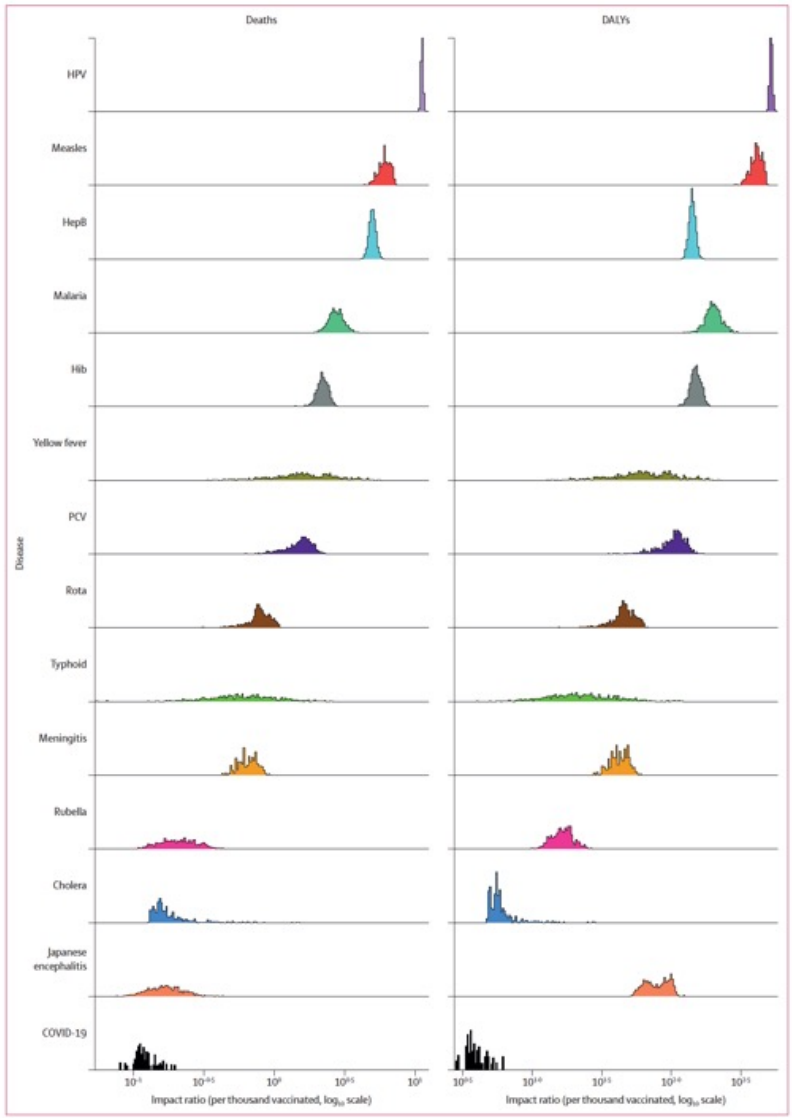

Figure 1: **Bootstrap mean impact ratios defined as deaths or disability-adjusted life-years (DALYs) averted per 1000 vaccinations across all subregions and activity types**
Diseases have been arranged by mean impact ratio value for the deaths averted. Deaths for rubella reflect deaths related to Congenital Rubella Syndrome. Malaria refers to the combined value of RTS,S and R21 vaccine effect. COVID-19 refers to an average of different COVID-19 vaccine product effects informed by the most prevalent vaccine product per country. Meningitis refers to the combined effect of MenA and MenACWYX vaccination. Each histogram contains 1000 bootstrapped mean estimates per vaccine for all relevant countries. Hib=Haemophilus influenzae type b. HepB=hepatitis B. HPV=Human papillomavirus. PCV=pneumococcal conjugate vaccine. Rota=Rotavirus.

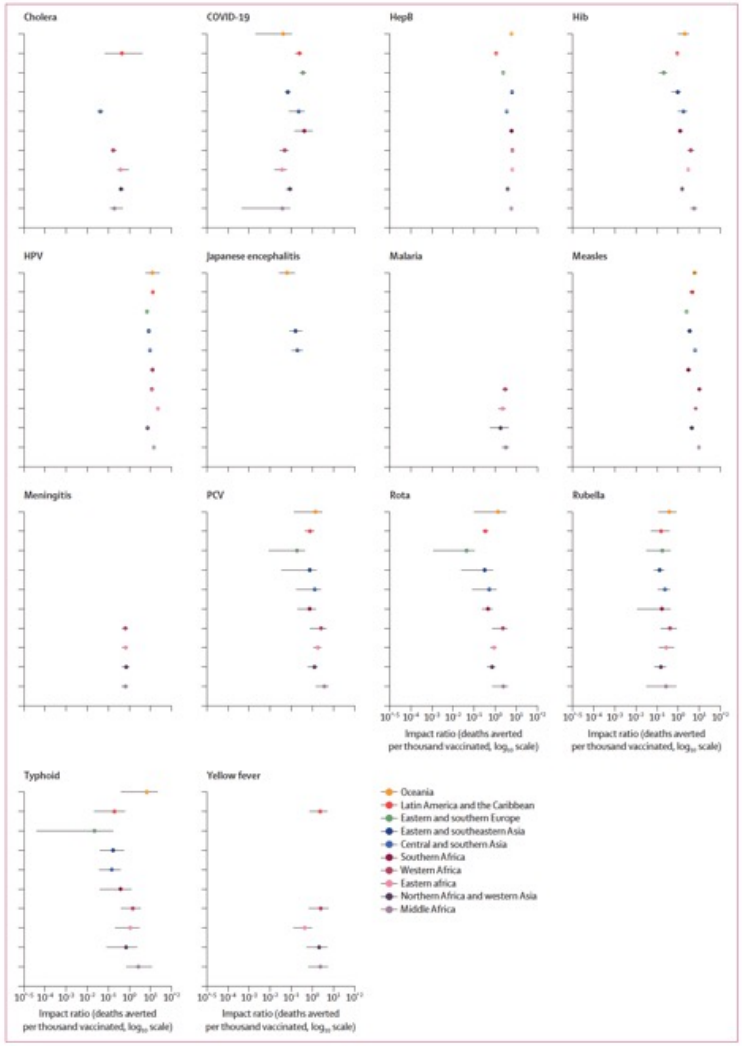

Figure 2: Bootstrap mean impact ratios and 95% CIs defined as deaths averted per 1000 vaccinations by subregion and disease for all activities

Dots indicate bootstrap mean impact ratios, and lines indicate 95% CIs (when the 95% CI is smaller than the length of the dot, it is shown as a white colour). Deaths for rubella reflect deaths related to Congenital Rubella Syndrome. Malaria refers to the combined value of RTS,S and R21 vaccine effect. COVID-19 refers to an average of different COVID-19 vaccine product effects informed by the most prevalent vaccine product per country. Meningitis refers to the combined effect of MenA and MenACWYX vaccination. Results for disability-adjusted life-years and results split by vaccination activity can be found in the appendix (pp 25–27). Hib=*Haemophilus influenzae* type b. HepB=hepatitis B. HPV=human papillomavirus. PCV=pneumococcal conjugate vaccine. Rota=rotavirus.

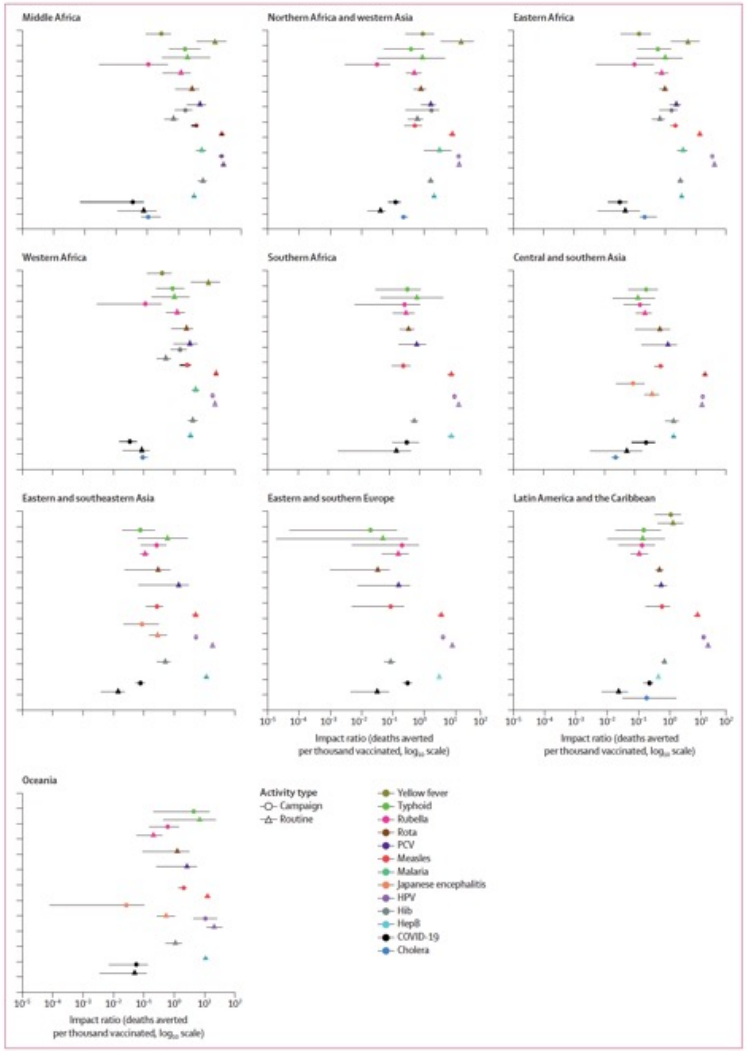

Figure 3: Bootstrap mean impact ratios and 95% CIs defined as deaths averted per 1000 vaccinated by disease, subregion, and activity

Dots or triangles indicate bootstrap mean impact ratios, and lines indicate 95% CIs. Deaths for rubella reflect deaths related to Congenital Rubella Syndrome. Malaria refers to the combined value of RTS,S and R21 vaccine effect. COVID-19 refers to an average of different COVID-19 vaccine product effects informed by the most prevalent vaccine product per country. Results for disability-adjusted life-years can be found in the appendix (pp 25–27). Hib=*Haemophilus influenzae* type b. HepB=hepatitis B. HPV=human papillomavirus. PCV= pneumococcal conjugate vaccine. Rota=rotavirus.

	Model	Code link
Cholera	Cholera-IVI-Kim	https://github.com/kimfinale/cholera_typhoid_vimc_ivi
Cholera	Cholera-JHU-Lee	https://github.com/HopkinsIDD/gavi_vimc_cholera
COVID	COVID-LSHTM-Liu	Results not presented in the current publication (appendix p 60)
COVID	COVID-IC-Ghani	https://mrc-ide.github.io/safir
HepB	HepB-Burnet-Scott	https://github.com/Burnet-Modelling/burnet-hbv
HepB	HepB-IC-Nayagam	https://github.com/mrc-ide/icl-hbv
HepB	HepB-Goldstein	No publicly available code
HPV	HPV-BU-Portnoy	Modelling outputs are based on three separate modelling approaches (appendix pp 43–44)
HPV	HPV-LSHTM-Jit	https://github.com/lshtm-vimc/prime
Malaria	Malaria-UAC-Glele-Kakai	https://github.com/RomainGleleKakai/Sub-national-malaria-model
Malaria	Malaria-IC-Okell	https://github.com/mrc-ide/VIMC_malaria
Malaria	Malaria-TKI-Penny	https://github.com/SwissTPH/openmalaria
Measles	Measles-PSU-Ferrari	https://github.com/bwlambert/pfilter_plus
Measles	Measles-LSHTM-Jit	https://github.com/lshtm-vimc/dynamice
Meningitis	MenA-Cambridge-Trotter	https://github.com/andromachi889/MMCV-model
Rubella	Rubella-UKHSA-Vynnycky	https://github.com/EmiliaVynnycky/Rubella-model-VIMC-runs-2023-24
Rubella	Rubella-UGA-Winter	https://github.com/UGA-IDD/MRTransmissionModel; https://github.com/UGA-IDD/globalRubellaIgG
Typhoid	Typhoid-IVI-Kim	https://github.com/kimfinale/cholera_typhoid_vimc_ivi
Typhoid	Typhoid-Yale-Pitzer	https://github.com/vepitzer/typhoidVIMC
Yellow fever	YF-IC-Gaythorpe	https://github.com/mrc-ide/YF_VIMC_Burden_orderly
Yellow fever	YF-UND-Perkins	https://github.com/TAlexPerkins/yf_ensemble
Hib	Hib-LSHTM-Clark	https://github.com/lshtm-vimc/UNIVAC_model
Hib	Hib-PCV-JHU-Tam	https://list.spectrumweb.org
Japanese encephalitis	JE-OUCRU-Clapham	https://github.com/tranquanc123/JE_burden_estimates
Japanese encephalitis	JE-UND-Moore	https://github.com/mooresea/JEV_estimation
PCV	PCV-LSHTM-NUS	No publicly available code but building on UNIVAC model
PCV	PCV-JHU-Tam	https://list.spectrumweb.org
Rota	Rota-Emory-Lopman	https://github.com/lopmanlab/VIMC_public
Rota	Rota-JHU-Tam	https://list.spectrumweb.org
Rota	Rota-LSHTM-Clark	https://github.com/lshtm-vimc/UNIVAC_model

Hib=*Haemophilus influenzae* type b. HepB=hepatitis B. HPV=human papillomavirus. PCV=pneumococcal conjugate vaccine. Rota=rotavirus.

Table 2: **Links to publicly available code for each modelling group**

Implications of all the available evidence

Vaccination continues to be one of the most effective public health interventions worldwide. However, impact varies across vaccines. We have estimated that the highest vaccine impact ratios are from the human papillomavirus vaccine and measles-containing vaccines. For other vaccines, the relative impact ratio varies by WHO subregion, with uncertainty distributions often overlapping. There are also differences in vaccine impact by dose and by immunisation activity type (ie, routine versus campaign). These findings highlight the complexity of prioritising vaccination efforts across a broad portfolio and provides one metric to consider within a suite of factors.

Das **Mantelzell-Lymphom (MCL)** ist eine seltene, bösartige Krebserkrankung des lymphatischen Systems. Es gehört zu den **reifen B-Zell-Lymphomen** (Non-Hodgkin-Lymphome) und entsteht durch die ungebremste Vermehrung entarteter B-Zellen. Biologisch zeigt es Eigenschaften sowohl von langsam wachsenden als auch von aggressiven Lymphomen. Bei rund **80 Prozent der Betroffenen** verläuft die Erkrankung jedoch rasch und erfordert schnelles Handeln.

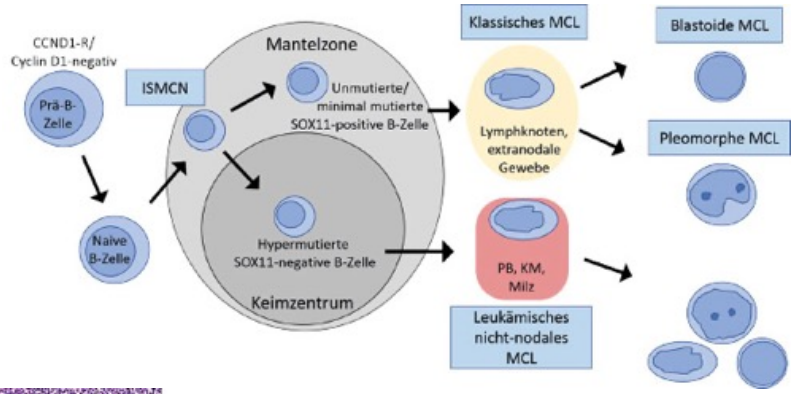

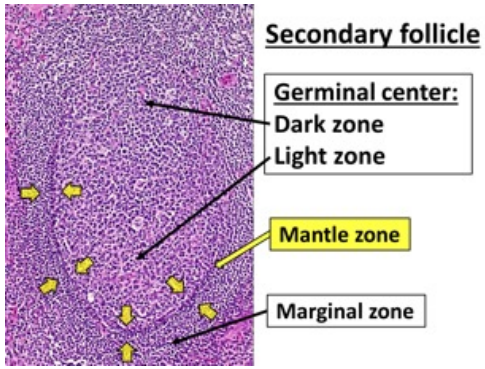

Genetic Testing: Pathologists look for a specific chromosomal abnormality known as the t(11;14) translocation, which causes the cell to overproduce the protein Cyclin D1. This mutation is the hallmark identifier for MCL.

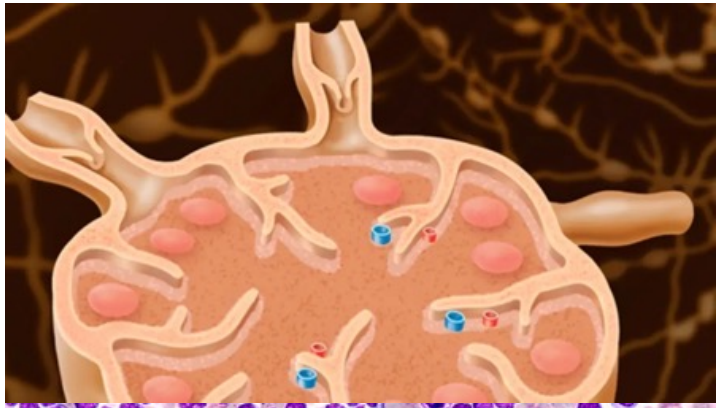

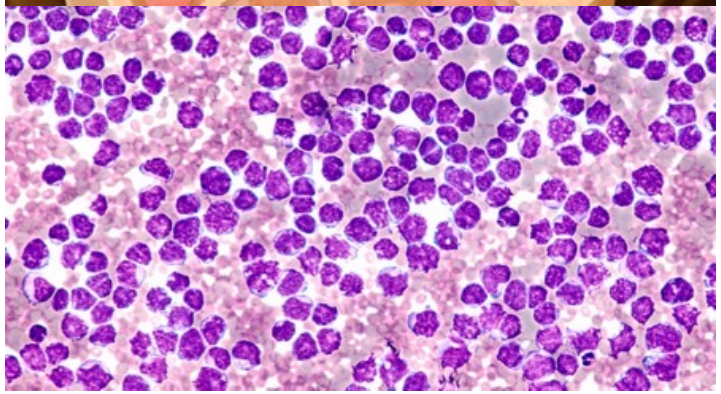

Ibrutinib ist ein zielgerichteter Bruton-Tyrosinkinase-(BTK-)Inhibitor zur Behandlung bestimmter B-Zell-Lymphome wie CLL, Mantelzell-Lymphom und Morbus Waldenström. Als Dauertherapie hemmt es das Krebswachstum, kann aber Nebenwirkungen wie Vorhofflimmern, Bluthochdruck und Infektionen verursachen.

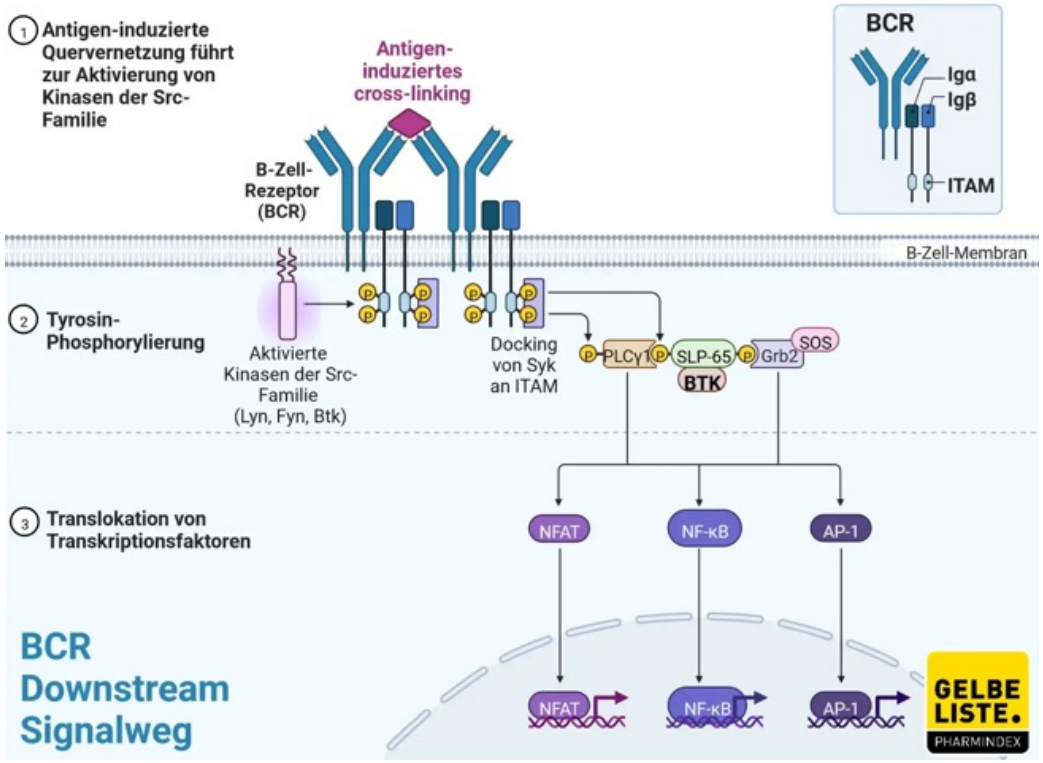

Addition of autologous stem-cell transplantation to an ibrutinib-containing first-line treatment in patients aged 18–65 years with mantle cell lymphoma (TRIANGLE): 4·5-year follow-up of a three-arm, randomised, open-label, phase 3 superiority trial of the European MCL Network

Summary

Background Adding ibrutinib to standard, first-line immunochemotherapy improves failure-free survival in adult patients aged 18–65 years with mantle cell lymphoma, according to the first results from the TRIANGLE trial. With prolonged follow-up, we investigated whether the addition of autologous stem-cell transplantation (ASCT) to an ibrutinib-containing regimen improves failure-free survival, and evaluated effects on overall survival.

Methods We conducted a three-arm, randomised, open-label, phase 3 superiority trial (TRIANGLE) in 165 secondary or tertiary clinical centres, with experience in mantle cell lymphoma treatment and the capability to perform ASCT or an association with such a centre, in 13 European countries and Israel. Patients aged 18–65 years with untreated, stage II–IV mantle cell lymphoma and suitable for ASCT were randomly assigned (1:1:1) to control group A or experimental groups A+I or I. Randomisation was done using computer-generated random numbers and stratified by study groups and Mantle Cell Lymphoma International Prognostic Index risk groups. Treatment in group A consisted of six alternating, 21-day cycles of R-CHOP (intravenous rituximab 375 mg/m² on day 0 or 1, cyclophosphamide 750 mg/m² on day 1, doxorubicin 50 mg/m² on day 1, vincristine 1·4 mg/m² on day 1 [up to a maximum of 2 mg], and oral prednisone 100 mg on days 1–5) and R-DHAP or R-DHAOx (intravenous rituximab 375 mg/m² on day 0 or 1, intravenous or oral dexamethasone 40 mg on days 1–4, high-dose intravenous cytarabine 2×2 g/m² for 3 h every 12 h on day 2, plus either intravenous cisplatin 100 mg/m² over 24 h on day 1 [R-DHAP] or intravenous oxaliplatin 130 mg/m² on day 1 [R-DHAOx]), followed by ASCT. In group A+I, oral ibrutinib (560 mg daily) was added on days 1–19 of R-CHOP cycles and as 2-year maintenance after ASCT. In group I, ibrutinib was given the same way, but ASCT was omitted. Rituximab maintenance was allowed in all treatment groups according to national guidelines. Three pairwise, one-sided, log-rank tests for the primary outcome (failure-free survival) were statistically monitored. The primary analysis was by intention to treat and included all randomly assigned patients, ignoring protocol deviations. Safety was assessed in randomly assigned patients who started any trial treatment component of the respective treatment phase. The trial is registered with ClinicalTrials.gov (NCT02858258) and is complete.

Findings Between July 29, 2016, and Dec 28, 2020, 870 patients (662 [76%] were male, 208 [24%] were female) were randomly assigned to group A (n=288), group A+I (n=292), or group I (n=290). After median follow-up of 54·9 months (95% CI 54·4–56·0), group A+I did not show superiority over group I, with 4-year failure-free survival of 82% (95% CI 78–87) versus 81% (76–86; hazard ratio [HR] 0·86 [one-sided 98·33% CI 0·00–1·27]; one-sided p=0·21). Group A+I remained superior to group A (82% [78–87] *vs* 70% [65–76]; HR 0·63 [one-sided 98·33% CI 0·00–0·89]; one-sided p=0·0026) and, as before, group A did not show superiority over group I (70% [65–76] *vs* 81% [76–86]; HR 1·45 [one-sided 98·33% CI 0·00–2·02]; one-sided p=0·99). 4-year overall survival was 88% (95% CI 84–92) in group A+I versus 81% (76–85) in group A (HR 0·59 [95% CI 0·38–0·92], p=0·0036) and 90% (87–94) in group I versus 81% (76–85) in group A (0·57 [0·36–0·90], p=0·0019). During maintenance or follow-up, the most common grade 3–5 adverse events were haematological disorders, reported in 127 (54%) of 234 patients in group A+I versus 74 (28%) of 269 in group I and 56 (23%) of 240 patients in group A, and infections, reported in 80 (34%) of 234 patients in group A+I versus 71 (26%) of 269 in group I and 37 (15%) of 240 patients in group A. Infections and infestations were the most common fatal adverse events during maintenance or follow-up, occurring in four (2%) of 234 patients in group A + I and five (2%) of 269 patients in group I.

Interpretation After a prolonged follow-up of 55 months, both ibrutinib-containing groups showed relevant improvements not only in failure-free survival—a modified form of progression-free survival—but also in overall survival. In contrast, the addition of ASCT to an ibrutinib-containing regimen had no supplementary benefit but increased toxicity. Induction treatment with ibrutinib and R-CHOP plus R-DHAP (or R-DHAOx), followed by 2 years of maintenance treatment with ibrutinib, should be considered as a new standard of care for younger patients with mantle cell lymphoma.

	Group A (n=288)	Group A + I (n=292)	Group I (n=290)
Age, years	57 (52–61)	57 (52–61)	57·5 (52–61)
Sex			
Male	218 (76%)	216 (74%)	228 (79%)
Female	70 (24%)	76 (26%)	62 (21%)
Race			
White	283 (98%)	283 (97%)	290 (100%)
Asian	0	1 (<1%)	0
Black	0	1 (<1%)	0
Other	5 (2%)	7 (2%)	0
Histology*			
MCL 9673/3	286 (99%)	288 (99%)	287 (99%)
ML, NOS 9590/3	0	1 (<1%)	0
NHL, NOS 9591/3	0	1 (<1%)	0
DLBCL 9680/3	0	0	2 (1%)
Splenic MZL 9689/3	0	1 (<1%)	0
FL 9690/3	1 (<1%)	0	0
MZL 9699/3	0	1 (<1%)	0
CLL 9823/3	1 (<1%)	0	0
HCL 9940/3	0	0	1 (<1%)
Ann Arbor Stage			
I	1/287 (<1%)	0	0
II	9/287 (3%)	11 (4%)	18 (6%)
III	24/287 (8%)	21 (7%)	28 (10%)
IV	253/287 (88%)	260 (89%)	244 (84%)
B symptoms	72/285 (25%)	79/291 (27%)	87/285 (31%)
ECOG performance status			
0	214 (74%)	213 (73%)	208 (72%)
1	69 (24%)	77 (26%)	77 (27%)
2	5 (2%)	2 (1%)	5 (2%)
LDH:ULN ratio	0·94 (0·78–1·19)	0·94 (0·77–1·18)	0·87 (0·74–1·12)
LDH>ULN	122 (42%)	120 (41%)	105 (36%)
MIPI score	5·62 (5·40–5·91)	5·64 (5·35–5·95)	5·61 (5·38–5·92)
Low-risk group	168 (58%)	168 (58%)	168 (58%)
Intermediate-risk group	79 (27%)	80 (27%)	77 (27%)
High-risk group	41 (14%)	44 (15%)	45 (16%)
Leukocytes (white blood cells, G/L)	7·34 (5·50–10·91)	7·09 (5·28–11·11)	7·40 (5·77–11·92)
Ki-67 index	18% (9·75–37·50); n=249	18% (11·56–40·00); n=262	19% (10·25–35·00); n=259
Ki-67 index ≥30%	81/249 (33%)	81/262 (31%)	83/259 (32%)
Blastoid cytology	28/253 (11%)	34/261 (13%)	31/265 (12%)
p53 expression >50%	25/201 (12%)	28/195 (14%)	31/206 (15%)
High-risk biology	34/201 (17%)	40/199 (20%)	44/208 (21%)

Data are n (%), n/N (%), or median (IQR). CLL=chronic lymphocytic leukaemia. DLBCL=diffuse large B-cell lymphoma. ECOG= Eastern Cooperative Oncology Group. FL=follicular lymphoma. G=giga. HCL=hairy cell leukaemia. LDH=lactate dehydrogenase. MCL=mantle cell lymphoma. MIPI=Mantle Cell Lymphoma International Prognostic Index. ML=malignant lymphoma. MZL=marginal zone lymphoma. NHL=non-Hodgkin lymphoma. NOS=not otherwise specified. ULN=upper limit of normal. *International Classification of Diseases for Oncology (ICD-O-3) histology code.

Table 1: **Baseline characteristics**

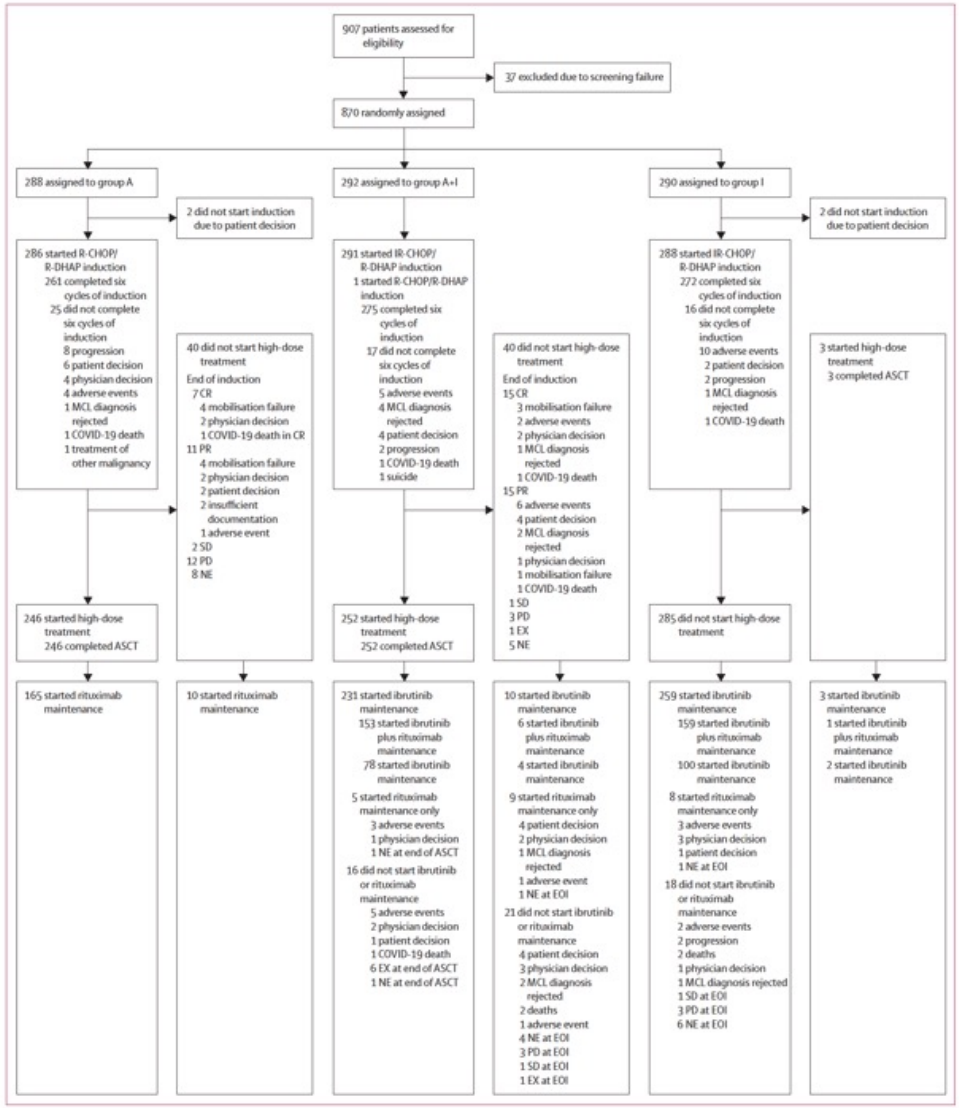

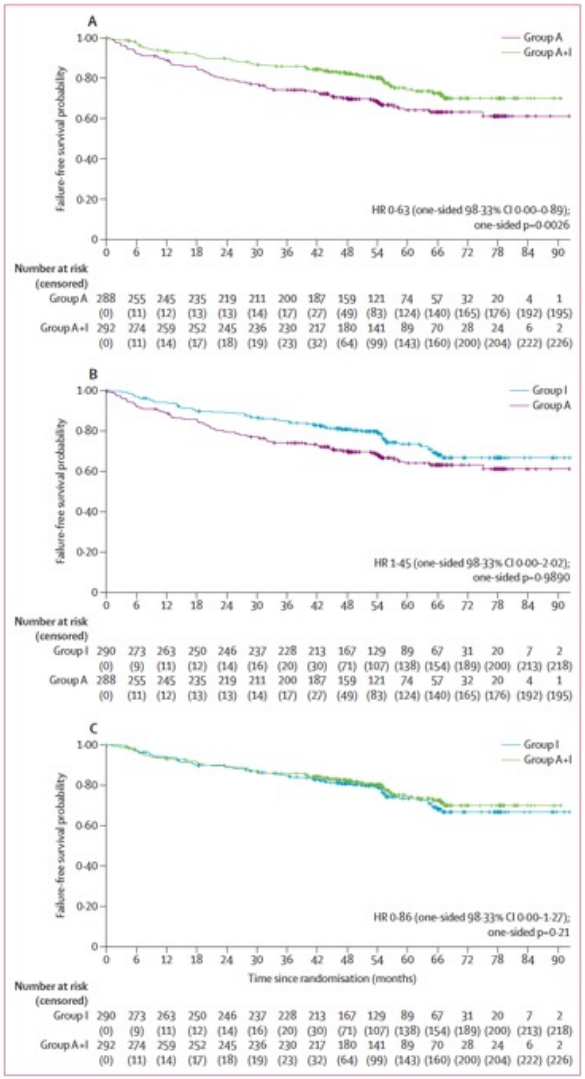

Figure 2: Failure-free survival for group A + I *vs* group A (A), group A *vs* group I (B), and group A + I *vs* group I (C)
HR=hazard ratio.

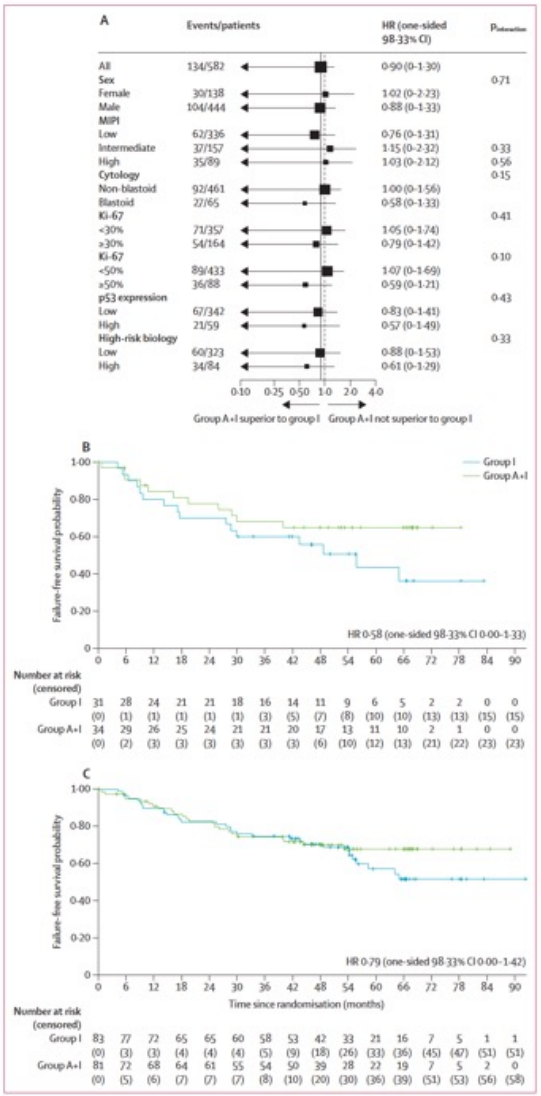

(Figure 3 continues on next page)

Figure 3: **Failure-free survival in subgroups for group A + I *vs* group I (A), in subgroups of patients with blastoid cytology (B), high Ki-67 with 30% cutoff (C), high Ki-67 with 50% cut-off (D), high p53 expression (E), and high-risk biology (F) for group A + I *vs* group I**
p values are for interactions. High-risk biology was classified as low (low, low intermediate, or high intermediate combined MIPI and low p53 expression) or high (high combined MIPI or high p53 expression). All results are uncorrected for the sequential design, and HRs are unadjusted and shown with one-sided 98·33% CIs corresponding to the primary one-sided hypotheses. No lower confidence limits for the treatment efficacy estimates are given. Superiority of group A + I versus group I would have been confirmed by an upper confidence limit smaller than 1·0 (A); due to reduced statistical power in the subgroups, the results are only hypothesis generating and not confirmatory. HR=hazard ratio. MIPI=Mantle Cell Lymphoma International Prognostic Index.

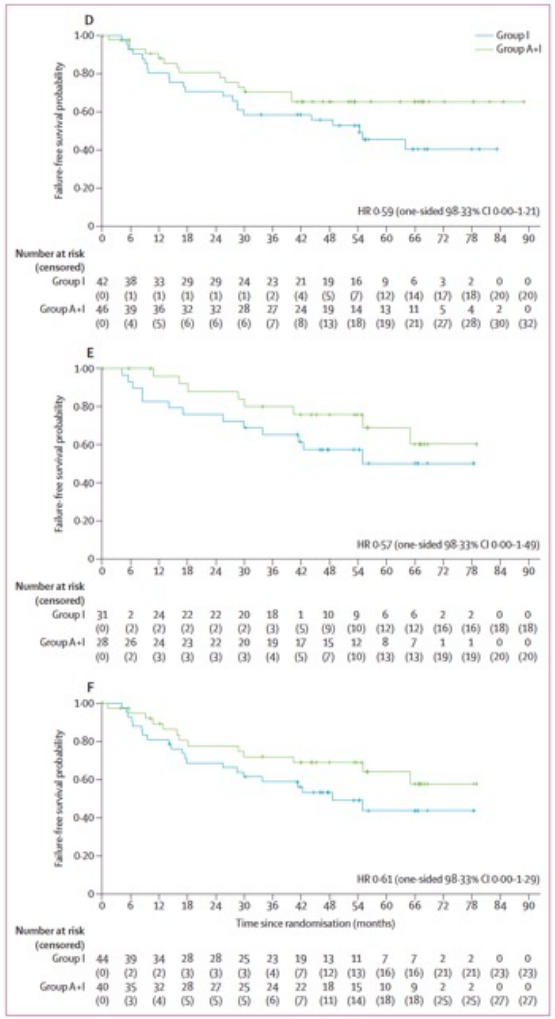

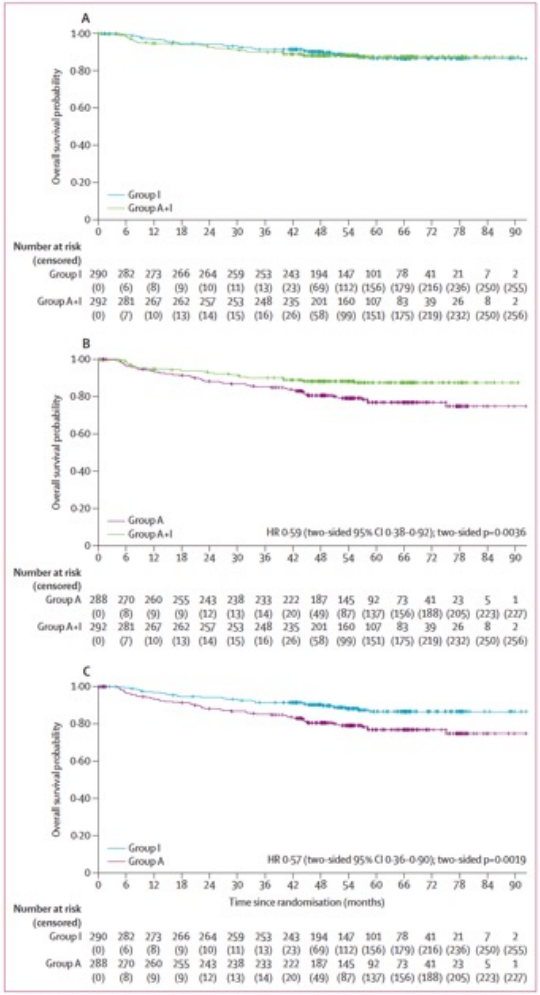

Figure 4: **Overall survival for group A + I *vs* group I (A), group A + I *vs* group A (B), and group A *vs* group I (C)**
HR=hazard ratio.

	During induction, IR-CHOP/R-DHAP (n=579)	During ASCT, IR-CHOP/R-DHAP (n=254)	During maintenance or follow-up	
			Group A+I (n=234)	Group I (n=269)
Blood and lymphatic system disorders	449 (78%)	163 (64%)	127 (54%)	74 (28%)
Neutrophil count decreased	301 (52%)	85 (33%)	110 (47%)	61 (23%)
Platelet count decreased	355 (61%)	112 (44%)	17 (7%)	9 (3%)
Anaemia	150 (26%)	58 (23%)	8 (3%)	5 (2%)
Febrile neutropenia	73 (13%)	73 (29%)	16 (7%)	7 (3%)
White blood cell decreased	93 (16%)	41 (16%)	13 (6%)	7 (3%)
Lymphocyte count decreased	41 (7%)	8 (3%)	2 (1%)	6 (2%)
Infections and infestations	73 (13%)	53 (21%)	80 (34%)	71 (26%)
Lung infection	9 (2%)	13 (5%)	37 (16%)	30 (11%)
Coronavirus infection	4 (1%)	0	12 (5%)	24 (9%)
Sepsis	12 (2%)	17 (7%)	5 (2%)	4 (1%)
Other	10 (2%)	12 (5%)	1 (<1%)	3 (1%)
Device-related infection	5 (1%)	7 (3%)	2 (1%)	1 (<1%)
Shingles	0	0	10 (4%)	1 (<1%)
Gastrointestinal disorders	69 (12%)	54 (21%)	15 (6%)	13 (5%)
Diarrhoea	21 (4%)	7 (3%)	7 (3%)	5 (2%)
Oral mucositis	9 (2%)	23 (9%)	0	2 (1%)
Nausea	18 (3%)	18 (7%)	0	0
Vomiting	18 (3%)	2 (1%)	1 (<1%)	2 (1%)
General disorders and administration-site conditions	38 (7%)	54 (21%)	7 (3%)	13 (5%)
Mucosal inflammation	6 (1%)	45 (18%)	2 (1%)	2 (1%)
Fever	6 (1%)	8 (3%)	0	5 (2%)
Fatigue	16 (3%)	3 (1%)	1 (<1%)	0
Metabolism and nutrition disorders	76 (13%)	22 (9%)	7 (3%)	8 (3%)
Hypokalaemia	34 (6%)	13 (5%)	2 (1%)	1 (<1%)
Investigations	36 (6%)	12 (5%)	13 (6%)	2 (1%)
γ-glutamyl transferase increased	11 (2%)	3 (1%)	7 (3%)	0
Nervous system disorders	28 (5%)	1 (<1%)	16 (7%)	13 (5%)
Syncope	9 (2%)	1 (<1%)	6 (3%)	3 (1%)
Respiratory, thoracic, and mediastinal disorders	17 (3%)	13 (5%)	8 (3%)	9 (3%)
Vascular disorders	33 (6%)	8 (3%)	5 (2%)	9 (3%)
Hypertension	24 (4%)	6 (2%)	1 (<1%)	4 (1%)
Cardiac disorders	19 (3%)	2 (1%)	9 (4%)	14 (5%)
Atrial fibrillation	11 (2%)	1 (<1%)	4 (2%)	7 (3%)
Injury, poisoning, and procedural complications	8 (1%)	4 (2%)	4 (2%)	10 (4%)
Neoplasms benign, malignant, and unspecified (including cysts and polyps)	2 (<1%)	0	8 (3%)	16 (6%)
Renal and urinary disorders	40 (7%)	3 (1%)	0	4 (1%)
Acute kidney injury	36 (6%)	2 (1%)	0	2 (1%)
Skin and subcutaneous tissue disorders	5 (1%)	11 (4%)	9 (4%)	1 (<1%)
Musculoskeletal and connective tissue disorders	8 (1%)	0	6 (3%)	10 (4%)

Grade 3–5 adverse events and preferred terms occurring in at least 3% of patients in any treatment group shown. MedDRA coded preferred terms and system organ class were reclassified to match Common Terminology Criteria for Adverse Events version 4.03 for all preferred terms that had occurred in more than ten patients. ASCT=autologous stem-cell transplantation. MedDRA=Medical Dictionary for Regulatory Activities. IR-CHOP=ibrutinib combined with R-CHOP. R-CHOP=intravenous rituximab 375 mg/m^2, intravenous cyclophosphamide 750 mg/m^2, intravenous doxorubicin 50 mg/m^2, intravenous vincristine 1·4 mg/m^2, and oral prednisone 100 mg. R-DHAP=intravenous rituximab 375 mg/m^2, intravenous or oral dexamethasone 40 mg, intravenous cytarabine 2 × 2 g/m^2, and intravenous cisplatin 100 mg/m^2.

Table 2: **Frequency of patients with at least one grade 3–5 adverse event by system organ class and preferred terms during induction, ASCT, and maintenance or follow-up in group A+I and group I**

Research in context

Evidence before this study

We did a PubMed search on Oct 30, 2025, without explicit publication date or language restriction, using the search terms "(mantle cell lymphoma) AND (ibrutinib OR autologous) AND randomized" to find all randomised, phase 3 trials investigating the role of autologous stem-cell transplantation (ASCT) or the Bruton's tyrosine kinase inhibitor ibrutinib as part of first-line treatment for younger, transplant-eligible patients with mantle cell lymphoma. Only two trials, both performed by the European Mantle Cell Lymphoma Network, matched the search criteria. The first randomised trial of the European Mantle Cell Lymphoma Network had established ASCT after response to first-line induction with chemotherapy or immunochemotherapy as standard of care in 2005. In 2024, the first results of the three-arm, randomised TRIANGLE trial indicated that the addition of fixed duration ibrutinib should become part of a cytarabine-containing induction immunochemotherapy and maintenance. These conclusions from the TRIANGLE trial were based on effects on failure-free survival, whereas results for overall survival had not yet formally been evaluated. Furthermore, the TRIANGLE trial remained ongoing to answer the final question of whether the addition of ASCT to an ibrutinib-containing first-line treatment was effective.

Added value of this study

With mature median follow-up of more than 4 years, the TRIANGLE trial shows improvements in both overall survival and failure-free survival when adding ibrutinib to first-line R-CHOP (rituximab, cyclophosphamide, doxorubicin, vincristine, and prednisone), alternating with R-DHAP (rituximab, dexamethasone, high-dose cytarabine, and cisplatin). The addition of ASCT to ibrutinib-containing, first-line treatment did not show superior efficacy and was associated with more frequent, severe side-effects. However, preplanned subgroup analyses suggested potentially prolonged disease control by ASCT in patients with mantle cell lymphoma who have high-risk biology, defined as high-risk combined Mantle Cell Lymphoma International Prognostic Index or high p53 expression, although these results were not adequately powered given the small sample sizes.

Implications of all the available evidence

In transplant-eligible adult patients aged 65 years or younger with mantle cell lymphoma, first-line treatment should consist of ibrutinib added to R-CHOP, alternating with R-DHAP, and followed by 2 years of ibrutinib maintenance without ASCT. Future studies are required to clarify the potential role of ASCT in patients with biologically aggressive mantle cell lymphoma.

Encephalitis is inflammation of the brain.

Early recognition of symptoms can save lives.

F.L.A.M.E.S

Encephalitis International

F — **Flu-Like Symptoms**
Fever, tiredness, nausea, aches and pains.

L — **Loss of Consciousness**
Becoming drowsy, confused or unresponsive.

A — **Acute Headache**
Head pain that feels different from ordinary headaches, and may include dizziness/blurred vision.

M — **Memory Problems**
Forgetting events or struggling to remember things clearly.

E — **Emotional or Behavioural Changes**
Acting out of character, hallucinations, unusual fears or suspicions, mood changes.

S — **Seizures**
Staring blankly, freezing, stiffening of the body, jerking or twitching movements, and falling to the ground.

Think **Brain in FLAMES**, Think **Encephalitis**

www.encephalitis.info/FLAMES

Encephalitis

Brain inflammation secondary to encephalitis is an urgent global emergency and presents multiple opportunities to reduce current substantial morbidity and mortality. Aetiologies can be divided into infectious and autoimmune causes. In this Seminar, we highlight pragmatic clinical approaches to recognise and distinguish the most common pathogenic viruses and emerging range of autoantibodies encountered in routine practice. These pre-test impressions are judiciously shaped by valuable, simple investigations—particularly serum and cerebrospinal fluid nucleic acid and autoantibody testing—to identify the precise causative agent. This clinically led approach ensures early recognition of encephalitis subtypes, facilitates the timely administration of antivirals and immunotherapies proven to improve patient outcomes, and minimises the frequent misdiagnosis of autoimmune encephalitis. Finally, we review emerging targeted therapeutic approaches, measurements of clinical encephalitis outcomes, and environmental and vaccine-centred strategies to improve prevention, diagnosis, and care for patients with encephalitis, cognisant of long-term patient, caregiver, and economic burdens.

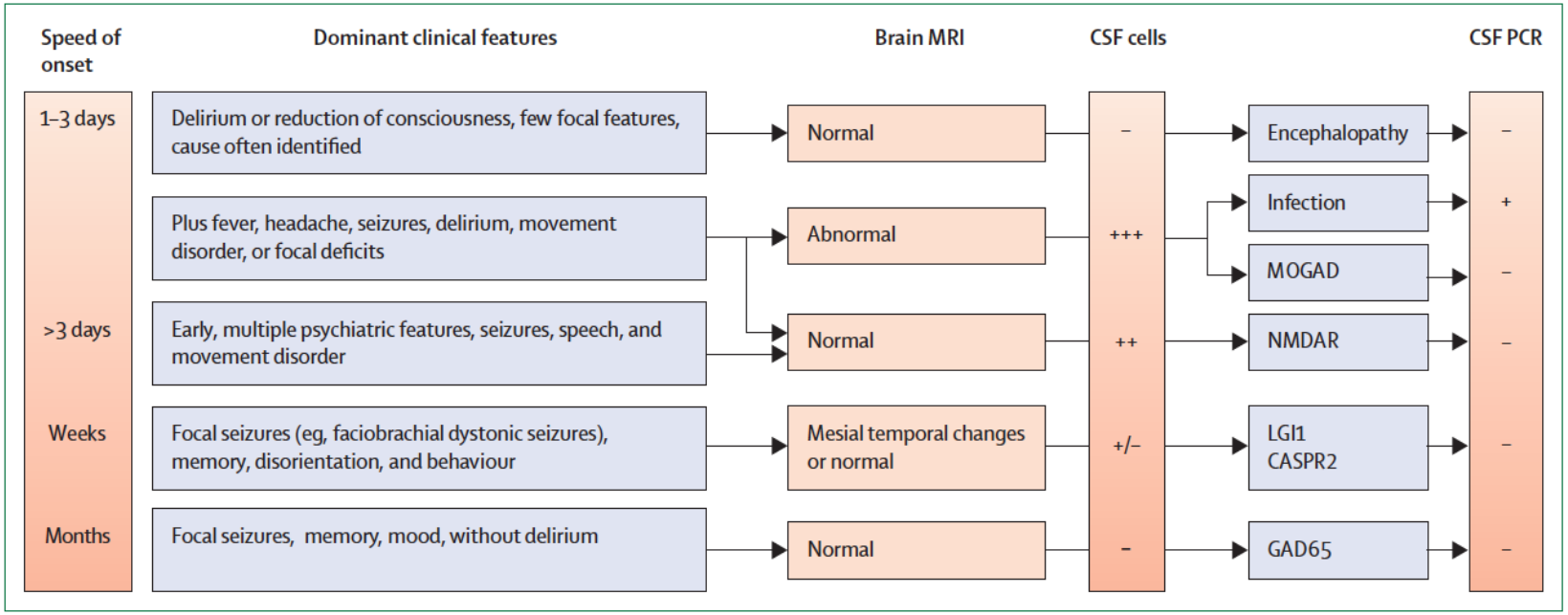

Figure 1: **Pragmatic approach to distinguish common forms of encephalitis**
Encephalopathy, infectious encephalitis, and forms of autoimmune encephalitis can be largely differentiated based on the speed of symptom onset, dominant clinical features, and by incorporating MRI, the presence of CSF cells, and PCR results. This clinical guide is intended to provide a simple, digestible approach to capture common encephalitis syndromes, without being definitive, and should be refined with data from figures 2 and 3, and appendix pp 4–29. CSF=cerebrospinal fluid. GAD65=glutamic acid decarboxylase 65. LGI1=leucine-rich glioma-inactivated 1. MOGAD=myelin oligodendrocyte glycoprotein antibody-associated disease. NMDAR=N-methyl-D-aspartate receptor.

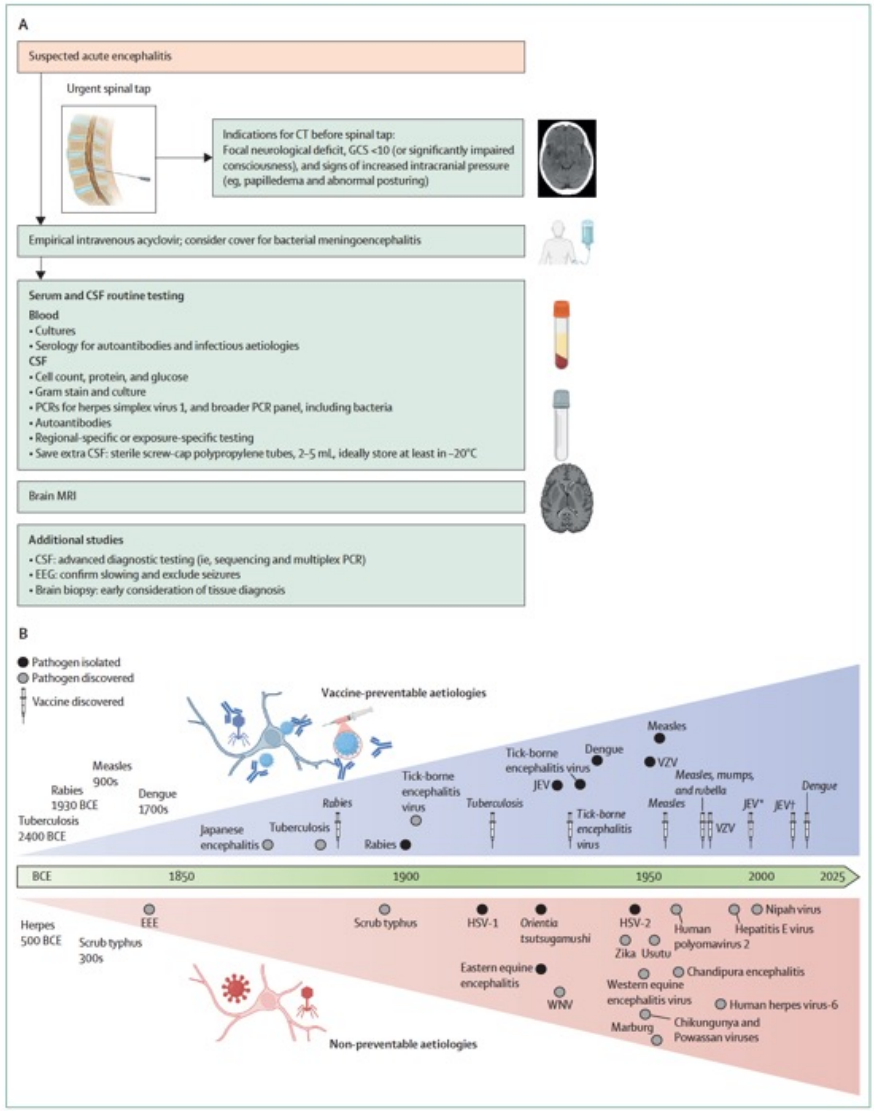

(Figure 2 continues on next page)

C

0% 20% 40% 60% 80% 100%

	Demographics		Clinical features									Investigations		
	Age	Male	Fever	Headache	Meningeal symptoms	Respiratory	Changes in mental status	Seizures	Focal signs	Vomiting	Rash	MRI	CSF	EEG
Japanese encephalitis virus	44	53	96	48	51	83	59	31	8	0	0	90	75	0
HSV-1	56	51	80	50	30	8	63	38	31	23	2	94	95	91
West Nile virus	60	70	81	47	35	19	51	8	20	48	19	55	100	0
Enterovirus	2	55	85	33	20	44	71	3	18	37	25	48	75	0
Varicella zoster virus	57	61	57	56	56	3	38	16	20	34	61	16	94	51

Figure 2: **Acute and infectious encephalitis—features and approach**

(A) Approach to diagnostic investivations in acute encephalitis, including safe expedition of CSF sampling[107,108] and timely, parallel testing of both infectious and autoimmune aetiologies from blood and CSF. (B) Pathogen discovery timeline, describing vaccine-preventable (blue, above line) and currently non-preventable aetiologies (pink, below line). Black dots represent when the virus was isolated, grey dots show when the virus was discovered, and syringes indicate when the vaccine was discovered. Created with BioRender.com. (C) Key clinical features of the five most common infectious encephalitis viruses, with percentages of each feature displayed in each cell, extracted from the five largest studies of each virus. Median age of onset shown. Zeros are entered for unreported data. CSF=cerebrospinal fluid. EEE= Eastern equine encephalitis. EEG=electroencephalogram. GCS=Glasgow Coma Score. HSV=herpes simplex virus. JEV=Japanese encephalitis virus. VZV=varicellar zoster virus. WNV=West Nile virus. *Mouse-brain derived. †Cell-culture derived.

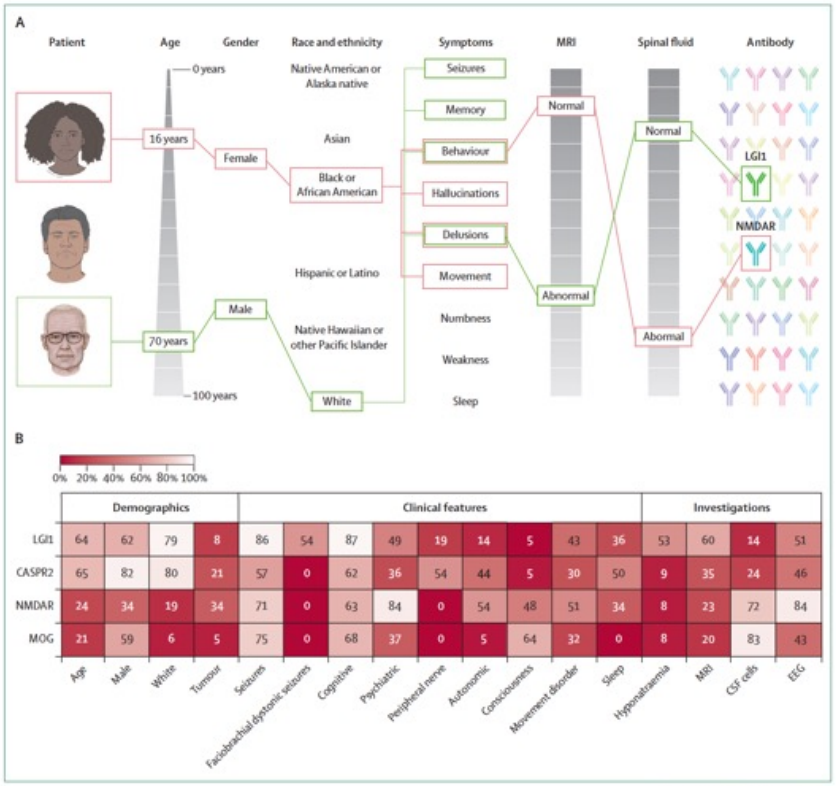

(Figure 2 continues on next page)

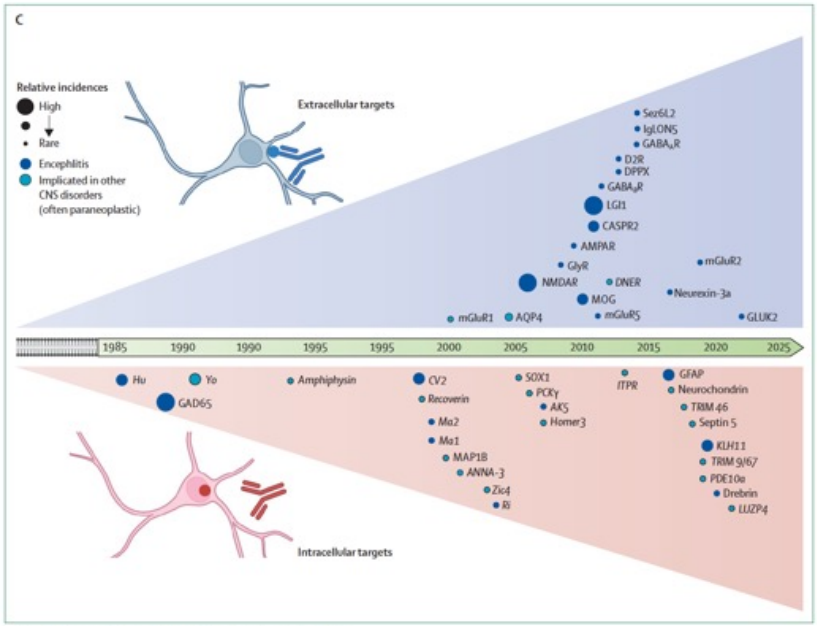

***Figure 3*: Autoimmune encephalitis features and discovery timeline**

(A) Fundamental clinical features across demographics, symptoms, and simple investigations direct the detection of autoantigen-reactive antibodies. Examples shown with LGI1 and NMDAR antibodies, which are somewhat skewed towards White and non-White populations, respectively. Used with permission of Mayo Foundation for Medical Education and Research, all rights reserved. (B) Demographics, clinical features, and investigations in autoimmune encephalitis. The percentages of each feature are extracted from the five largest studies of each of the five most common autoantibodies. Median age of onset shown. Zeros are entered for unreported data. (C) Timeline of discovery for autoantibodies targeting extracellular (above line) and intracellular (below line) epitopes. Many are implicated in autoimmune encephalitis. Created with BioRender.com. CSF=cerebrospinal fluid. EEG=electroencephalogram. GAD65=glutamic acid decarboxylase 65. LGI1=leucine-rich glioma-inactivated 1. MOG=myelin oligodendrocyte glycoprotein. NMDAR=N-methyl-D-aspartate receptor.

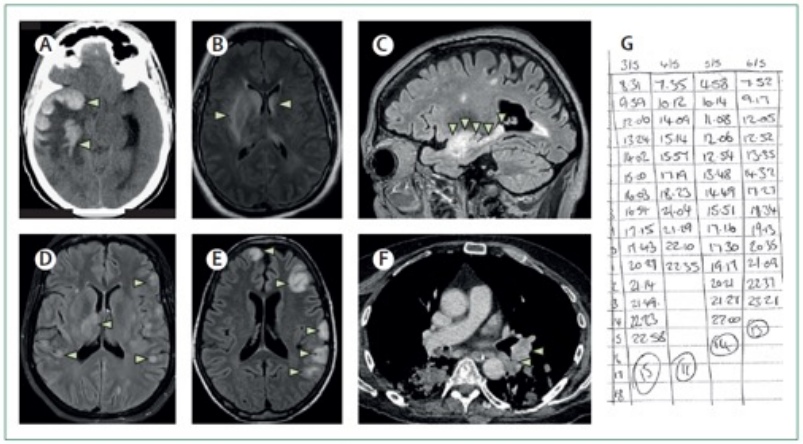

Figure 4: **Brain imaging and patient diary in infectious and autoimmune encephalitis**
(A) CT head scan showing haemorrhage (arrows) and oedema (hypodense) in right temporal lobe secondary to herpes simplex virus-1 encephalitis. (B) Left and right basal ganglia involvement (arrows) with Japanese encephalitis virus. (C) Limbic encephalitis associated with autoantibodies against the $GABA_B$ receptor, with high signal intensity in the hippocampus and amygdala on FLAIR imaging (arrows). (D) FLAIR imaging showing multifocal bilateral subcortical and right thalamic hyperintensities (arrows) associated with myelin oligodendrocyte glycoprotein antibodies. (E) Multifocal fluffy cortical and juxtacortical FLAIR hyperintensities (arrows) seen with $GABA_A$-receptor antibody encephalitis. (F) Left hilar lymph nodes (arrows) associated with small cell lung cancer and $GABA_B$ receptor antibodies. (G) Diary of a patient with leucine-rich glioma-inactivated 1 antibody encephalitis recording 1 day of focal seizures per column. Daily totals are circled.

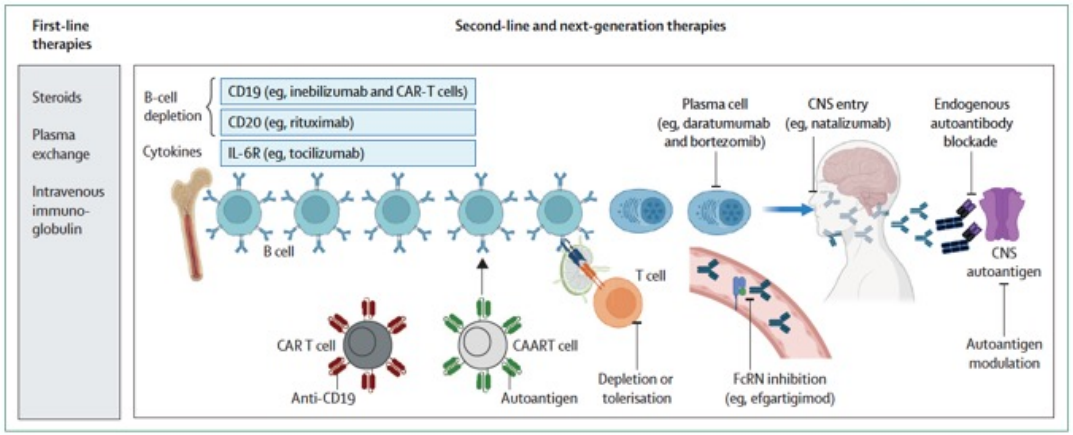

Figure 5: **Established and emerging immunotherapies for treating autoimmune encephalitis**
After first-line therapies, second-line immunotherapies should be considered, including B-cell depletion with CD19 or CD20-targeting medications, CAR T cells, IL-6R blockade with tocilizumab or satralizumab (ie, cytokine modulation), and drugs that delete plasma cells, including daratumumab (targeting CD38, which is also expressed on some B cells) and the proteosome inhibitor bortezomib. Emerging options include inhibition of leukocyte entry to the CNS (eg, natalizumab), blockade of FcRN IgG uptake to prolong the half-life of IgG (eg, with efgartigimod), blockade of endogenous antibody binding (eg, with monovalent antibody decoy therapy), direct pharmacological autoantigen binding to overcome autoantibody effects (eg, allosteric modulators), CAART cells (which express the autoantigen to induce selective deletion of autoantigen-reactive B cells), and various T-cell tolerisation or modulation approaches, to deny help to B cells. Depicted key neuroimmune compartments involved in the generation of pathogenic autoantibodies include bone marrow (the source of B cells and early T cells) and lymph nodes (a key site of crosstalk between B cells and T cells). CAR T=chimeric antigen receptor T cells. CAART=chimeric autoantibody receptor T cells. FcRN=Fc receptor neonatal. IL-6R=interleukin-6 receptor.

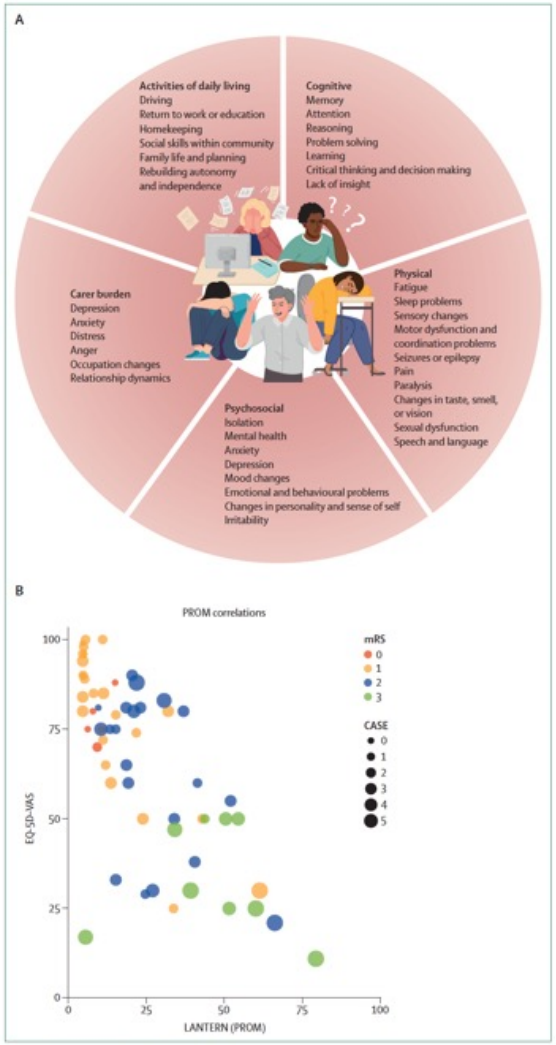

Figure 6: **Patient outcomes after encephalitis**
(A) Multiple functional domains are affected by infectious and autoimmune encephalitis. (B) In LGI1-antibody encephalitis, the patient-rated quality of life score (EQ-5D-VAS) correlates most closely with the patient-reported outcome measure (PROM), rather than the clinician-assessed modified Rankin score (mRS) or clinical assessment scale in autoimmune encephalitis (CASE).[126]

Conclusion

The past few years have reclassified many enigmatic and idiopathic forms of encephalitis with molecularly precise, aetiology-based definitions. However, improved physician education regarding clinical presentations, targeted research agendas and funding to improve diagnostic capacities, and global public health initiatives are essential to meet the WHO-designated, urgent public health aim of reducing the overall encephalitis burden for survivors and their caregivers.

Signe de cils in peripheral facial palsy

Panel

Learning points

- Signe de cils refers to the apparent elongation or increased prominence of the eyelashes on the affected side in peripheral facial palsy, due to orbicularis oculi dysfunction
- Its presence should prompt clinicians to differentiate peripheral from central facial palsy and to recognise subtle features distinguishing bilateral from unilateral involvement

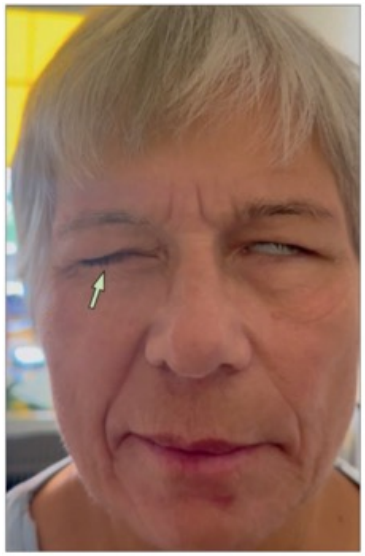

Figure 2 The presence of a signe de cils

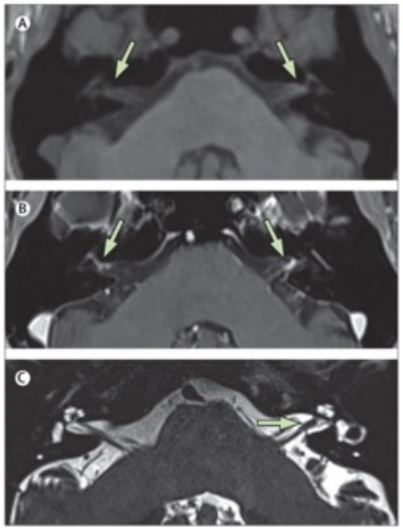

Figure 3 Focal nodular thickening and contrast enhancement of facial nerve on brain MRI

A positive antibody cerebrospinal fluid (CSF)–serum index for borrelia (IgG index 4·24) that came back from our laboratory 5 days after the lumbar puncture confirmed the acute neuroborreliosis. The chemokine C-X-C ligand 13 (CXCL13) in CSF was more than 800 pg/mL (reference: normal <250 pg/mL; in cases of suspected early neuroborreliosis in adults, if no antibiotics have been administered, CSF CXCL13 levels >250 pg/mL are measured). The specificity of results using the 250 pg/mL threshold is then greater than 95%. To increase specificity without substantially reducing sensitivity, a threshold of 500 pg/mL can be considered and levels less than 250 pg/mL make early, untreated neuroborreliosis highly unlikely.

Figure 4 Residual findings after 7 days of therapy showing persistent signe de cils

Pyocine sind natürliche, bakterientötende Proteine (Bakteriozine), die vom Bakterium *Pseudomonas aeruginosa* gebildet werden. Sie dienen der Bekämpfung von Konkurrentenstämmen und werden intensiv als neuartige, zielgerichtete Antibiotika gegen multiresistente Krankheitserreger erforscht

Die drei Hauptklassen

Pyocine werden basierend auf ihrer Struktur und Wirkungsweise in drei Gruppen unterteilt:

•**R-Typ & F-Typ:** Sie ähneln den Schwanzstücken von Bakteriophagen (Viren) und töten Zellen durch Perforation der bakteriellen Zellmembran.

•**S-Typ:** Kleinere, lösliche Proteine, die als Enzyme wirken und beispielsweise die DNA oder die Proteinsynthese in der Zielzelle zerstören.

Warum sie für die Medizin wichtig sind

•**Targeted Killing:** Sie wirken hochspezifisch auf *Pseudomonas aeruginosa* oder nahe verwandte Stämme, während die restliche, gesunde Mikrobiota geschont wird.

•**Kampf gegen Resistenzen:** Sie können Antibiotikaresistenzen umgehen und sind in der Lage, bakterielle Biofilme aufzubrechen.

•**Fokus der aktuellen Forschung:** Künstlich modifizierte Pyocine (Chimäre) werden als sogenannte "lebende Therapeutika" entwickelt, die im Labor sogar erfolgreich darauf ausgelegt werden können, spezifische Erreger wie *E. coli* anzugreifen.

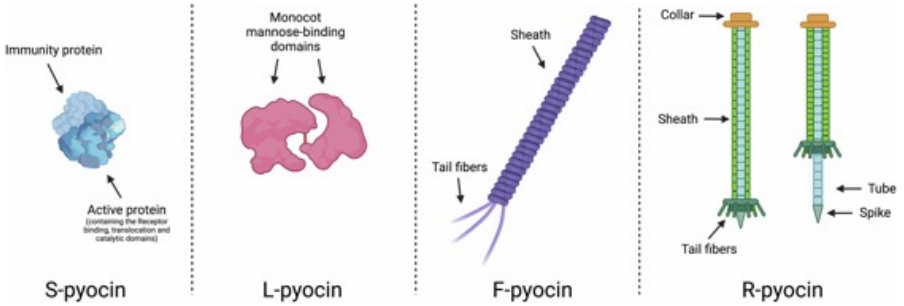

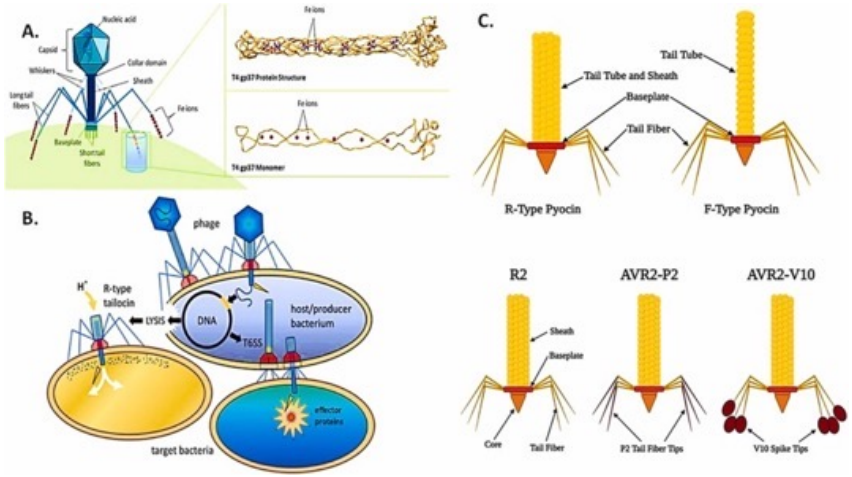

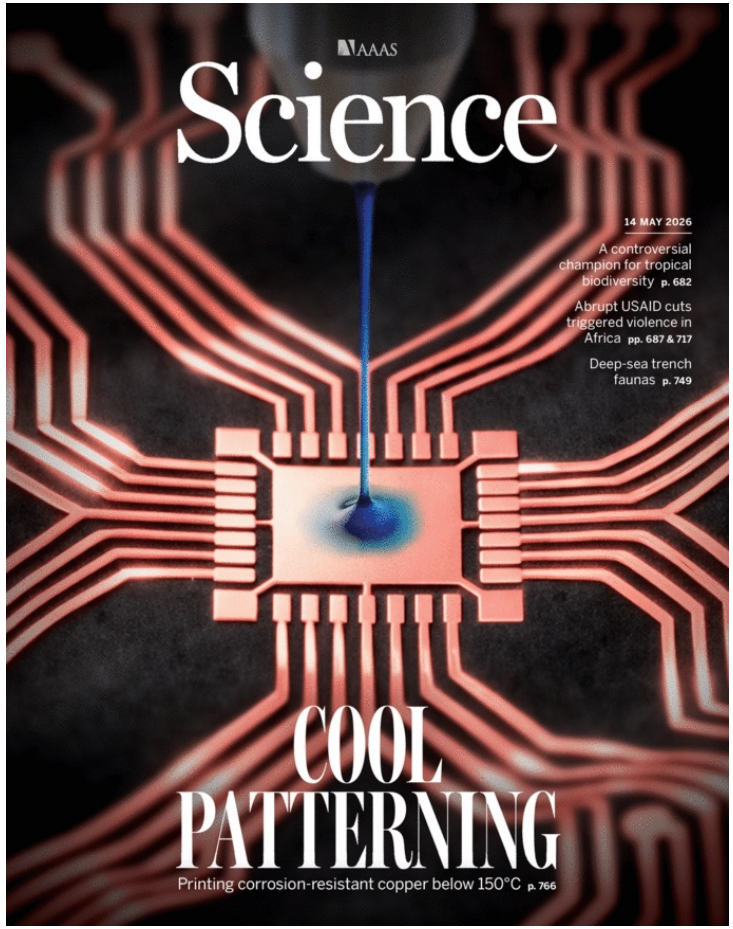

Scaffolds toughen bacteria-based therapy

Engineered cells can sense disease and deliver drugs at a site of pathology. These living therapeutics provide localized, self-sustaining responses to environmental changes, such as inflammation and pathogenic signals, that conventional drugs cannot offer. A promising chassis for living therapeutics is bacteria, which can be genetically programmed to release drugs in response to an external signal. However, bacteria require physical enclosure to prevent uncontrolled spread and toxicity. Biomaterials such as hydrogels and core-shell capsules have only demonstrated short-term containment of up to 2 weeks in culture. Harimoto *et al.* report a hydrogel scaffold with engineered stiffness and toughness that confines bacteria for up to 6 months in culture. When the system harbored bacteria producing pyocin, it cleared an infection in a mouse model of joint replacement. This could advance living therapeutics from short-lived proof-of-concept systems to durable, programmable medicines.

Hierarchical scaffold for on-demand therapy

Engineered bacteria can sense signals from infections in the surrounding tissue and release therapeutic molecules to treat the site of infection inside a body. Hierarchical biomaterial scaffold consists of bacteria-containing gelatin microgel enclosed in a larger polyvinyl alcohol scaffold. This provides a safe enclosure to suppress bacterial proliferation while withstanding pressure from the surrounding tissue to prevent fracture. The biomaterial scaffold can pass small molecules to and from the surrounding medium for delivering nutrients, biomarkers, and drugs to treat infection for a prolonged period.

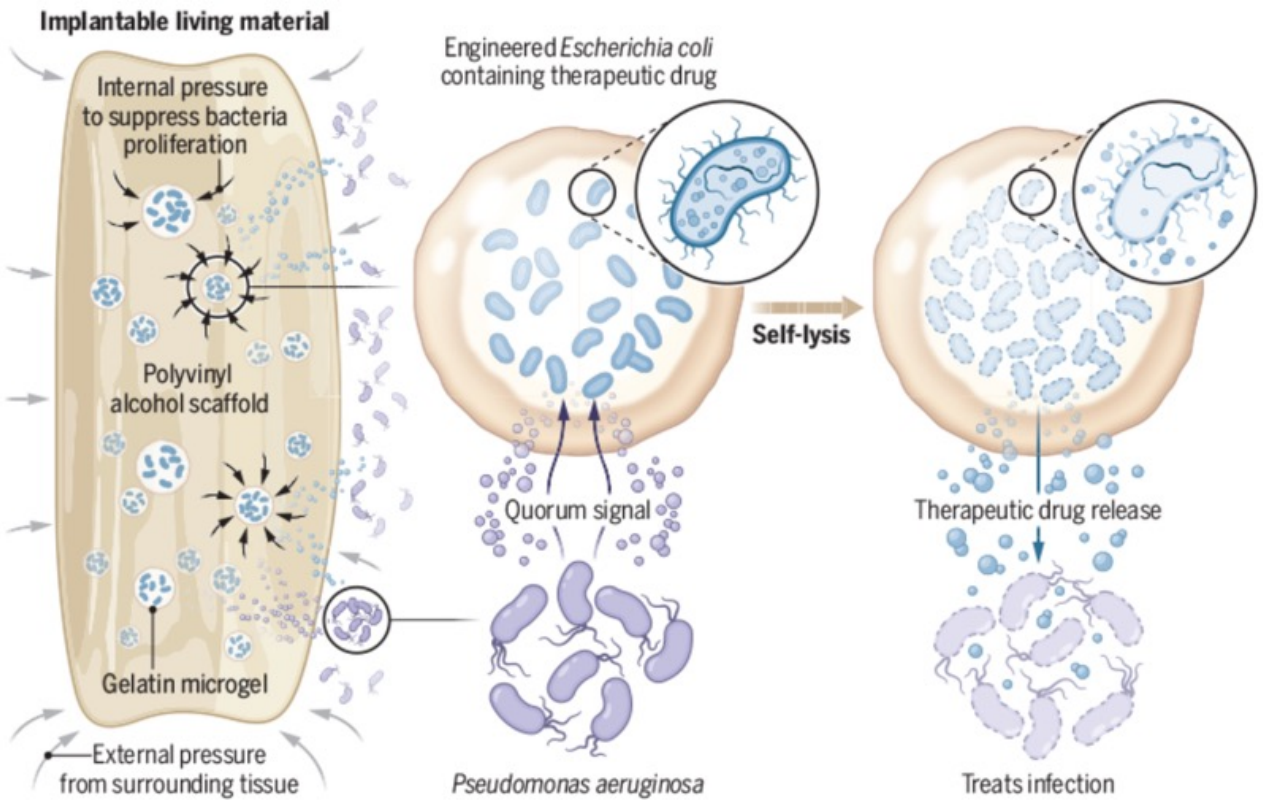

Implantable living materials autonomously deliver therapeutics using contained engineered bacteria

Microbes are increasingly used as living therapeutics, yet their uncontrolled dissemination in the body has remained a clinical roadblock. Physical containment remains largely unattainable owing to eventual bacteria escape. In this work, we present an implantable material that encapsulates and confines bacteria, wherein synthetically engineered microbes produce therapeutic payloads from within. We developed a hydrogel scaffold with dual mechanical features: high stiffness to regulate bacterial proliferation and high toughness to resist material fracture under physiological stress. This design achieved complete bacterial containment for 6 months and withstood multiple forms of mechanical loading that otherwise caused catastrophic material failure. By genetically engineering embedded bacteria, we endowed the material with environmental sensing and on-demand therapeutic release capabilities and demonstrated autonomous treatment in a murine prosthetic joint infection model.

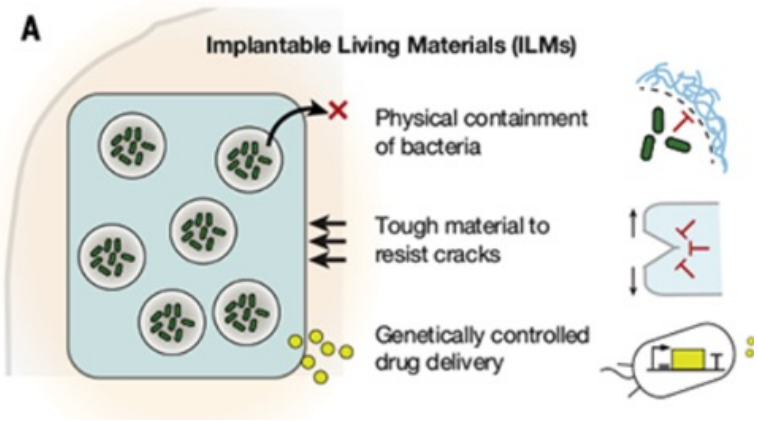

Design and mechanical characterization of ILMs. (**A**) Schematic of the ILM platform, in which a tough hydrogel scaffold encapsulates therapeutic bacteria. The material provides physical containment, resists both internal proliferative forces and external mechanical stresses, and enables genetically controlled therapeutic release.

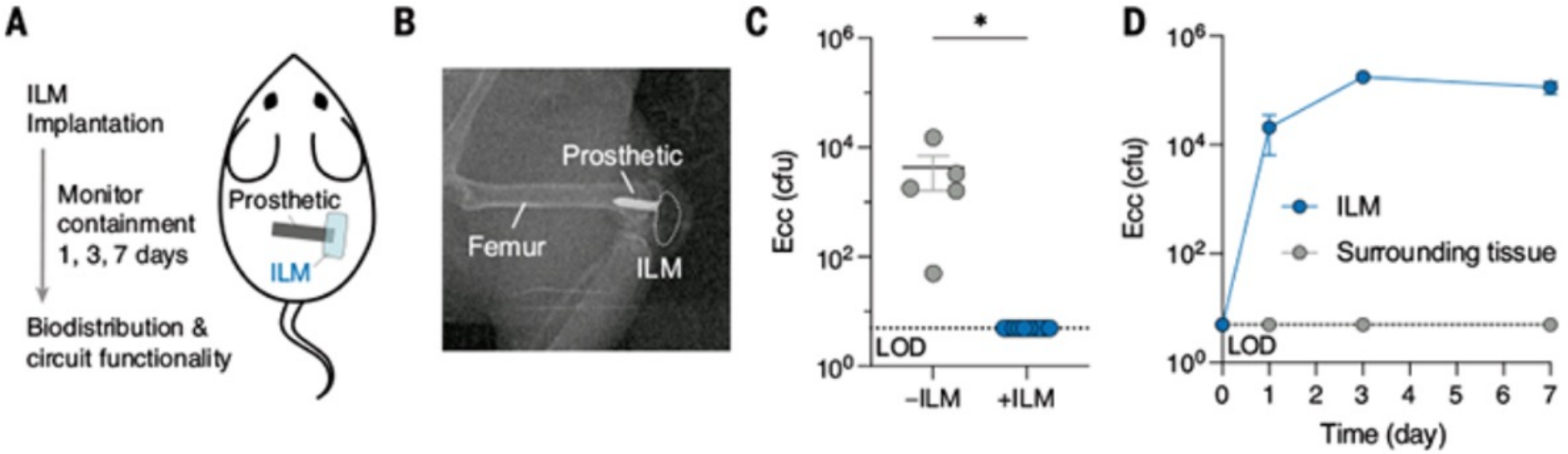

ILMs confine engineered bacteria and treat infection in a murine joint implant model. (**A**) Experimental design to assess in vivo containment and safety of ILMs. (**B**) Representative x-ray of a mouse femur implanted with a stainless-steel prosthesis and an ILM. (**C**) Viable Ecc recovered from surrounding joint tissue 1 day after implantation. LOD = 5 CFUs per animal (dotted line). Data are means ± SEMs; all replicates are shown. $*P < 0.05$; unpaired *t* test. (**D**) Bacterial counts in joint tissue and within ILMs over 7 days. LOD = 5 CFUs per animal (dotted line). Data are means ± SEMs; $n \geq 5$ independent replicates.

A 59,000-year-old tooth reshapes what we know about Neanderthal dentistry

Some 59,000 years ago, a Neanderthal developed a toothache.

What happened next was, in many ways, astonishing.

This individual figured out the source of their pain, deep inside a molar. They probably sought help to plan an invasive medical intervention. Then, they opened wide — no numbing gels or cotton wads to help — just a pointy rock grinding against a throbbing tooth.

This painful prehistoric dentistry saga unfurls from an ancient molar with a circular drill hole, discovered in a cave once inhabited by Neanderthals in southwestern Siberia. In a study published in PLOS One on Wednesday, scientists rule out other explanations for the hollowed-out hole, pushing back the known history of human dentistry by about 40,000 years.

Earliest evidence for invasive mitigation of dental caries by Neanderthals

Neanderthal medical knowledge has long attracted scholarly interest. Evidence suggests they cared for sick, injured, and elderly group members, with possible use of medicinal plants. However, it remains uncertain whether such practices reflect deliberate medical strategies or instinctive self-medication akin to that observed in non-human primates. Here, we analyze and interpret traces of deliberate artificial manipulation of Chagyrskaya 64, a Neanderthal lower left second molar found in Chagyrskaya Cave (Altai Krai, Russia). The tooth exhibits a large human-generated concavity on the occlusal surface, created during the lifetime of the individual. Traceological and microtomographic analyses of the observed modifications, combined with experimental verification, reveal that the concavity in Chagyrskaya 64 is indicative of the earliest documented instance of caries treatment involving the drilling/rotating with a lithic perforator, ca. 59 ka. Evidence of two distinct types of manipulations requiring different tools, in addition to the drilling/rotating technique, necessitating complex finger movements, indicates that the Chagyrskaya Cave Neanderthals possessed the cognitive capacity to intuit the source of pain, comprehend the feasibility of its elimination, and deliberately select the most efficacious dental intervention. These patterns bring Neanderthal behavior closer to modern humans and differentiate that behavior from the instinctive actions of other primates.